EVANS-HAMILTON, INC.
Western Region
6306 21st Ave. NE
Seattle, Washington 98115

A STUDY OF CURRENT PROPERTIES AND MIXING USING DROGUE MOVEMENTS OBSERVED DURING SUMMER AND WINTER IN CENTRAL PUGET SOUND, WASHINGTON

FINAL REPORT

by

Curtis C. Ebbesmeyer and Jonathan M. Helseth

for the

Municipality of Metropolitan Seattle

June 1975

Approved by:

Curtis C. Ebbesmeyer
Principal Investigator

ABSTRACT

As one of the Puget Sound Interim Studies, groups of drogues (i.e., current followers) were released over the West Point sewage outfall at depths of maximum effluent concentration. Through statistical analysis of subsequent drogue positions, the relative dilution of maximum concentration has been determined using an appropriate form of the Lagrangian diffusion equation during seven ebb, seven flood and two slack tidal phases in summer and winter.

By separating the eddy spectrum at the drogue group's effective diameter (average = 0.9 km) larger scale eddies appear as shear of the mean flow, whereas smaller scale eddies appear as turbulence characterized by an eddy diffusivity (average = 2.2×10^4 cm^2 s^{-1}). During established tidal currents the effluent is primarily stirred by the mean flow and large-scale eddies, thereby producing complex patterns of relatively concentrated filaments and patches. During slack tides, increased fluid accelerations rearrange and divide the larger eddies resulting in an increased supply of small-scale eddies, which more effectively disperse patches and filaments.

The net result is about a 1:10 dilution of maximum concentration over four hours during major flood or ebb tides compared with more rapid dilution proportional to t^{-x}, $x > 1.2$, during slack tides. Some effluent patches may retain their identity through several tidal phases as observed in photographs of dye injected into the Puget Sound Model. Those photographs also show an eddy in West Point's lee on selected flood tides as confirmed on two occasions by drogue trajectories.

Table of Contents

Table of Contents

List of Tables

List of Plates

List of Figures

List of Figures

List of Figures

Cooperative Efforts

This work represents one of the Puget Sound Interim Studies initiated by the Municipality of Metropolitan Seattle (Metro). More specifically, this study is designed to provide a quantitative description of currents and mixing in support of a major dye study undertaken concurrently by the Applied Physics Laboratory (APL) at the University of Washington (UW). A closely related study of effluent dispersal using the Puget Sound Model of the UW Department of Oceanography provided supporting data for both studies.

Acknowledgements

This work was performed under Purchase Order 10661 from Metro located at 600 First Avenue, Seattle, Washington 98104.

The drogues were constructed by Beth Chiodo and Dick Sylwester at Shoreline Community College. We are grateful to them and Jack Serwold, coordinator of the Marine Technician Program at Shoreline Community College for their fine work. Drogues were monitored from U.S. Geological Survey research vessel Hydor under the expert navigation of Bill Clique, and a National Oceanic and Atmospheric Administration survey vessel kindly supplied by Captain G.L. Short and navigated by Ray Schmidt. Sextant fixes were taken by Beth Chiodo, Joseph Glasscock, Lincoln Loehr, Jolene Patricelli and Dave Thomson. Joseph Glasscock, Jolene Patricelli and Darrell Terry plotted and digitized the fixes.

We are also grateful to Bill Bendiner and Richard D. Tomlinson for

providing liaison with APL and Metro, respectively. Under separate contract John H. Lincoln at the UW Department of Oceanography took 16-mm film of the Puget Sound Model. With his guidance we reviewed that unique film and took pictures of selected frames.

We also wish to acknowledge the continued guidance of Professor Emeritus Clifford A. Barnes at the UW Department of Oceanography and Professor Akira Okubo at the Marine Sciences Research Center, State University of New York, Stony Brook, New York.

I. Summary

This study is designed to provide a quantitative description of currents and mixing in support of a comprehensive dye study undertaken concurrently by the Applied Physics Laboratory* (abbreviated APL). The objective of that study is to trace sewage effluent stained with a fluorescent dye as it flows away from the West Point outfall during the summer period 30 August-4 September 1974 and the winter period 25 February-4 March 1975 (Figure 1).

Methods and initial results of the summer drogue study were reported by Ebbesmeyer and Okubo (1974). The present study reports the winter observations with a reanalysis of the summer data. The observations of both summer and winter may be described briefly as follows: groups of drogues (usually seven) were released over the outfall during selected tidal phases at nominal depths of maximum dye concentration (50 m in summer; 20 m in winter). Drogue positions, obtained from two small craft using sextants at 5-15 minute intervals, were plotted and then processed on a high speed computer using statistical regression procedures and an appropriate form of the Lagrangian diffusion equation. Table 1 shows general information for releases of 16 drogue groups.

The analysis separates the eddy spectrum at the drogue group's effective diameter (average = 0.9 km) so that larger scale eddies appear as shear of the mean flow (see Table 2), and smaller scale eddies appear as turbulence characterized by an eddy diffusivity (Table 3:average = 2.2×10^4 cm^2 s^{-1}). During established tidal currents the effluent is

*At the University of Washington, Seattle, Washington.

primarily stirred by the mean flow and large-scale eddies, thereby producing complex patterns of concentrated filaments and patches. Maximum concentrations within patches require about four hours or five kilometers to achieve a 1:10 dilution.* After an initial interval of slower decay, maximum concentrations decay at the rate of approximately $t^{-1.2}$ (Figure 2*).

During slack tide, increased fluid accelerations rearrange and divide the larger eddies resulting in an increased supply of small-scale eddies. The result is an increased rate of dilution according to t^{-2} to t^{-4} for patches toward shore, while patches toward mid-channel may only experience decay rates moderately faster than $t^{-1.2}$.

Figure 3 shows drogue plumes for all releases. Superpositions of these on corresponding photographs of dye injected into the Puget Sound Model show that drogue plumes often approximate dye plumes (cf., Plates I,II). Deviations occur due to dye recirculated from previous tidal phases. Drogue trajectories tend to follow the more concentrated filaments and patches.

The photographs also indicate an asymmetrical distribution of patchiness between ebb and flood tides, possibly as a result of net freshwater accumulation flowing northward. During flood tides two types of patchiness are often evident: (1) effluent patches dispersed between mid-channel and Magnolia Bluff; (2) an eddy in West Point's lee circulating counterclockwise. Ebbs produce a characteristic filamentary dispersion sweeping northward around Meadow Point. Selected patches were observed to maintain their identity for up to 15 hours.

---

*Because of assumptions basic to the Lagrangian diffusion equation these dilutions should be treated as estimates of maximum dilution.

Table 1. General information for summer and winter drogue studies.

Date	Tidal phase	Tidal range (m)	# drogues launched	Depth (m)	Hour first drogue launched	Hour last drogue retrieved	Elapsed time (h)
8-30-74	Flood	3.2	7	50	13.4	19.5	6.1
8-31-74	"	3.1	7	50	12.2	19.1	6.9
9- 1-74	"	3.0	7	50	11.5	17.6	6.1
9- 2-74	"	2.9	7	50	12.8	18.5	5.7
2-25-75	"	2.1	5	20	14.5	17.3	2.8
9- 3-74	Ebb	2.3	6	50	7.3	12.1	4.8
2-26-75	"	3.0	7	20	8.5	11.8	3.3
2-27-75	"	3.4	6	20	7.9	12.2	4.3
2-28-75	"	3.6	7	20	8.2	11.7	3.5
3- 1-75	"	3.7	7	20	8.7	14.7	6.0
3- 2-75	"	3.6	7	20	9.5	14.3	4.8
3- 3-75	"	3.4	7	20	9.5	15.4	5.9
9- 3-74	Slack		4	50	12.7	14.7	2.0
2-28-75	"		7	20	13.1	16.2	3.1
2-26-75	Shilshole flood	2.6	5	20	13.8	17.8	4.0
2-27-75	Flood eddy	2.9	6	20	14.2	18.7	4.5

Table 1 Cont'd.

Date	Tidal phase	Interval analyzed for current properties	Initial area of group (km^2)	Final area of group (km^2)	Average drogue speed ($cm\ s^{-1}$)	Average wind speed* (kn)
8-30-74	Flood	14.2-15.8	.741	.612	32.8	5.9
8-31-74	"	13.1-16.3	.366	8.75	18.1	5.3
9- 1-74	"	12.8-16.9	.816	4.99	19.1	6.7
9- 2-74	"	13.7-17.4	.288	3.42	23.4	7.0
2-25-75	"	14.8-16.8	.0644	.418	27.3	15.0
9- 3-74	Ebb	8.2- 9.5	.411	.501	29.0	7.8
2-26-75	"	9.0-11.2	.0775	.496	37.8	14.1
2-27-75	"	8.8-11.7	.0685	.254	36.7	5.7
2-28-75	"	8.8-11.2	.166	.471	42.9	12.4
3- 1-75	"	9.3-13.0	.124	2.49	36.1	7.7
3- 2-75	"	9.9-13.6	.340	.443	42.4	20.1
3- 3-75	"	9.8-15.0	.175	.621	46.9	16.9
9- 3-74	Slack	13.2-14.1	.256	.806	18.8	7.8
2-28-75	"	13.7-15.8	.137	.254	17.9	12.4
2-26-75	Shilshole flood	15.5-17.3	.0868	.241	17.0	14.1
2-27-75	Flood eddy	14.8-18.3	.0382	.206	13.5	5.7

* 24 hour averages. Summer values from Sea-Tac airport. Winter values from UW weather station at West Point (courtesy of E. E. Collias).

Table 2. Average centroid speed and properties of the mean flow and eddies larger than drogue groups.

Date	Tidal phase	Centroid speed (cm s^{-1}) mean	std. dev.	Horizontal divergence (10^{-4} s^{-1}) mean	std. dev.	Relative vorticity (10^{-4} s^{-1}) mean	std. dev.
8-30-74	Flood	32.8	2.10	-.535	1.72	-4.33	.908
8-31-74	"	18.1	6.60	2.89	2.93	1.96	1.41
9-1 -74	"	19.1	3.39	1.21	.178	-.566	1.09
9-2 -74	"	23.4	6.91	1.29	1.81	1.52	.703
2-25-75	"	27.3	11.0	2.43	.739	1.04	1.48
9-3 -74	Ebb	29.0	3.26	.344	1.06	-1.81	.644
2-26-75	"	37.8	4.66	1.83	1.77	3.16	2.74
2-27-75	"	36.7	7.63	1.05	1.99	.877	1.72
2-28-75	"	42.9	1.04	1.05	1.13	.928	2.07
3-1 -75	"	36.1	4.09	2.17	1.13	-.833	.609
3-2 -75	"	42.4	1.37	.279	.989	-.747	.626
3-3 -75	"	46.9	7.18	.764	.858	-.290	.567
9-3 -74	Slack	18.8	2.15	4.96	2.38	1.72	1.84
2-28-75	"	17.9	8.05	.633	1.25	-2.58	1.89
2-26-75	Shilshole flood	17.0	6.06	1.52	3.55	-.924	2.38
2-27-75	Flood eddy	13.5	6.56	1.11	3.78	.144	2.88

Table 2. Cont'd.

Date	Tidal phase	Stretching deformation (10^{-4} s^{-1}) mean	std. dev.	Shearing deformation (10^{-4} s^{-1}) mean	std. dev.	No. of data points
8-30-74	Flood	-.474	1.52	-.724	.928	13
8-31-74	"	-.309	3.30	-.876	1.07	29
9-1 -74	"	.748	.538	-.240	1.30	38
9-2 -74	"	.0781	1.93	-.116	1.17	34
2-25-75	"	.115	2.15	.326	1.26	17
9-3 -74	Ebb	.484	.354	-3.70	.755	10
2-26-75	"	4.40	2.88	1.07	1.56	19
2-27-75	"	1.14	3.98	1.52	2.64	26
2-28-75	"	-.767	2.79	-1.67	2.18	21
3-1 -75	"	.0881	.361	.531	.357	34
3-2 -75	"	.554	.920	.675	1.09	34
3-3 -75	"	.419	.591	-.282	1.57	51
9-3 -74	Slack	-.756	1.44	-1.76	2.75	6
2-28-75	"	-.566	.838	.972	1.57	18
2-26-75	Shilshole Flood	-1.80	3.33	2.49	2.96	15
2-27-75	Flood eddy	-1.17	6.56	.123	2.72	32

Table 3. Horizontal eddy diffusivity and mean division between large and small scale eddies.

Date	Tidal phase	Horizontal eddy diffusivity (10^4 cm^2 s^{-1})	Mean division* between large and small scale eddies (km)	No. of data points
8-30-74	Flood	.711	.836	13
8-31-74	"	9.23	1.63	29
9-1 -74	"	4.78	1.64	38
9-2 -74	"	5.58	1.38	34
2-25-75	"	.208	.516	17
9-3 -74	Ebb	.799	.824	10
2-26-75	"	2.08	.680	19
2-27-75	"	.386	.400	26
2-28-75	"	.289	.576	21
3-1 -75	"	.445	1.16	34
3-2 -75	"	.904	.692	34
3-3 -75	"	.494	.584	51
9-3 -74	Slack	2.03	.728	6
2-28-75	"	.221	.472	18
2-26-75	Shilshole Flood	.852	.616	15
2-27-75	Flood eddy	.156	.360	32

*Diameter of drogue group.

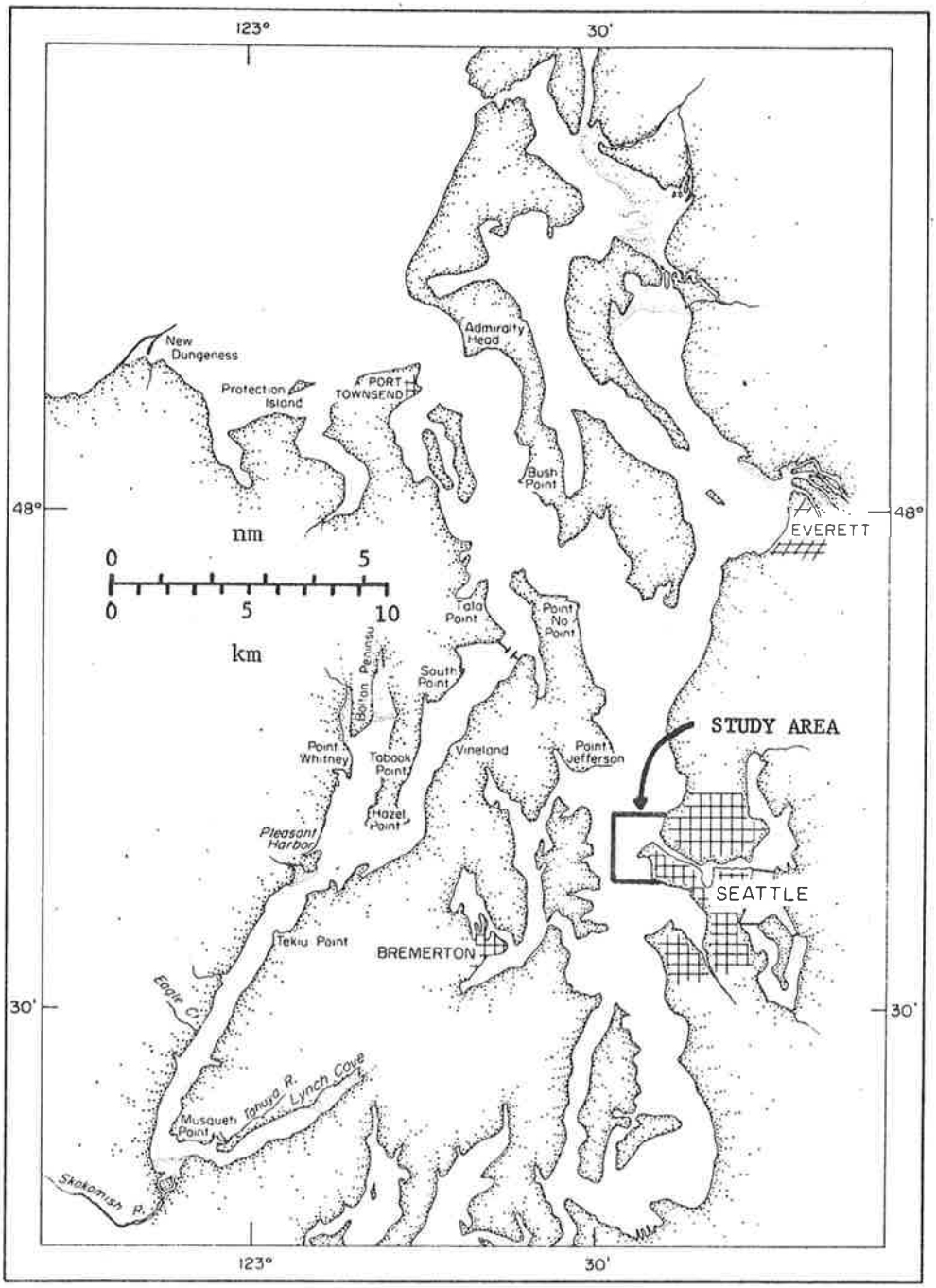

Figure 1. Puget Sound and study area.

Plate I. Photograph of dye injected into Puget Sound Model during flood tide of 27 February 1975. Note eddy in West Point's lee and three patches between Magnolia Bluff and mid-channel. For comparison with corresponding drogue plume and trajectories see Figures 3a3 and 8a3, respectively.

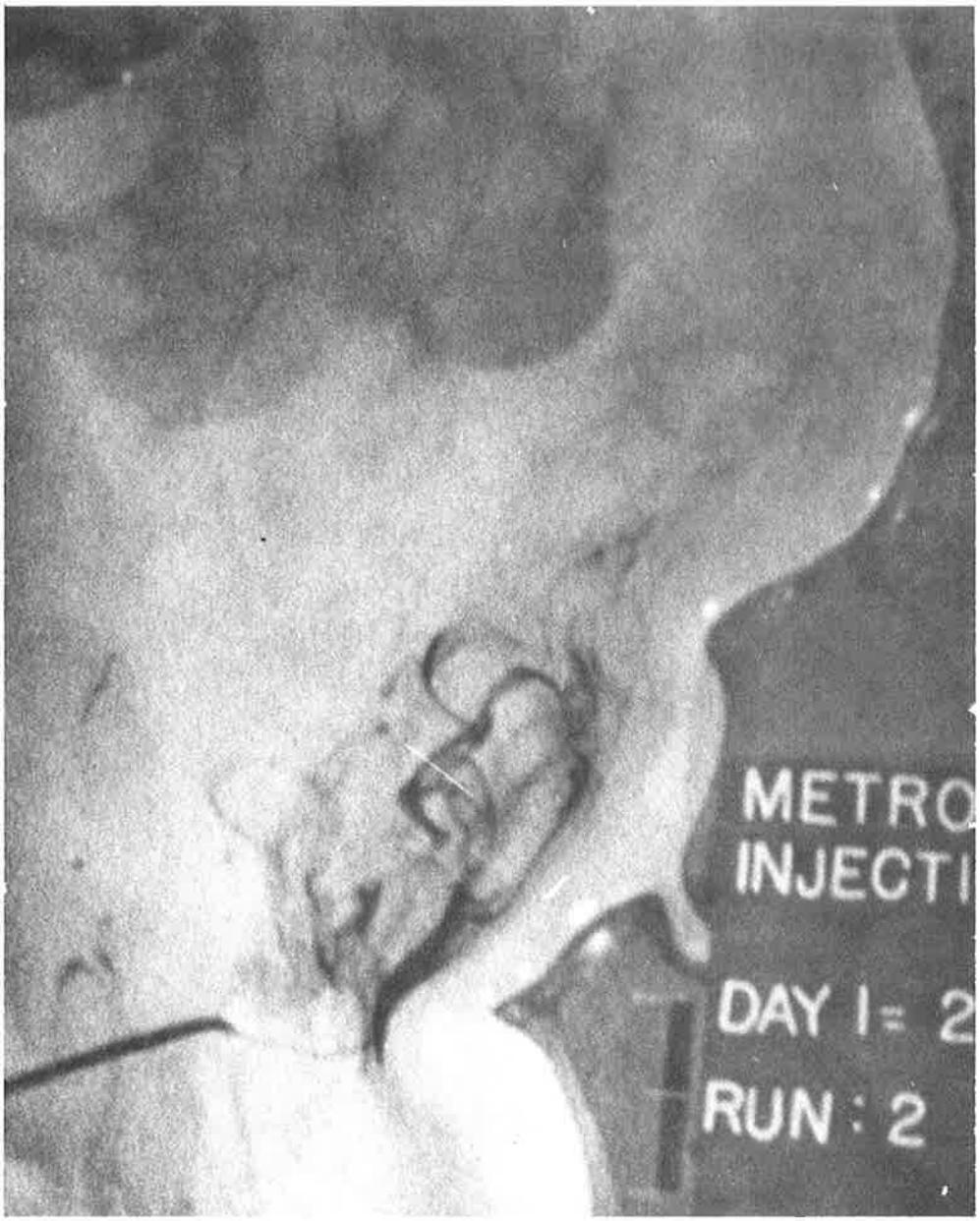

Plate II. Photograph of dye injected into Puget Sound Model during ebb tide of 1 March 1975. For comparison with corresponding drogue plume and trajectories see Figures 3b4 and 8b4, respectively.

ELAPSED TIME (hours) after initial dilution by diffuser

5.0

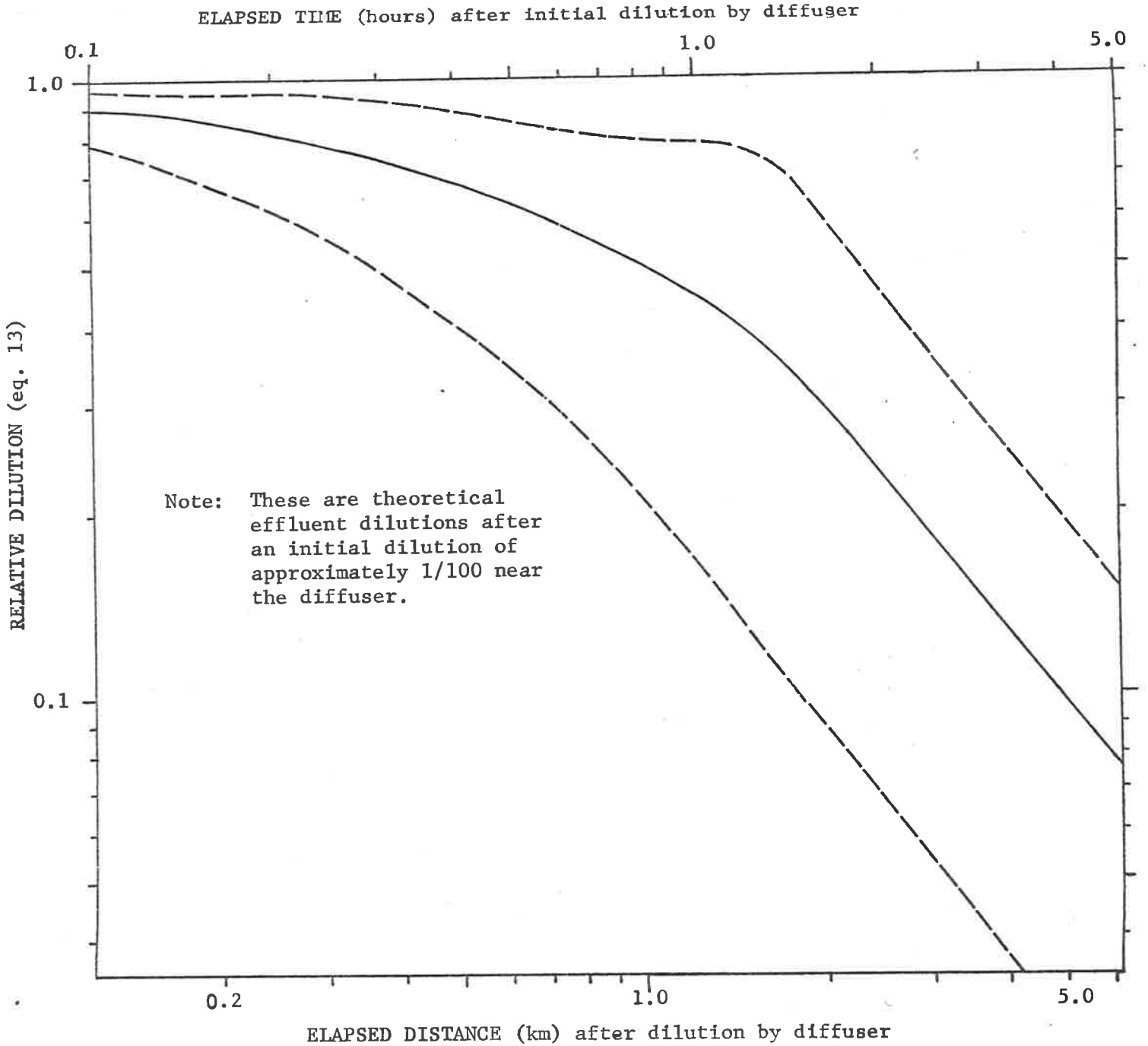

Figure 2a. Average and limits of relative dilution of maximum concentration. Average consists of five flood and seven ebb tides listed in Tables 1-3.

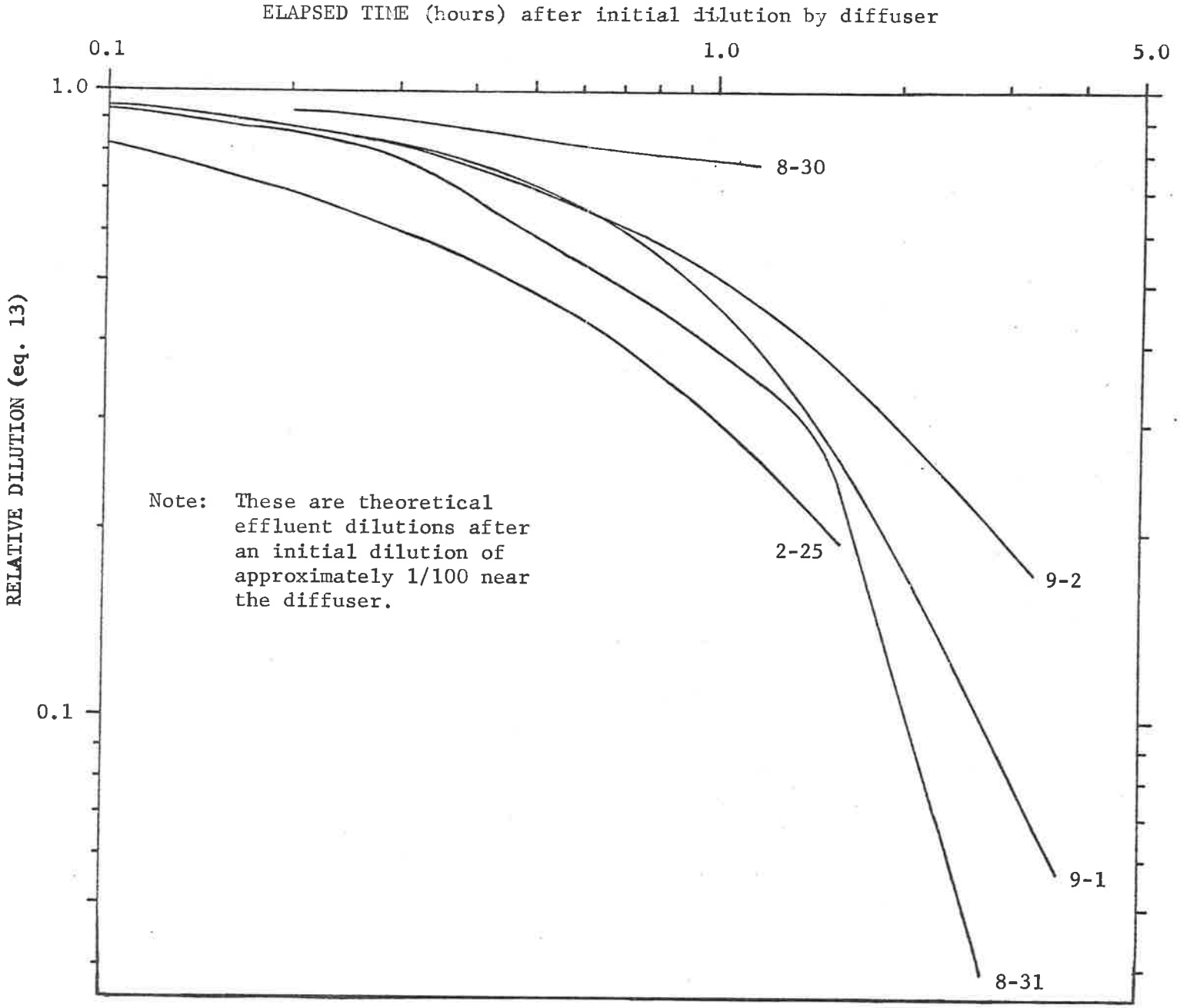

Figure 2b1. Relative dilution of maximum concentration for flood tides versus elapsed time.

ELAPSED DISTANCE (km) after initial dilution by diffuser

Figure 2b1. Relative dilution of maximum concentration for flood tides versus elapsed time.

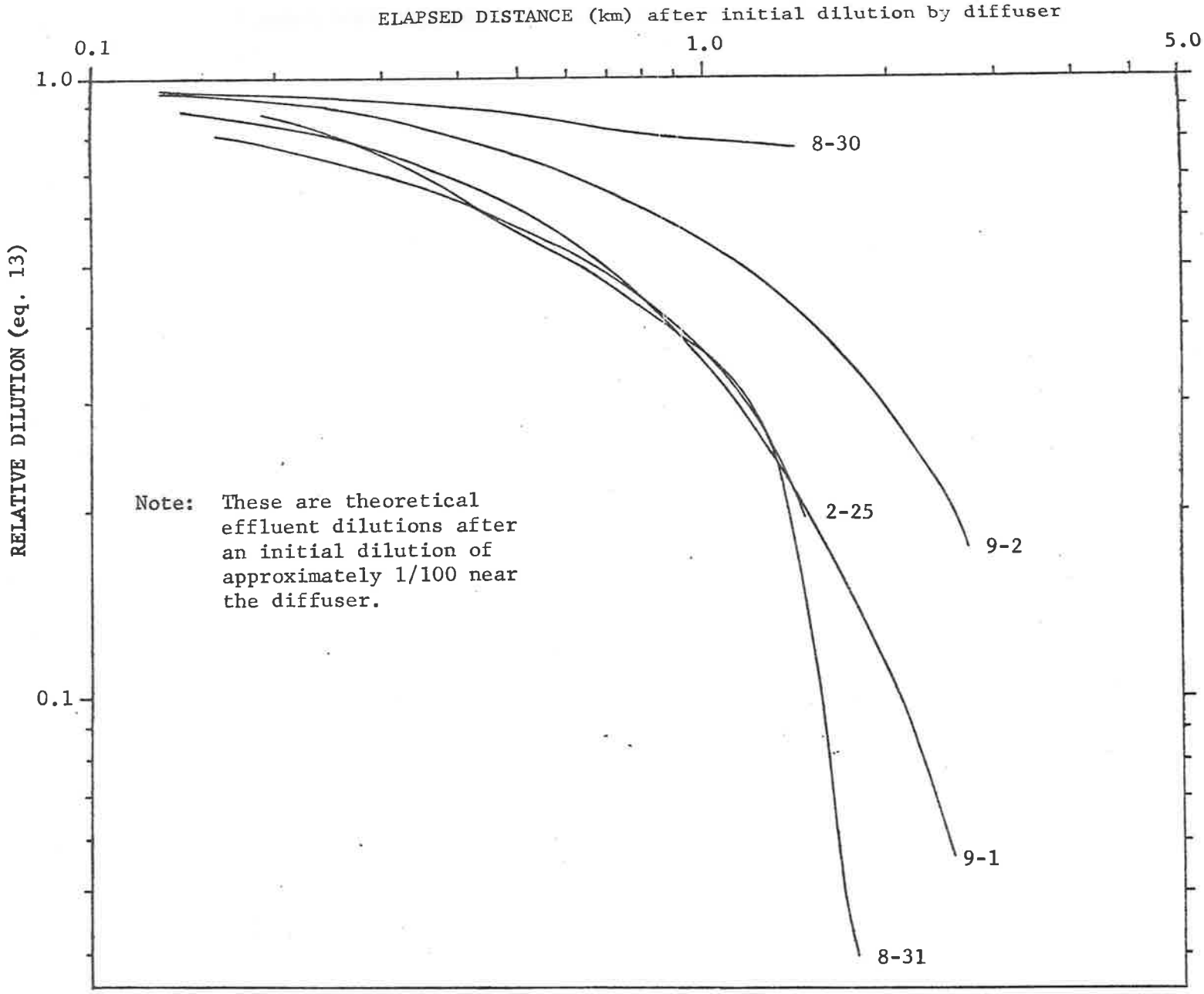

Figure 2b2. Relative dilution of maximum concentration for flood tides versus elapsed distance.

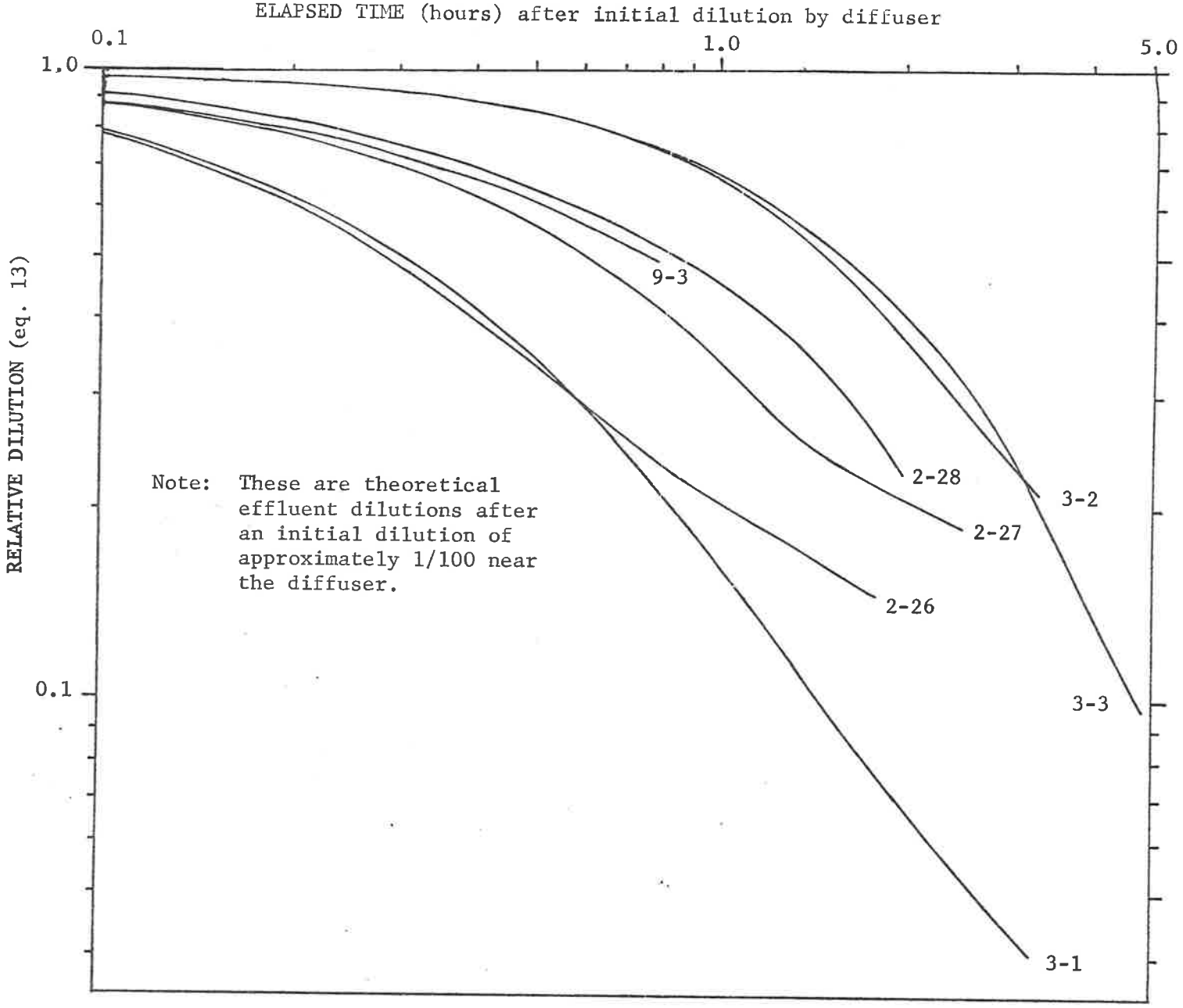

Figure 2c1. Relative dilution of maximum concentration for ebb tides versus elapsed time.

ELAPSED DISTANCE(km) after initial dilution by diffuser

1.0

10.0

Figure 2c1. Relative dilution of maximum concentration for ebb tides versus elapsed time.

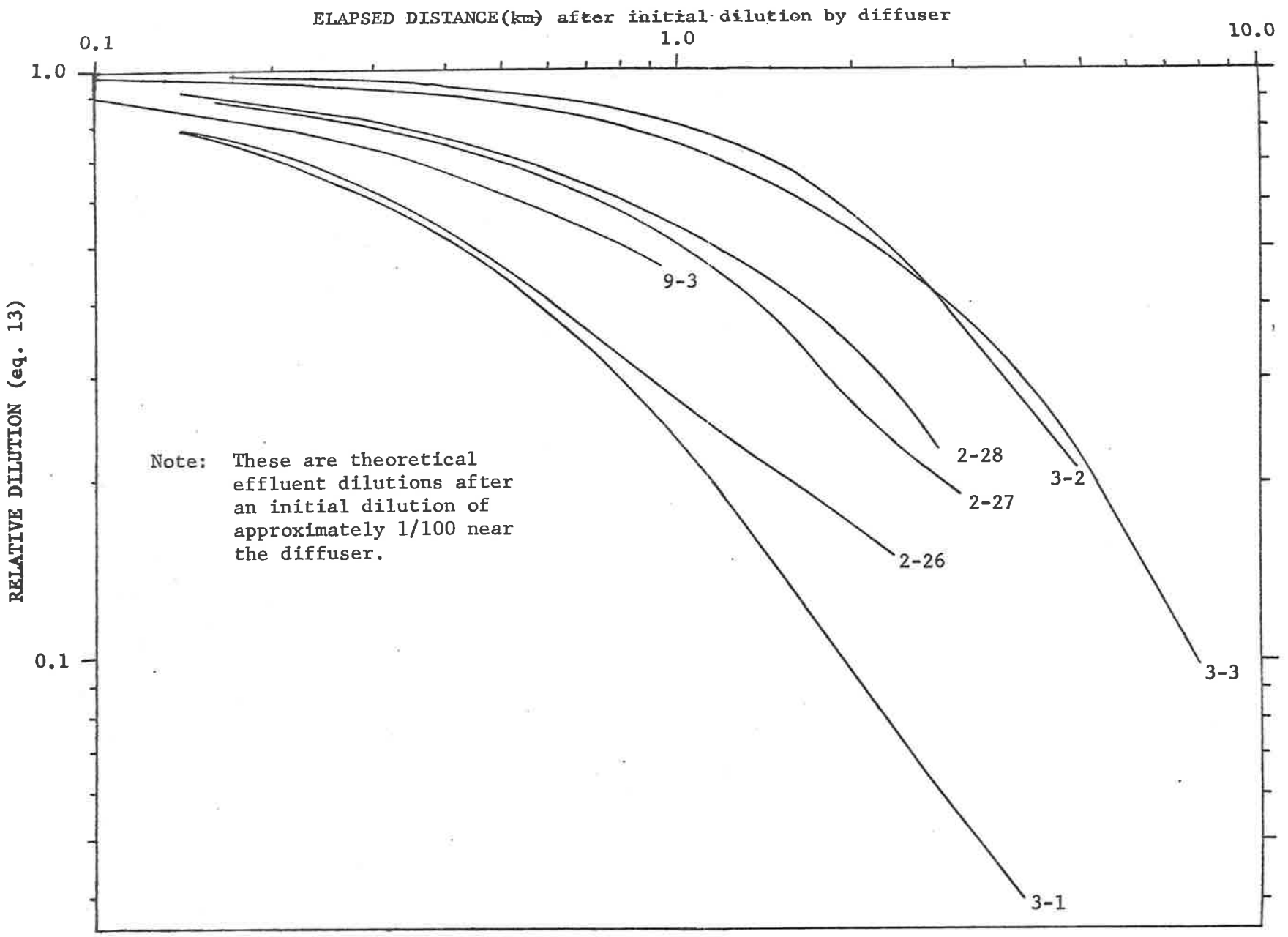

Figure 2c2. Relative dilution of maximum concentration for ebb tides versus elapsed distance.

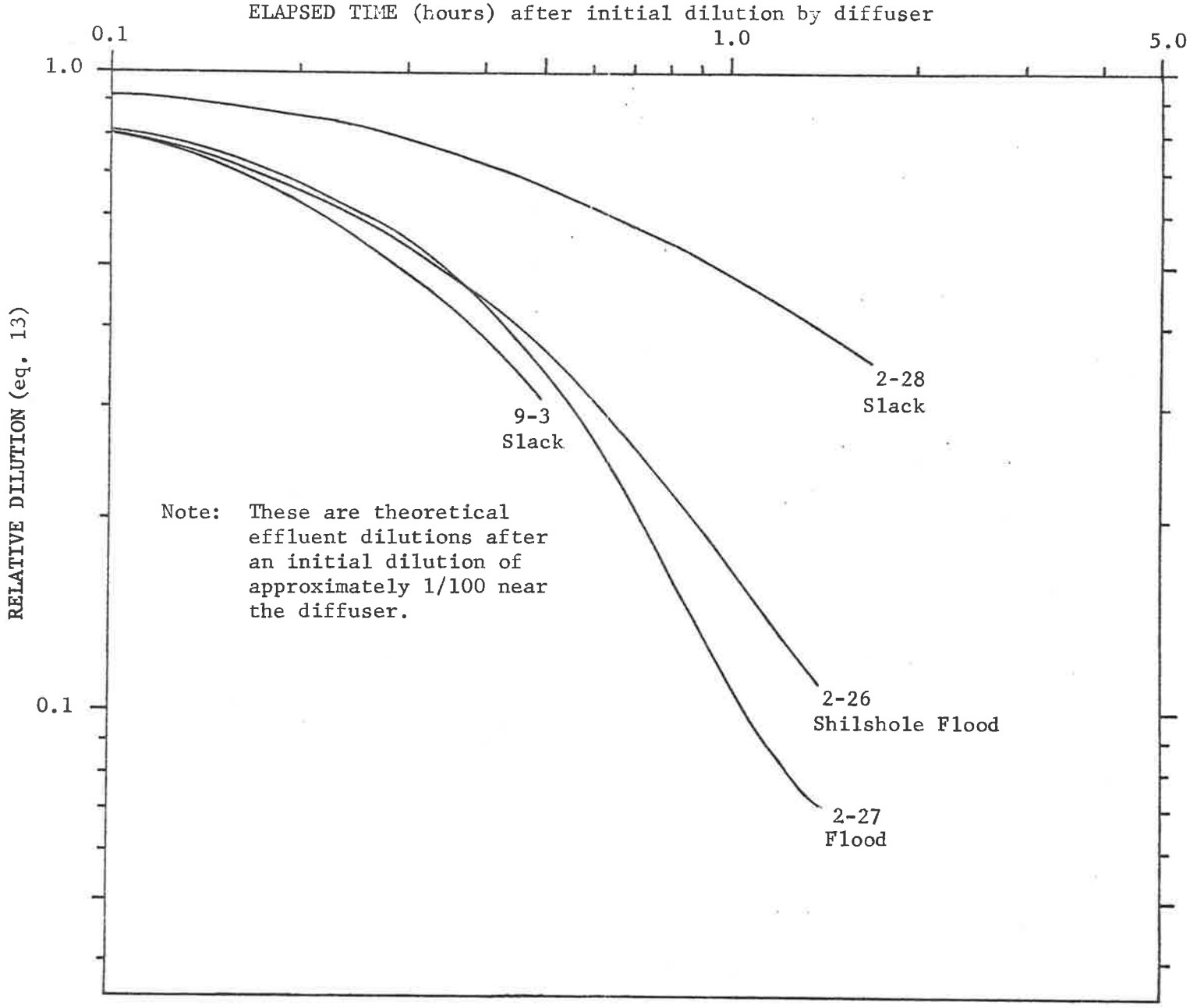

Figure 2d. Relative dilution of maximum concentration for slack tides, Shilshole flood and flood eddy.

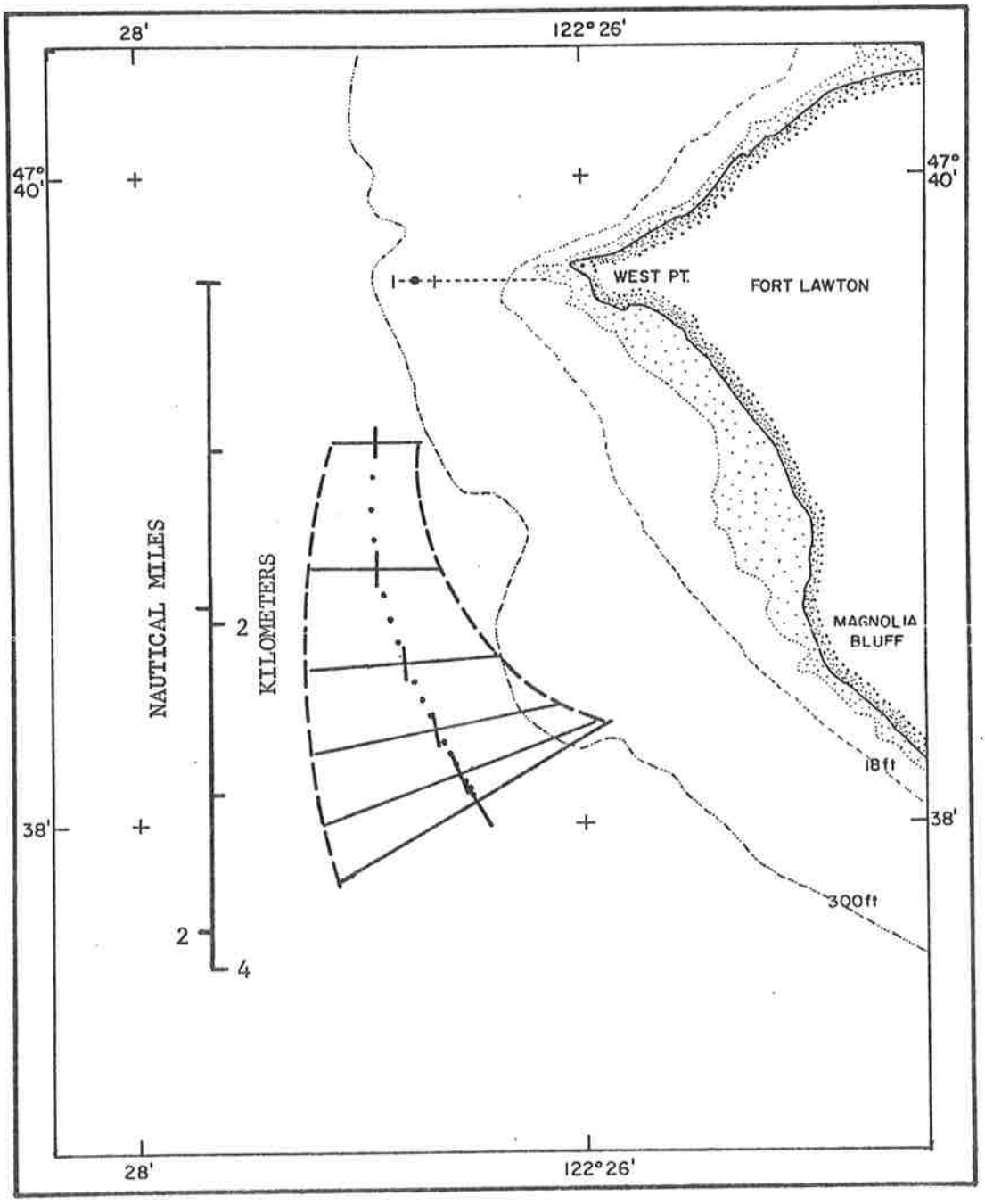

Figure 3a1. Drogue plume (dashed line) for flood tide on 25 February 1975. Dots mark centroid every six minutes. Selected principal axes of drogue areas contain 95% of drogue positions.

Figure 2d. Relative dilution of maximum concentration for slack tides, Shilshole flood and flood eddy.

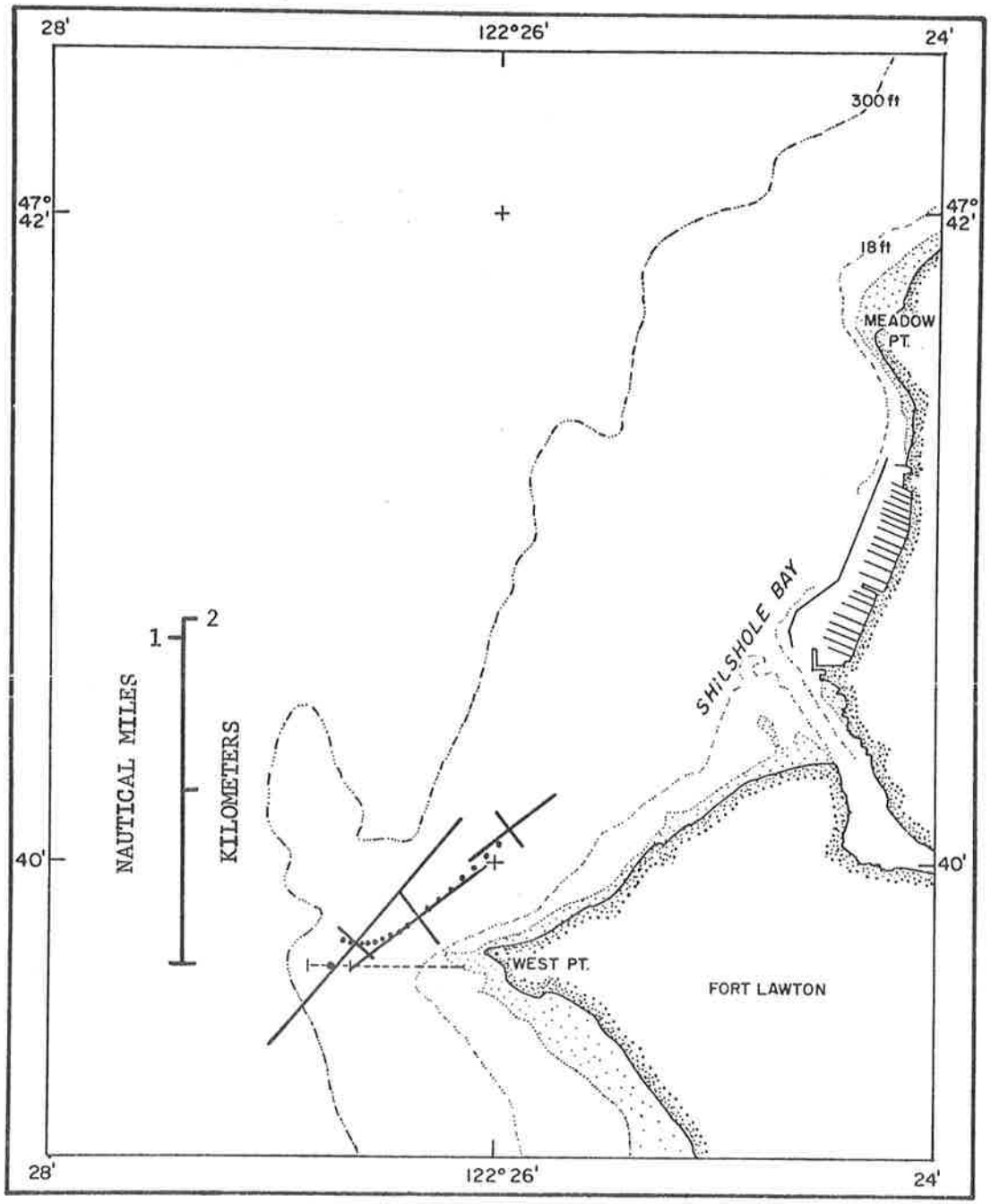

Figure 3a2. Drogue plume for Shilshole flood tide on 26 February 1975. Dots mark centroid every six minutes. Selected principal axes of drogue areas contain 95% of drogue positions.

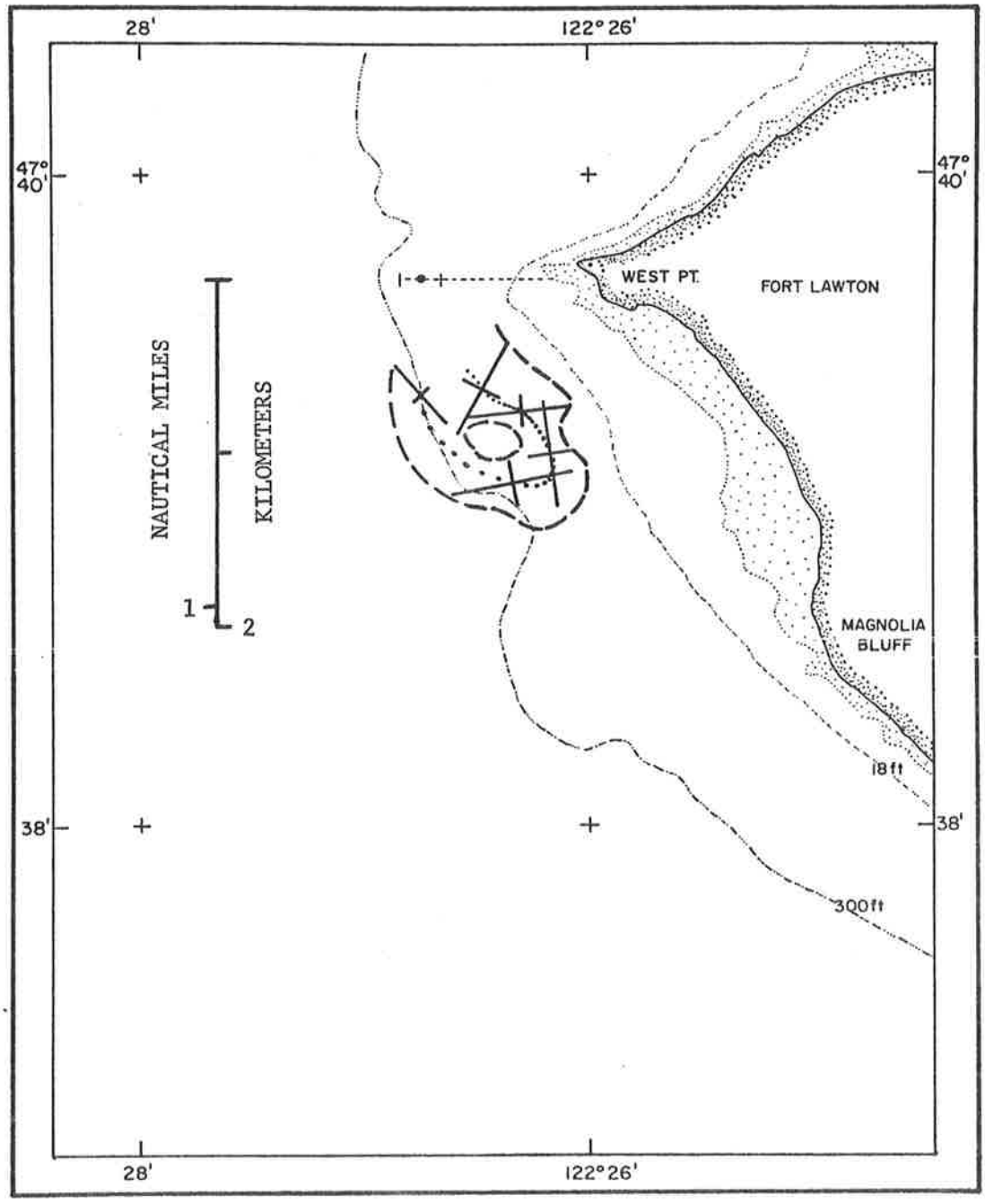

Figure 3a3. Drogue plume (dashed line) for flood eddy on 27 February 1975. Dots mark centroid every six minutes. Selected principal axes of drogue areas contain 95% of drogue positions.

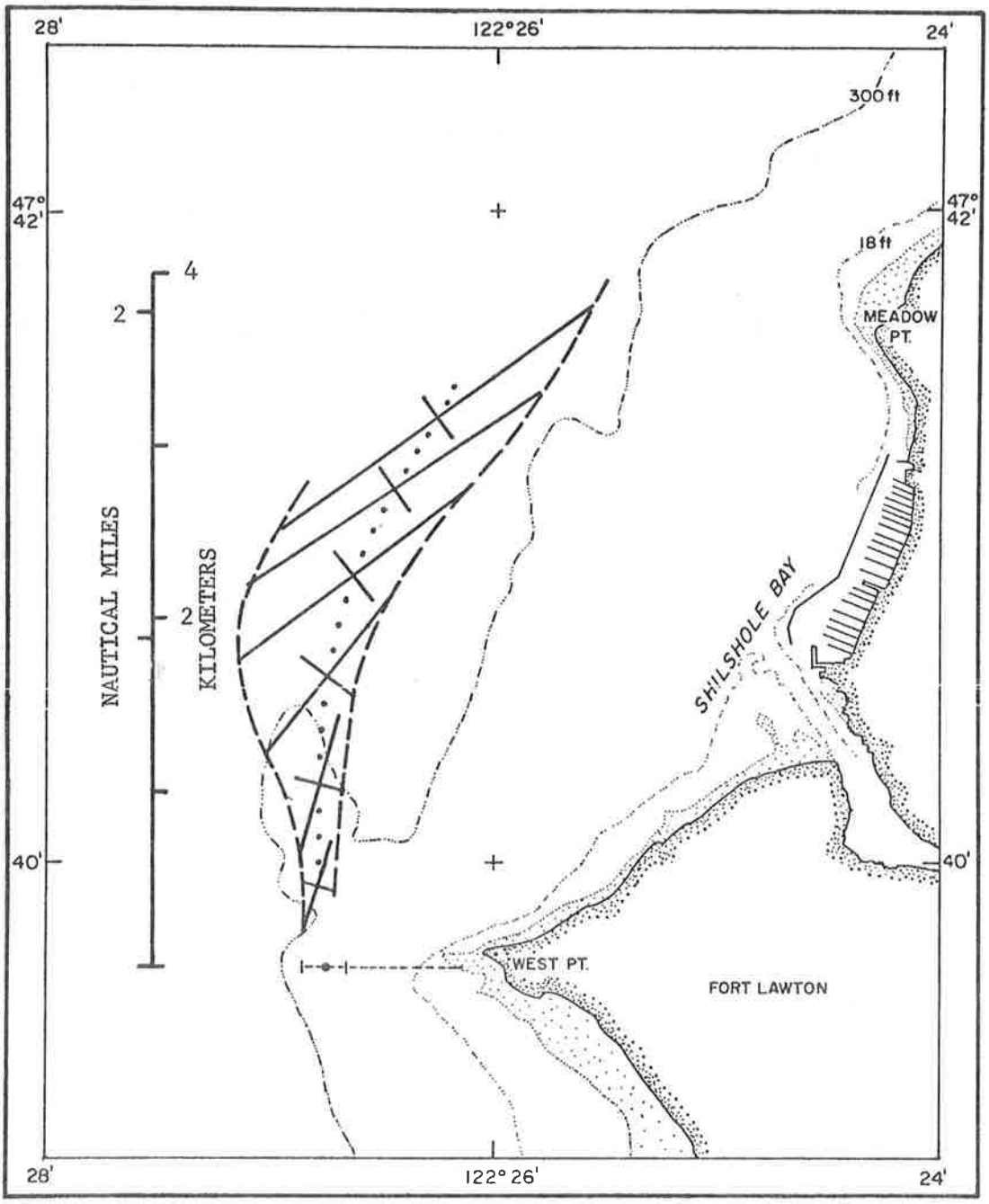

Figure 3b1. Drogue plume (dashed line) for ebb tide on 26 February 1975. Dots mark centroid every six minutes. Selected principal axes of drogue areas contain 95% of drogue positions.

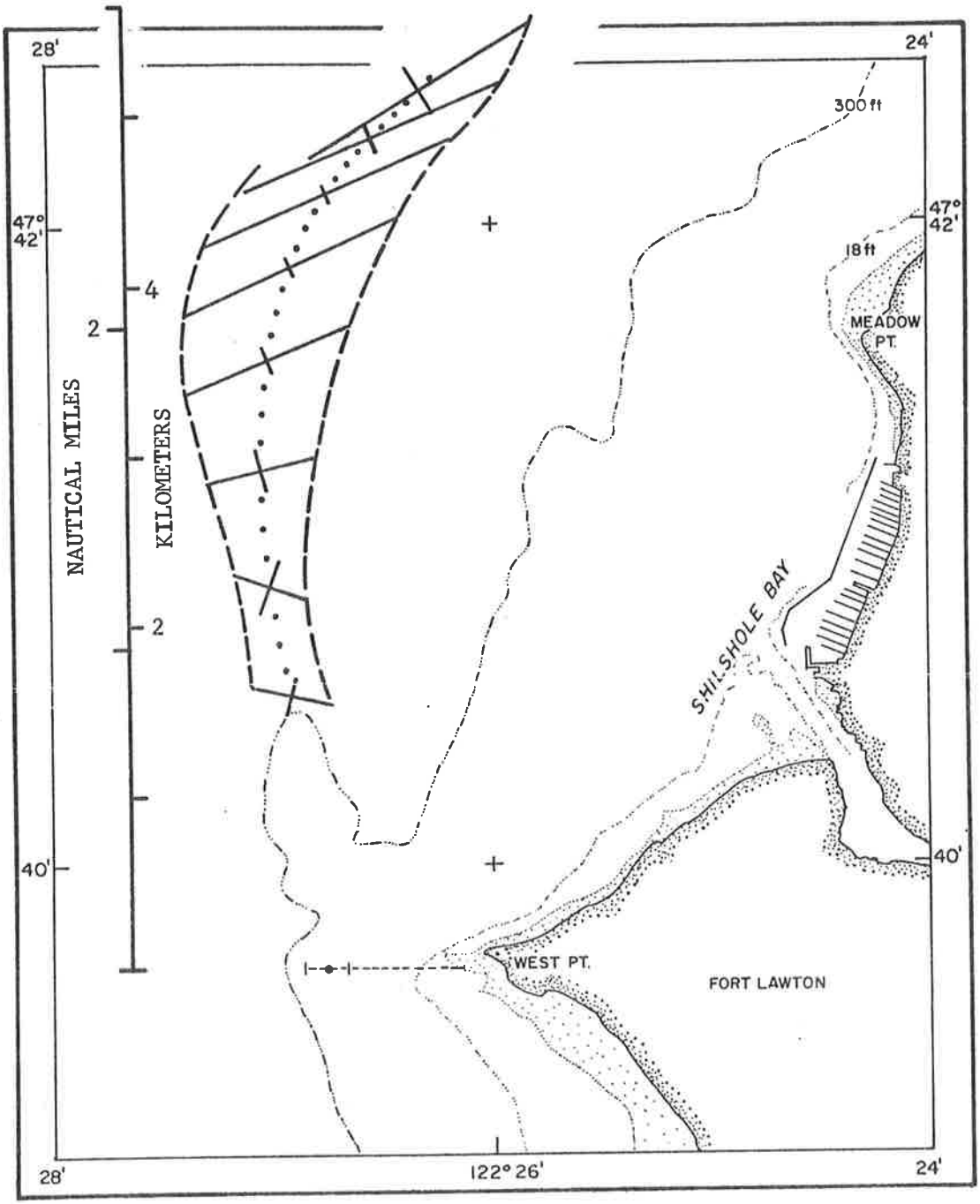

Figure 3b2. Drogue plume (dashed line) for ebb tide on 27 February 1975. Dots mark centroid every six minutes. Selected principal axes of drogue areas contain 95% of drogue positions.

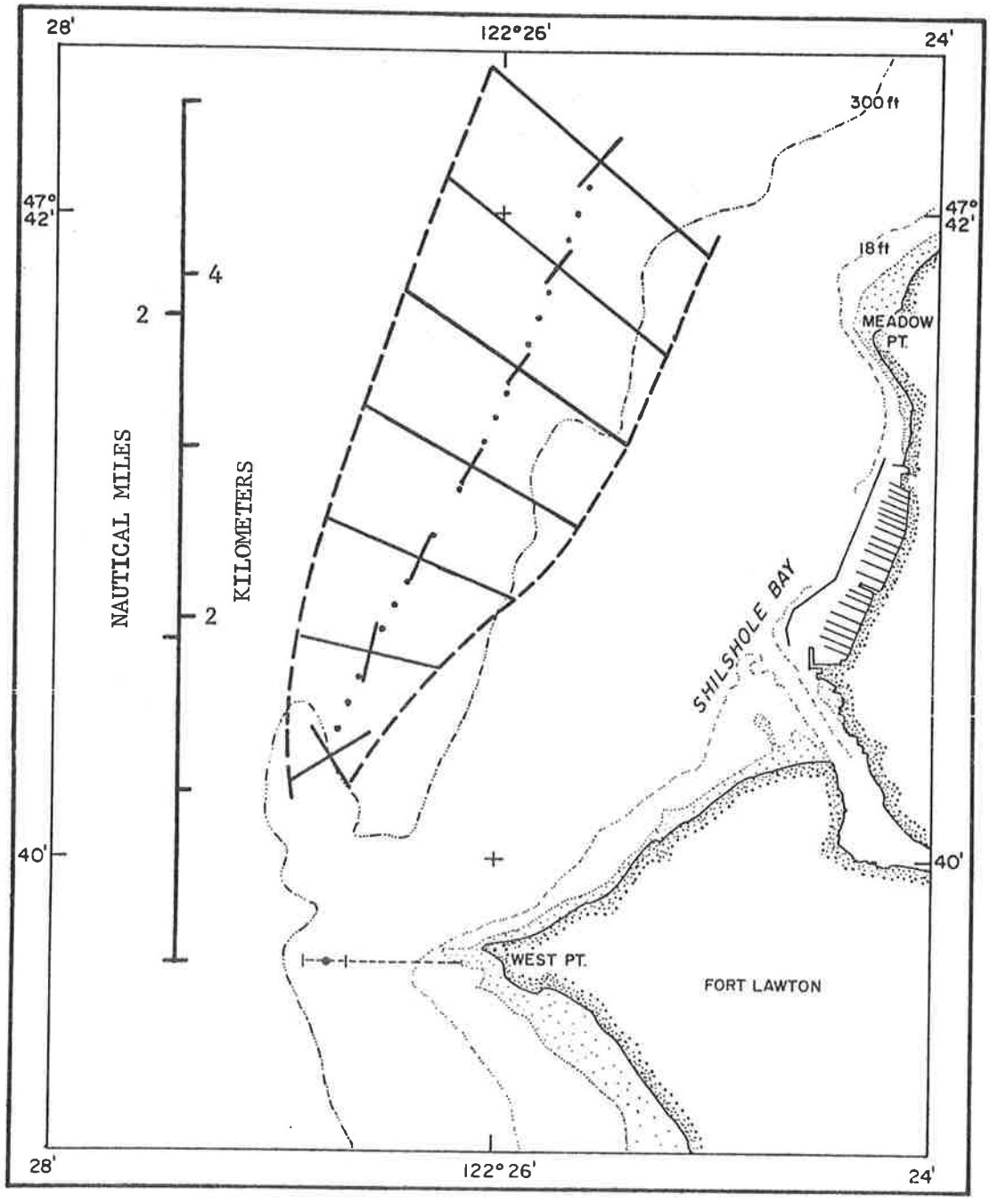

Figure 3b3. Drogue plume (dashed line) for ebb tide on 28 February 1975. Dots mark centroid every six minutes. Selected principal axes of drogue areas contain 95% of drogue positions.

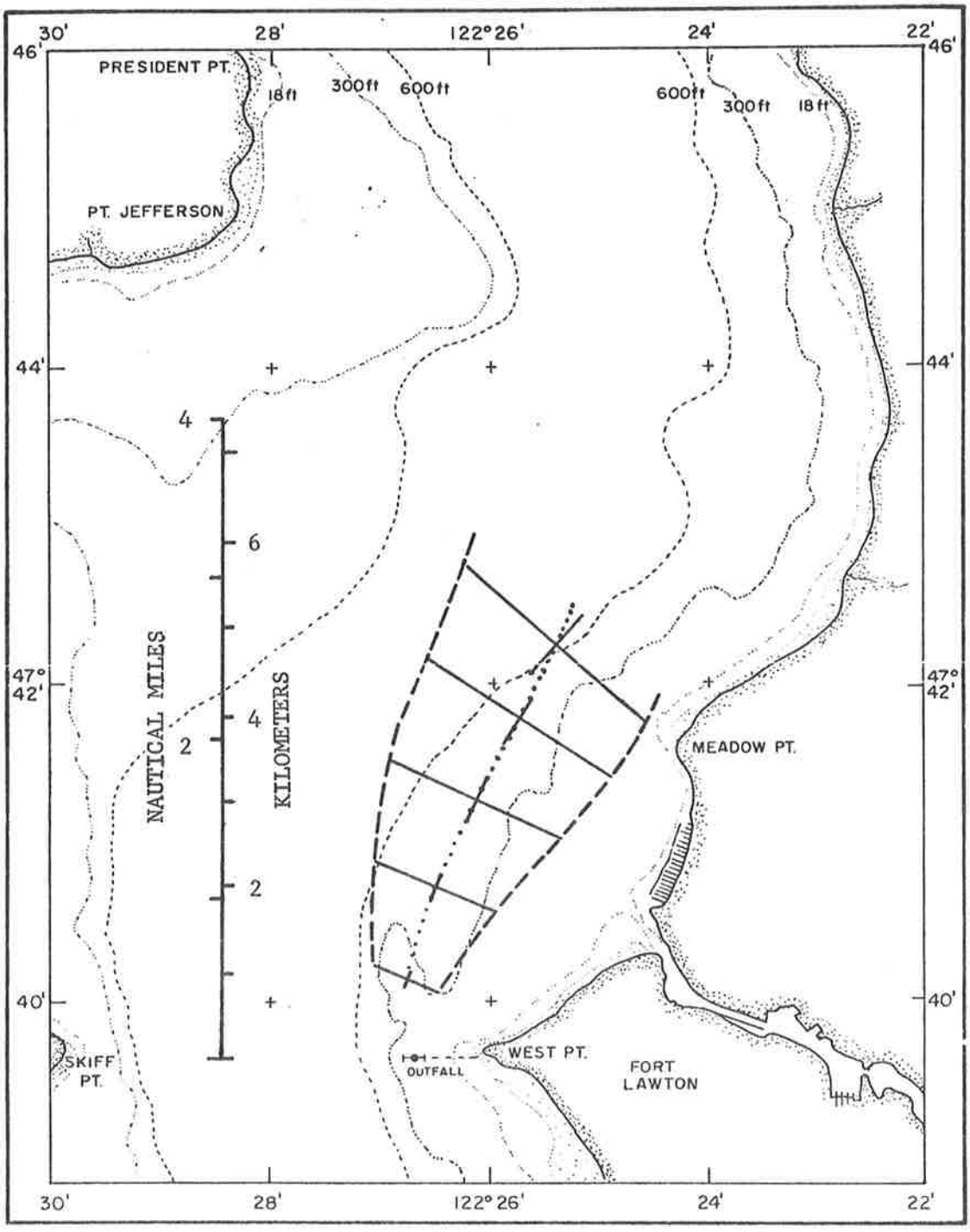

Figure 3b4. Drogue plume (dashed line) for ebb tide on 1 March 1975. Dots mark centroid every six minutes. Selected principal axes of drogue areas contain 95% of drogue positions.

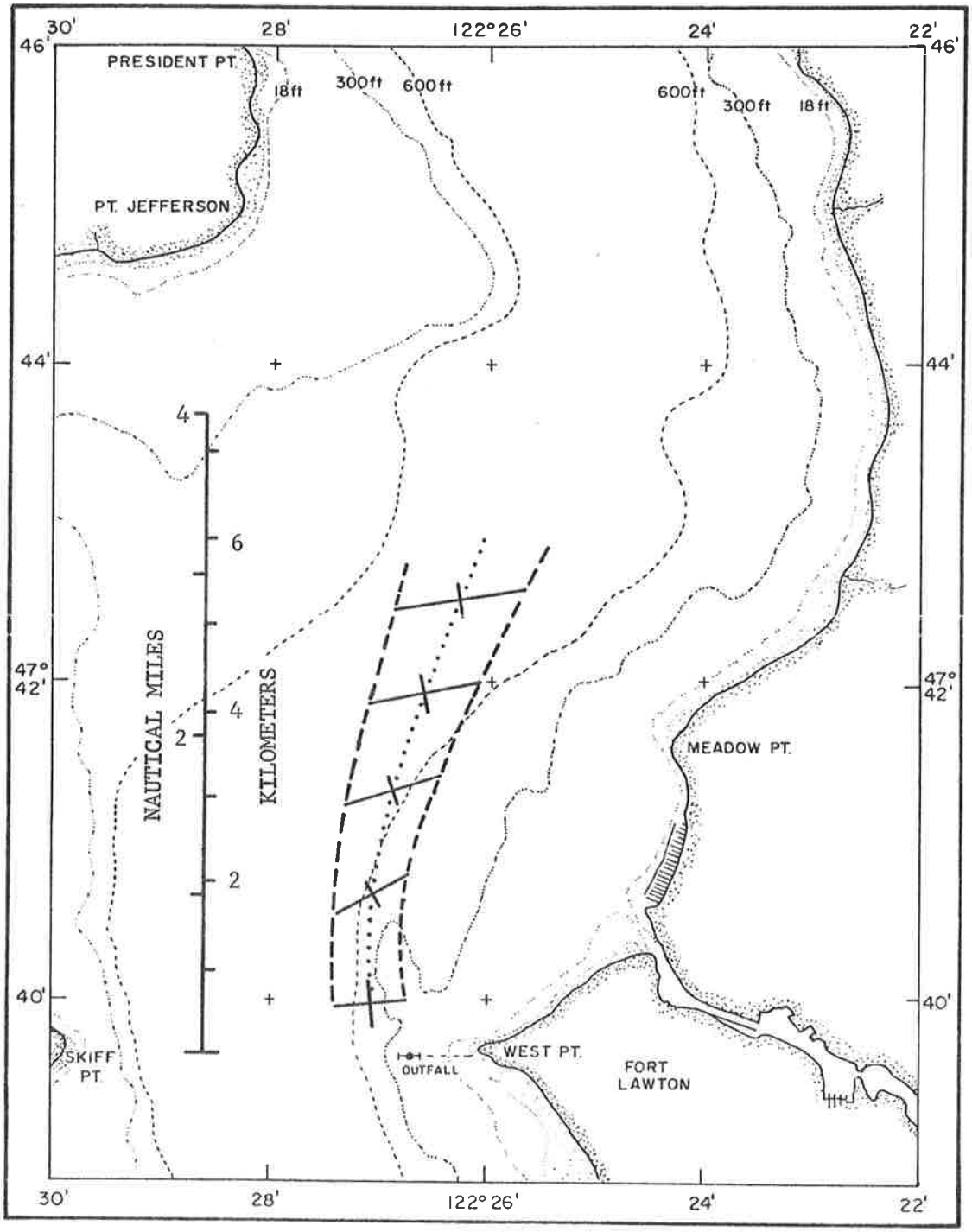

Figure 3b5. Drogue plume (dashed line) for ebb tide on 2 March 1975. Dots mark centroid every six minutes. Selected principal axes of drogue areas contain 95% of drogue positions.

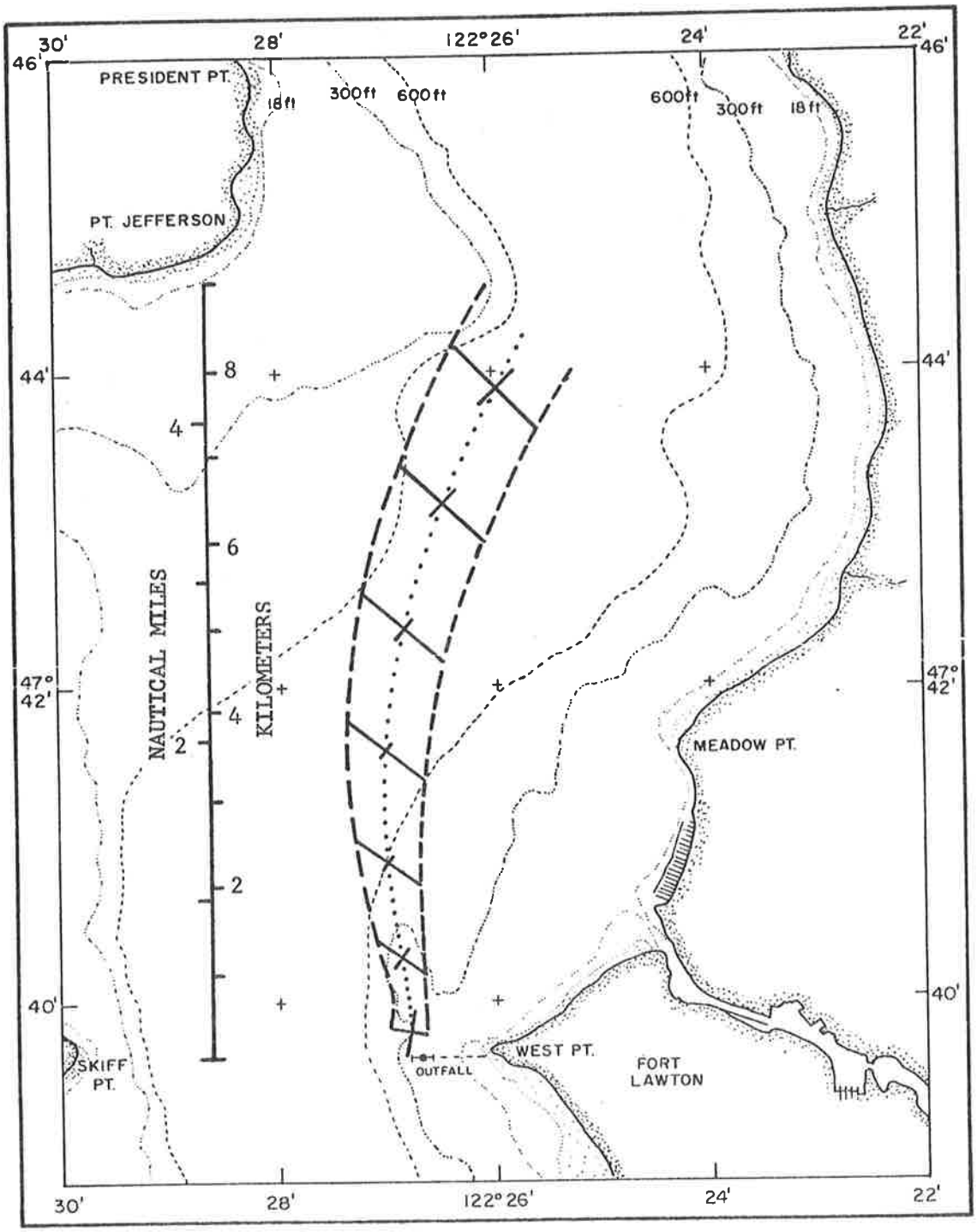

Figure 3b6. Drogue plume (dashed line) for ebb tide on 3 March 1975. Dots mark centroid every six minutes. Selected principal axes of drogue areas contain 95% of drogue positions.

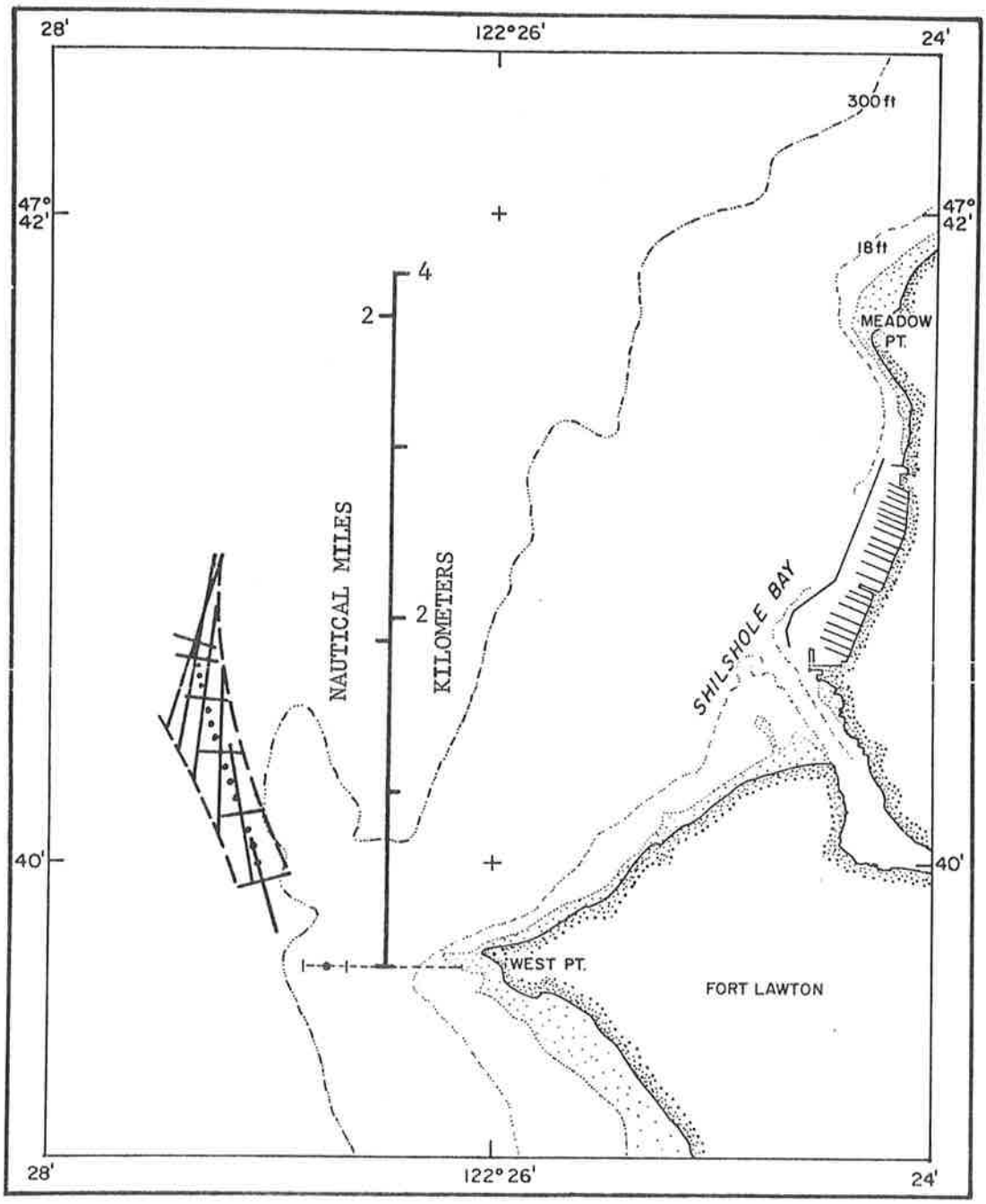

Figure 3c. Drogue plume (dashed line) for slack tide on 28 February 1975. Dots mark centroid every six minutes. Selected principal axes of drogue areas contain 95% of drogue positions.

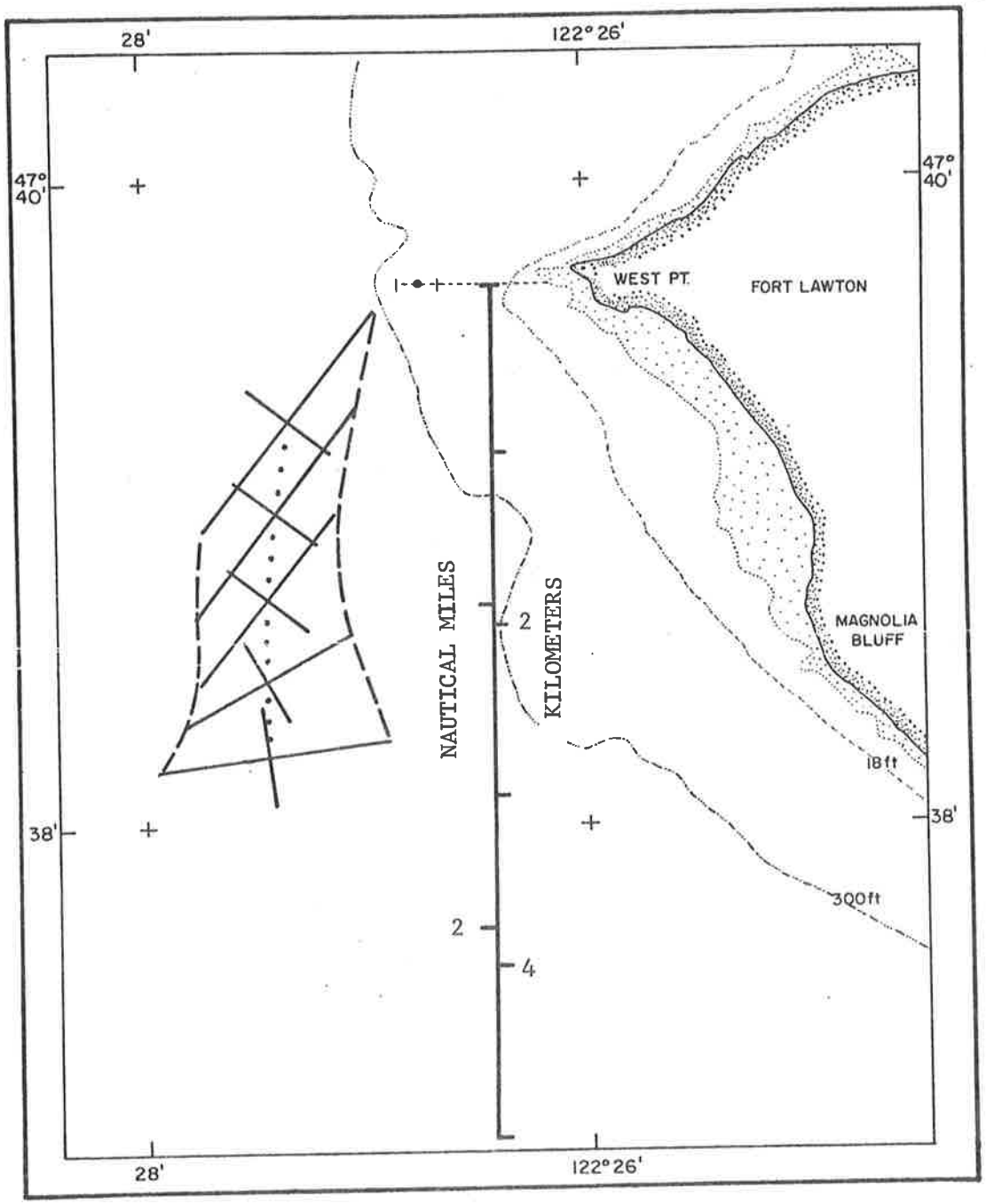

Figure 3d1. Drogue plume (dashed line) for flood tide on 30 August 1974. Dots mark centroid every six minutes. Selected principal axes of drogue areas contain 95% of drogue positions.

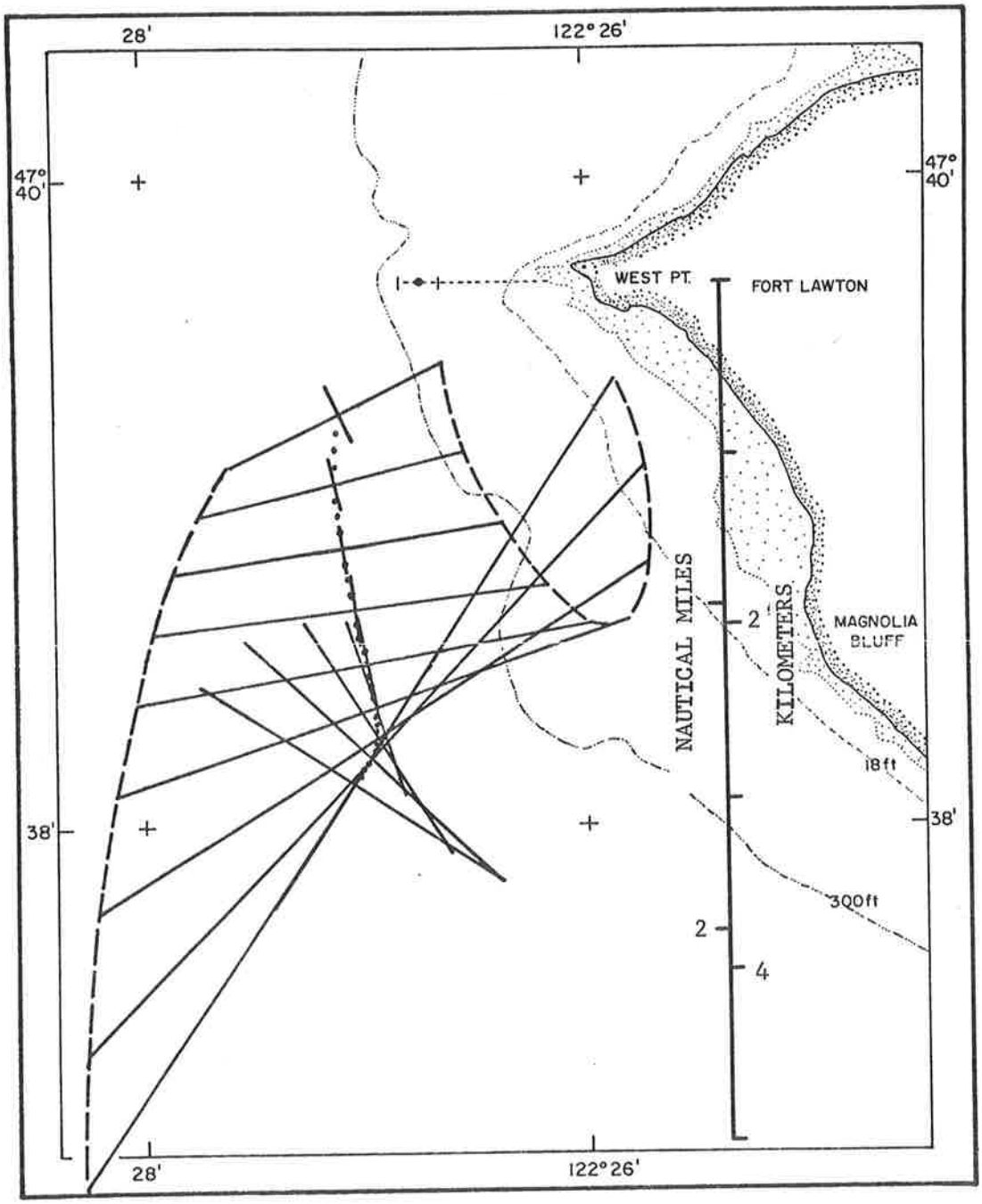

Figure 3d2. Drogue plume (dashed line) for flood tide on 31 August 1974. Dots mark centroid every six minutes. Selected principal axes of drogue areas contain 95% of drogue positions.

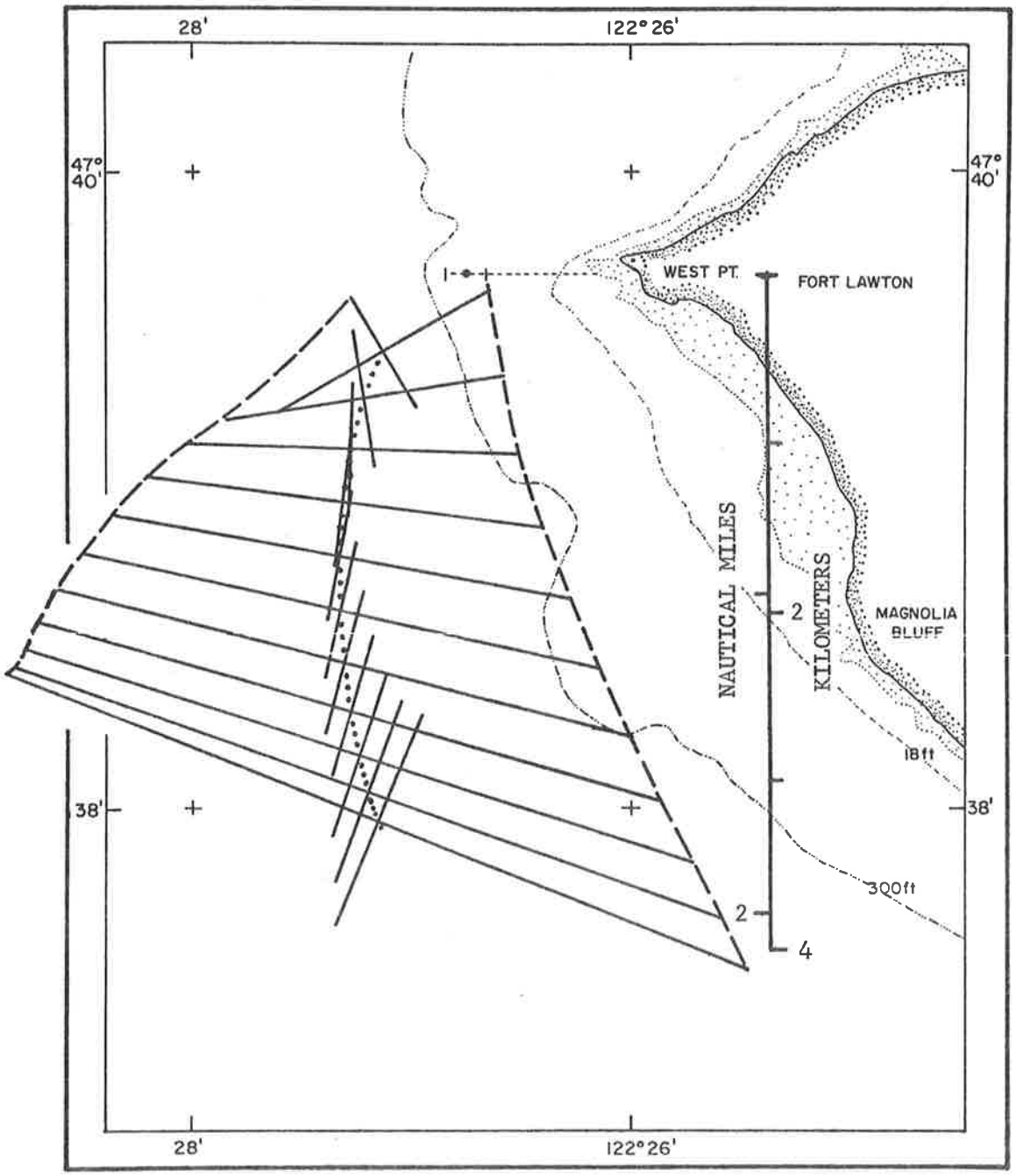

Figure 3d3. Drogue plume (dashed line) for flood tide on 1 September 1974. Dots mark centroid every six minutes. Selected principal axes of drogue areas contain 95% of drogue positions.

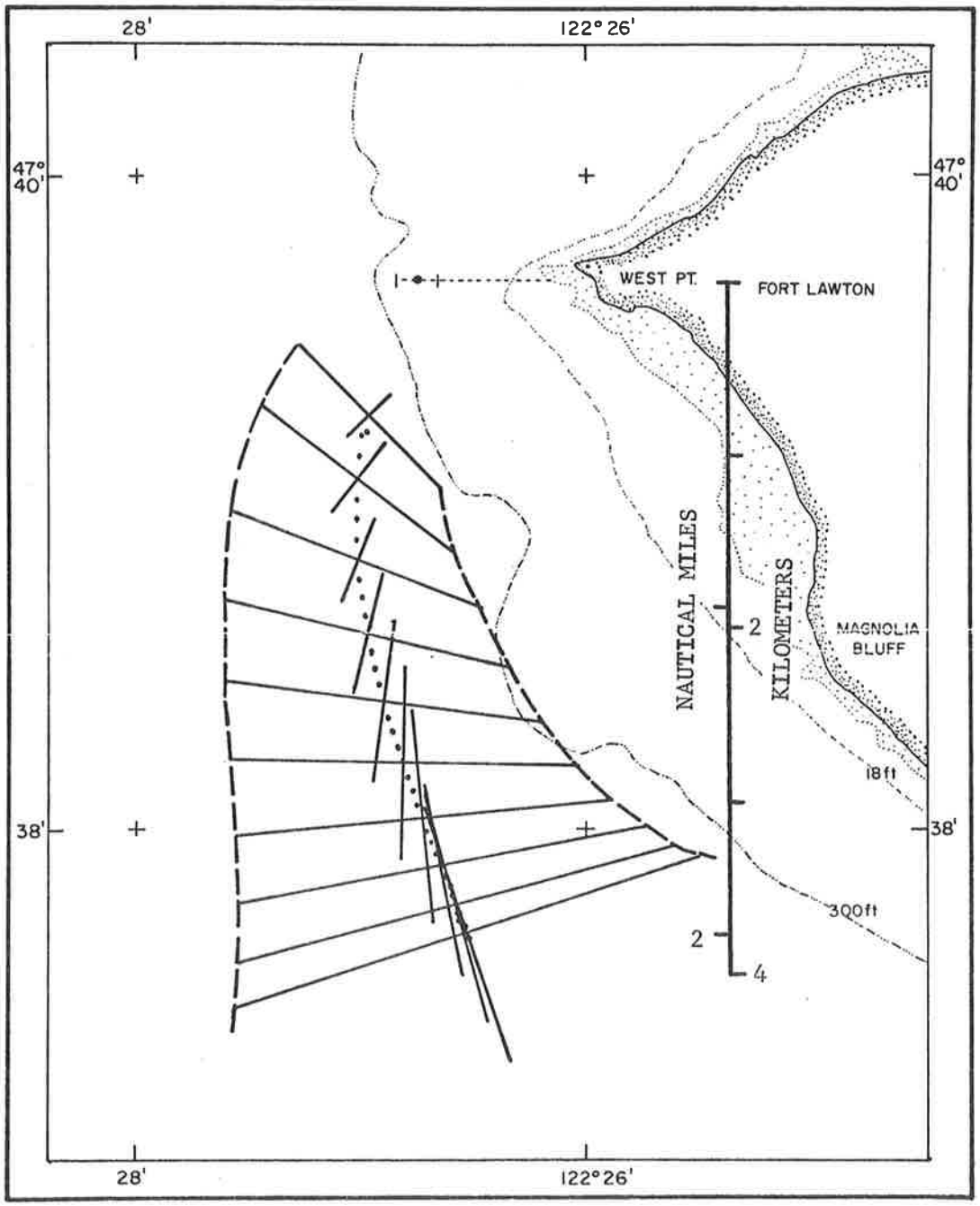

Figure 3d4. Drogue plume (dashed line) for flood tide on 2 September 1974. Dots mark centroid every six minutes. Selected principal axes of drogue areas contain 95% of drogue positions.

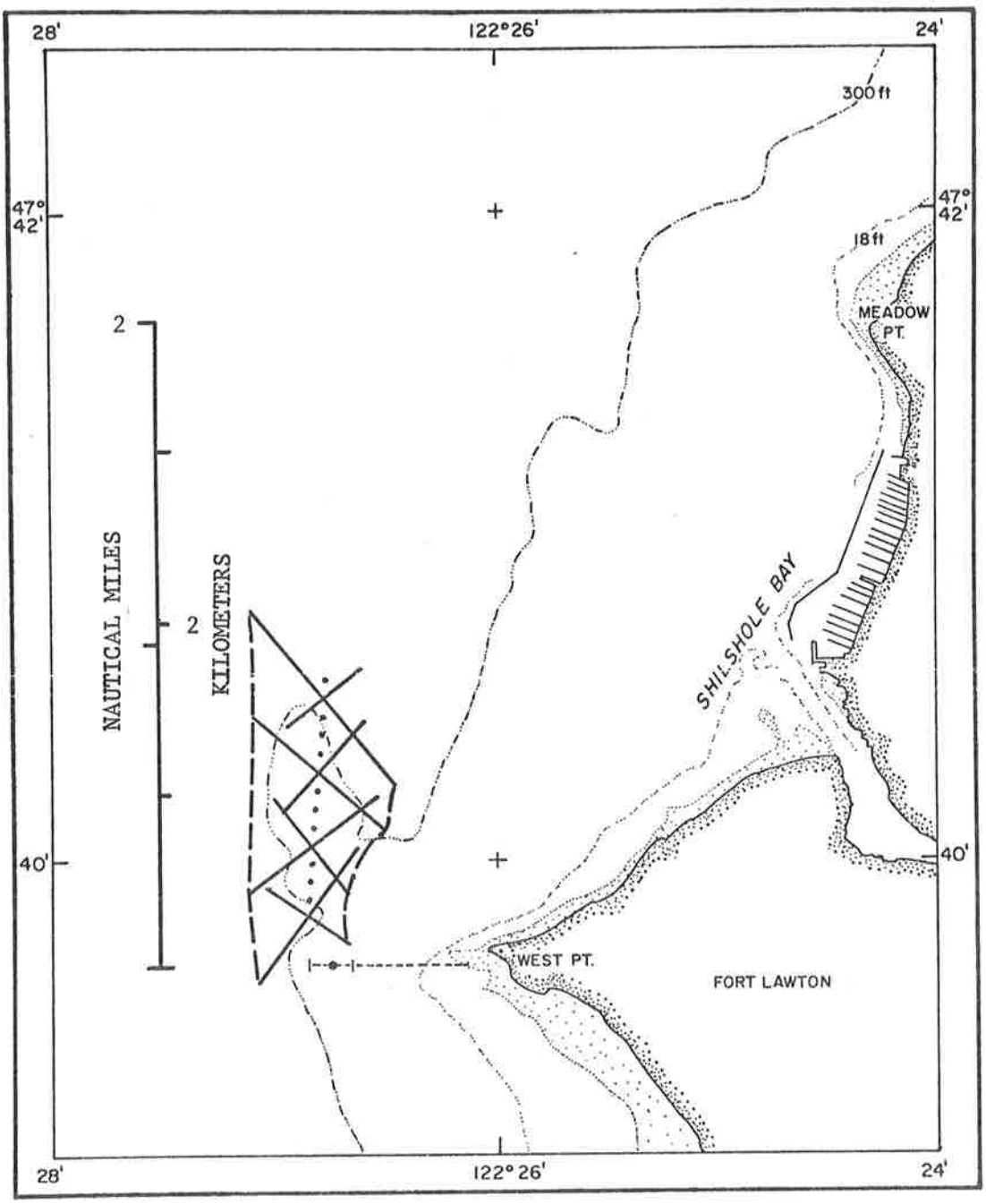

Figure 3e. Drogue plume (dashed line) for ebb tide on 3 September 1974. Dots mark centroid every six minutes. Selected principal axes of drogue areas contain 95% of drogue positions.

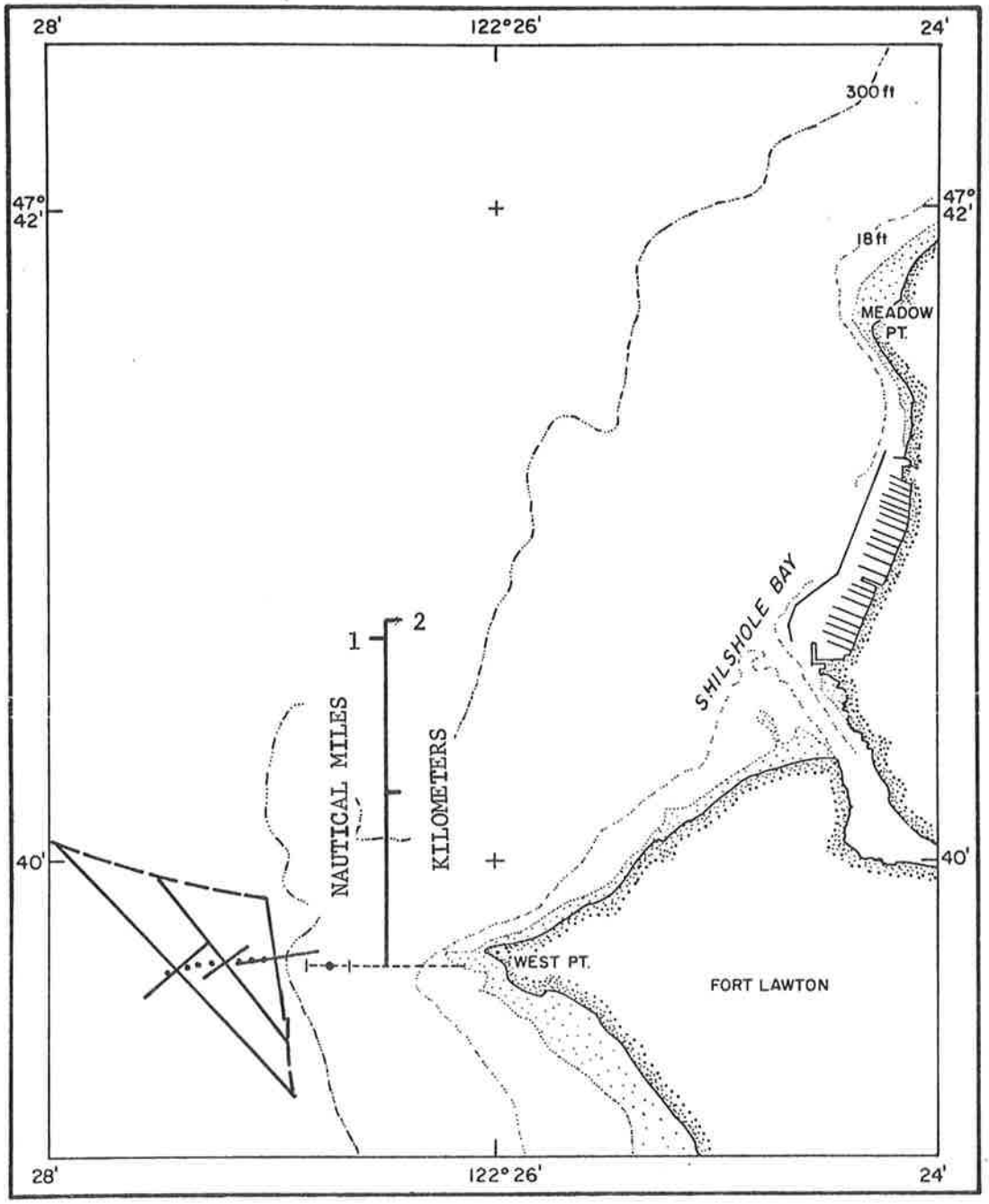

Figure 3f. Drogue plume (dashed line) for slack tide on 3 September 1974. Dots mark centroid every six minutes. Selected principal axes of drogue areas contain 95% of drogue positions.

II. Introduction

This study is designed to provide a quantitative description of currents and associated mixing in support of concurrent observations of dye pumped continuously from the West Point sewage outfall. The observations of dye concentration were performed under a separate contract to APL. In that study rhodamine B* dye was continuously injected into sewage within the treatment plant located close onshore at West Point. The sewage and dye enter Puget Sound approximately 1100 m west of West Point at a nominal depth of 73 m. The combined effluent rises to an intermediate depth controlled primarily by prevailing density structure. The resulting vertical and horizontal dye distribution was observed by APL using a towed instrument package. Preliminary analysis of those observations on board ship showed that 50 m approximated the depth of maximum dye concentration in summer, and 20 m in winter. Groups of drogues (usually seven) were then placed at those depths near the beginning of major flood and ebb tidal phases (Table 1 and Figure 4).

III. Methods

A. Drogue design

A drogue may be defined as a device which is theoretically free to follow currents. Practical considerations often result in a drogue which rides at a fixed depth by suspension from a surface float. Optimum design maximizes current drag on the drogue relative to drag on its

*A fluorescent bluish red dye.

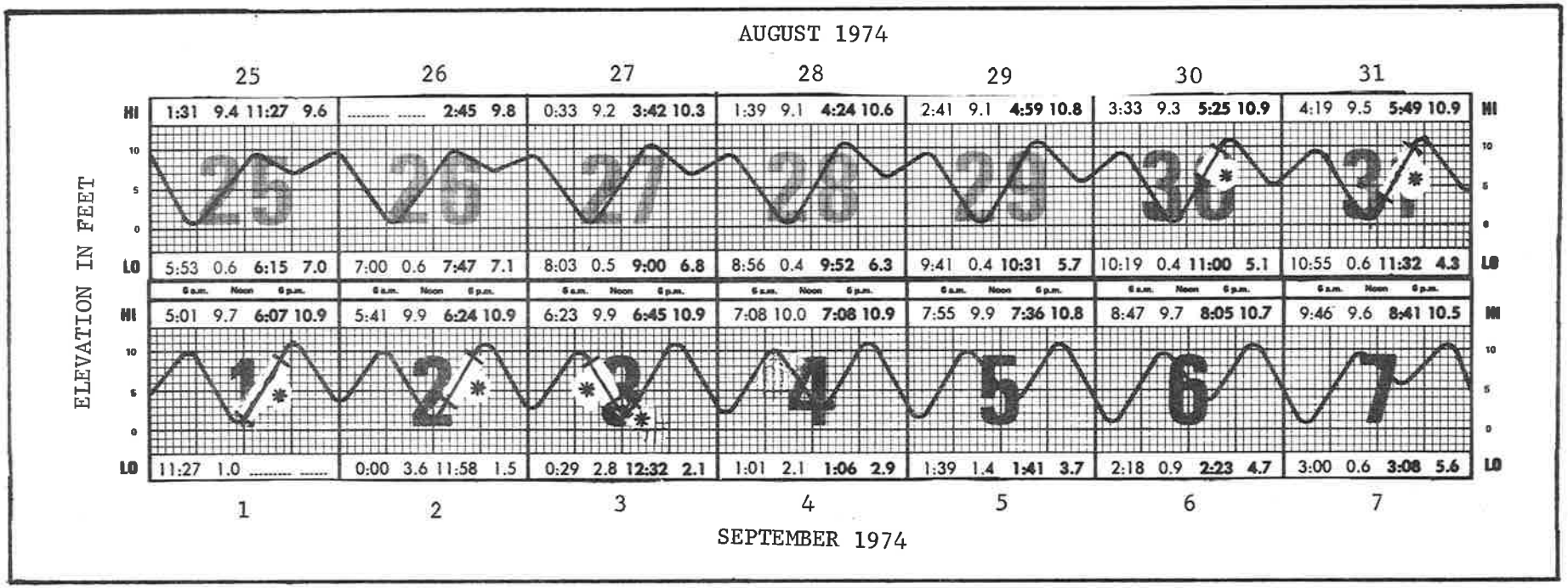

Figure 4. West Point tides during August and September. Observational periods denoted by a single asterisk were analyzed for current properties and relative dilutions.

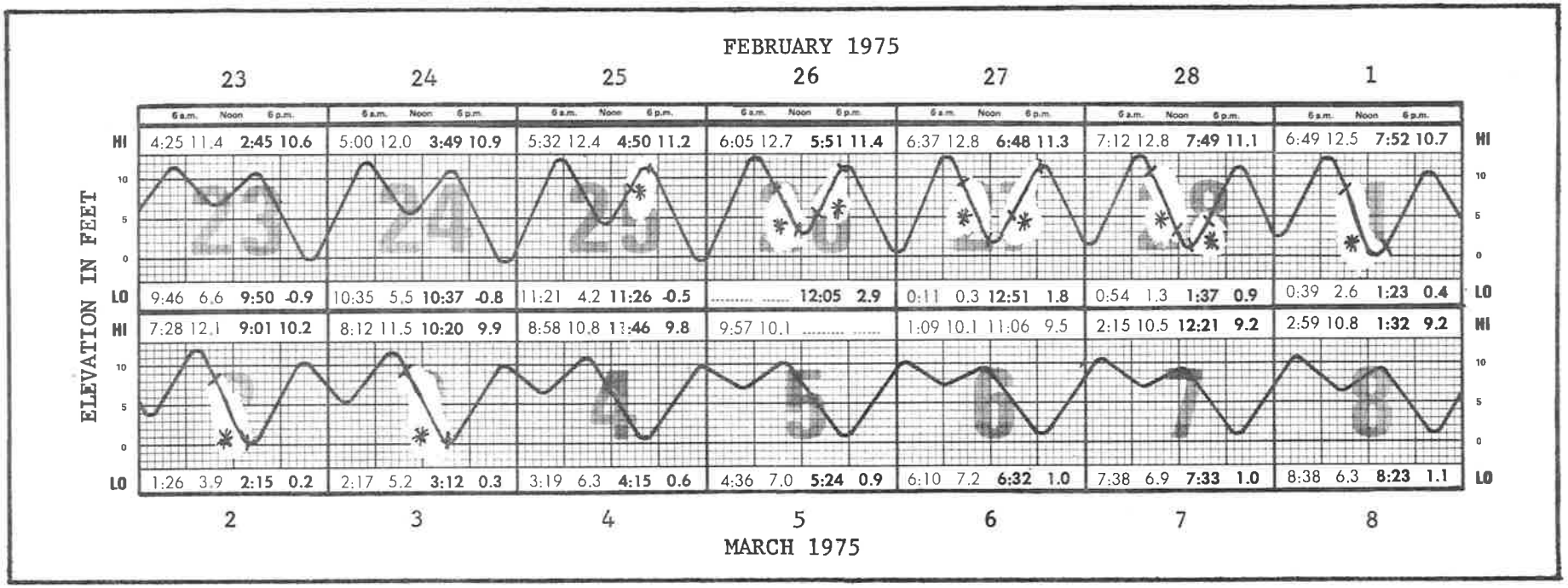

Figure 4 cont. West Point tides during February and March 1975. Observational periods denoted by a single asterisk were analyzed for current properties and relative dilutions.

suspending elements. The drogue used in this study is patterned after a design used previously for extensive field studies in Great Lakes Michigan and Erie (Okubo and Verber, 1967 and Okubo and Farlow, 1967).

The design consists* of two rectangles of coated lightweight nylon sewn over small diameter zinc-coated electrical conduit (Figure 5). The conduits and nylon were fastened at the center and the frame guyed with small diameter braided nylon cord. The surface float consisted of polyurethane sandwiched between square pieces of plywood previously coated with fiber glass. Nylon cord (1/8") connected the drogue and surface float. Assuming a wind speed of 10 knots and a current of one knot, the drag on the drogue's suspending elements is approximately five percent of that on the drogue itself. A several pound weight suspended about ½ meter below the drogue kept it nearly vertical and also resulted in a descent time of approximately five minutes.

B. Field procedure

Shortly after dawn two small craft arrived over the outfall near times of high or low water. In an established tidal current 5-8 drogues were launched within a several hundred meter diameter. After observing positions for 4-5 hours drogues were retrieved usually near midday and dusk. By assigning small craft to selected drogues the position of each could be obtained at least once every 15 minutes. Two observers in each craft obtained drogue positions using micrometer drum sextants during daylight hours of sufficient visibility. Table 1 summarizes general information for sixteen experiments during seven flood, seven ebb and two

*Identical drogues were used in summer and winter periods.

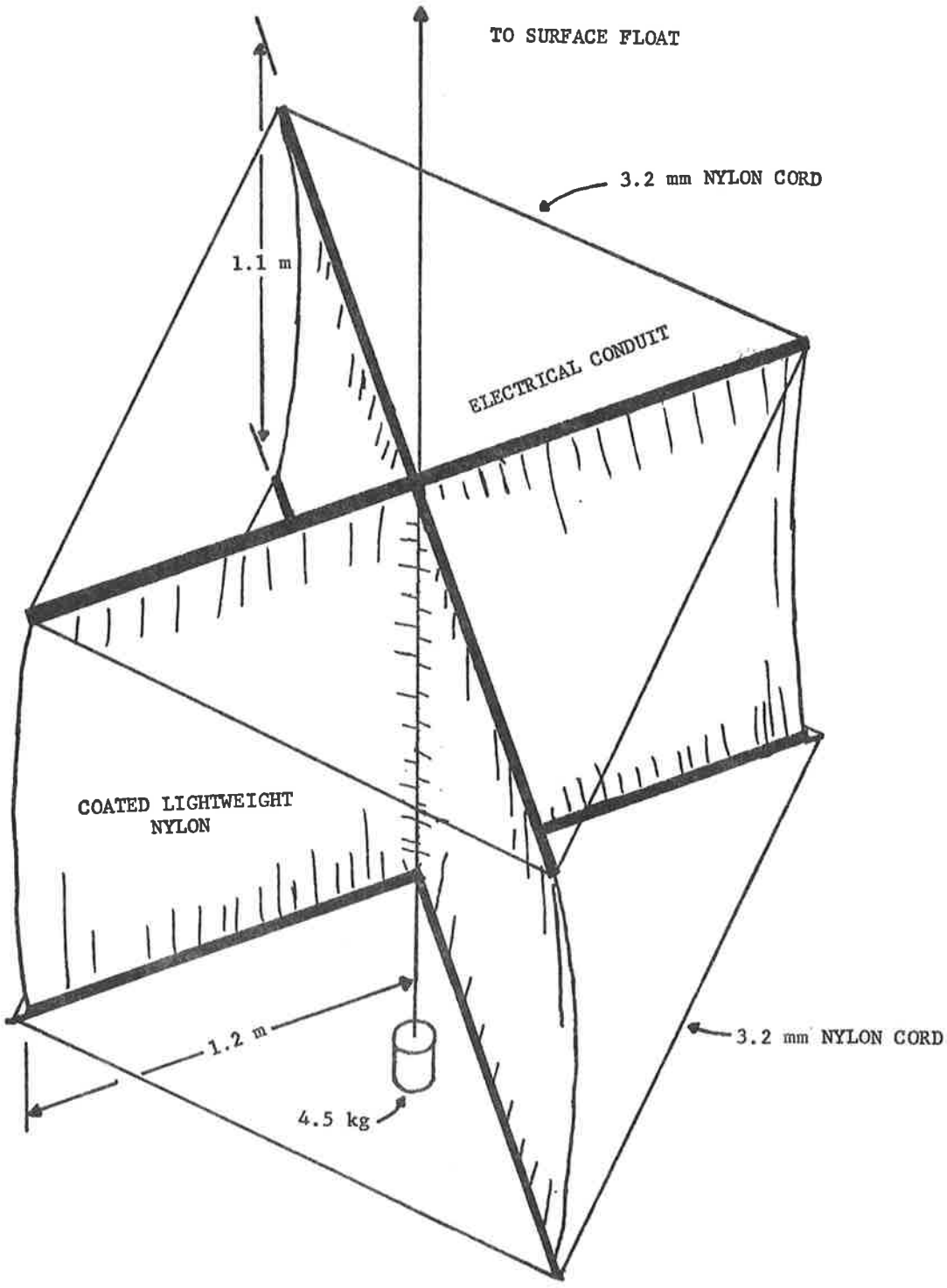

Figure 5. Sketch of drogue.

slack tidal phases.

C. Statistics of drogue position

Sextant fixes were first plotted using a three arm protractor; then digitized on a master grid with x, y reckoned positive toward east and north, respectively; and finally interpolated at six minute intervals using polynomial curves fitted to the time series of x and y by means of least squares. The following statistics were computed from the interpolated positions:

1. Centroid position and speed.
2. Orientation of the principal axes.
3. Standard deviations along the principal axes.

The principal axes are mutually perpendicular and pass through the centroid with respect to which the standard deviation is either maximum (σ_{ma} along the major axis) or minimum (σ_{mi} along the minor axis). Two standard deviations along these axes form an ellipse of area $A = 4\pi\sigma_{ma}\sigma_{mi}$ which contains 95% of the observed drogue positions. Henceforth this area will be referred to as 'drogue area,' A. We define a 'drogue plume' by contouring successive positions of two standard deviations measured from the centroid along major axes (cf. Okubo, 1970, p. 93).

Mean standard deviation for n drogues is defined geometrically as

$$\hat{\sigma} \equiv (\sigma_{ma}\sigma_{mi})^{\frac{1}{2}} \tag{1}$$

where

$$\hat{\sigma}_{ma}^2 = \frac{1}{n-1}\sum_{i=1}^{n}(r_i - \bar{r})^2$$

$$\hat{\sigma}_{mi}^2 = \frac{1}{n-1}\sum_{i=1}^{n}(s_i - \bar{s})^2$$

where r, s refer to coordinates in the principal axis frame and the centroid $(\bar{r},\bar{s})$ is located at

$$\bar{r} = \frac{1}{n} \sum_{i=1}^{n} r_i$$

$$\bar{s} = \frac{1}{n} \sum_{i=1}^{n} s_i$$

In eq. (1) the denominator n-1 replaces the more common n. According to Cramer (1966, p. 182) this formulation approximates the variance of a continuous population as observed with n discrete samples. Calculation of centroid position requires no correction. The 'hats' ($\hat{}$) denote use of this corrected standard deviation.

D. Divergence, vorticity, deformation rates and frictional torque

These properties of mean current shear were computed from interpolated positions using linear regression procedures described in Appendix B.

Drogue area is approximately related to horizontal divergence by

$$\gamma = \frac{1}{A} \frac{dA}{dt} \tag{2}$$

so that

$$A = \exp \left[\int_{o}^{t} \gamma(t')dt' \right] \tag{3}$$

If we associate A with a vertical cylinder of water having unit volume and height D, then for this volume to be conserved $D \alpha A^{-1}$, or

$$D = \exp - \left[\int_o^t \gamma(t')dt' \right] \tag{4}$$

where the integral will be referred to as the integrated divergence.

The vertical component of the absolute vorticity ($\zeta + f$) obeys the following dynamic equation

$$\left.\begin{aligned} &\frac{d}{dt}(\zeta+f) + (\zeta+f)\gamma + \left(\frac{\partial v}{\partial z}\frac{\partial w}{\partial x} - \frac{\partial u}{\partial z}\frac{\partial w}{\partial y}\right) - 2\Omega\cos\phi\frac{\partial w}{\partial y} + w\frac{\partial f}{\partial y}\tan\phi = \\ &- \left(\frac{\partial \alpha}{\partial x}\frac{\partial p}{\partial x} + \frac{\partial \alpha}{\partial y}\frac{\partial p}{\partial y}\right) + \left(\frac{\partial Fy}{\partial x} - \frac{\partial Fx}{\partial y}\right) \end{aligned}\right\} \tag{5}$$

where
- ζ : vertical component of relative vorticity
- f : vertical component of planetary vorticity (1.08×10^{-4} s^{-1})
- γ : horizontal divergence
- u,v,w : x, y, z components of velocity
- Ω : earth's angular rotation
- ϕ : latitude
- α : specific volume of sea water
- p : pressure
- F_x, F_y : x, y - components of frictional forces

If we ignore the terms involving the vertical velocity and also the baroclinic term, (5) is reduced to

$$\frac{d}{dt}(\zeta+f) + (\zeta+f)\gamma = T_f \tag{6}$$

where $T_f \equiv \frac{\partial Fy}{\partial x} - \frac{\partial Fx}{\partial y}$: frictional torque.

Dividing (6) by D, the vertical height of a water column and using the relation (4), we obtain

$$\frac{d}{dt}\left(\frac{\zeta+f}{D}\right) = \frac{T_f}{D} \tag{7}$$

Equation (7) states that without frictional torque, potential vorticity, $\frac{\zeta+f}{D}$, is conserved:

$$\frac{\zeta+f}{D} = \text{constant} \tag{8}$$

E. Dilution of maximum concentration

The dilution of the maximum concentration, S_m, within an effluent patch formed at t = 0 is approximated by the following Lagrangian diffusion equation adapted from Okubo (1966):

$$\frac{S_m}{Q} \simeq \left\{ 2\pi(\sigma_T + \sigma_{mao})(\sigma_T + \sigma_{mio}) \left[\overline{(F_1^2 + G_1^2)}\,\overline{(F_2^2 + G_2^2)} - \overline{(F_1F_2 + G_1G_2)}^2 \right]^{\frac{1}{2}} \right\}^{-1} \tag{9}$$

where: (1) Q is the amount of substance released per unit depth at t = 0.

(2) σ_{mao}, σ_{mio} are standard deviations along the major and minor axes at t = 0, respectively.

(3) σ_T is the standard deviation due to small-scale eddies

$$\sigma_T^2 = 2\bar{K}t \tag{10}$$

(4) $\bar{K}$ is the time average horizontal eddy diffusivity

$$\bar{K} = \frac{1}{t}\int_o^t K(t')dt' \tag{11}$$

(5) K is the instantaneous eddy diffusivity

$$K \equiv \frac{1}{2t}\left(\sigma_{ma}\sigma_{mi} - \sigma_{maM}\sigma_{miM}\right) \tag{12}$$

in which σ_{maM}, σ_{miM} are major and minor axes, respectively, of the drogue group after subtraction of turbulent displacements from drogue positions.

(6) F_1, F_2, G_1, G_2 are the Lagrangian displacement properties which depend on time and characterize the mean flow (see Appendix C for details of computations).

(7) The overbars denote use of the time average process as used in eq. (11).

Equation (9) assumes that vertical mixing is negligible and that the eddy spectrum may be separated into two major parts: eddies larger than the drogue group (i.e., large-scale eddies) appear as shear of the mean flow and eddies smaller than the drogue group (i.e., small-scale eddies) appear as turbulence.

From eq. (9) we define the relative dilution of the maximum concentration as:

$$\text{Relative dilution} \equiv \frac{S_m(t)}{S_m(t=0)} \tag{13}$$

F. Photographs of dye injected into the Puget Sound Model

As part of another study for Metro, J.H. Lincoln* took 16-mm film of dye injected at the West Point outfall in the Puget Sound Model. We reviewed that footage magnified several times and shot pictures of 16-mm frames near times coinciding with the beginning, mid-point and end of drogue runs from 26 February-2 March 1975. Additional pictures were made of two dye patches which maintained their identity for 12 and 15 hours. Two of the more interesting pictures are shown in Plates I and II.

IV. Results and discussion

A. Drogue dispersion

Application of these methods results in drogue plumes (Figure 3); divergence, vorticity and deformation rates due to the mean flow and large-scale eddies (Table 2); and eddy diffusivities due to small-scale eddies (Table 3). The separation between these two scales varies with time according to the drogue group's instantaneous size. From Table 3 for ebb and flood tides the mean separation is 0.9 km.

Additional analysis shows that the mean flow and large-scale eddies are primarily responsible for drogue dispersion during established tidal

*Dept. of Oceanography, University of Washington, Seattle, Washington.

phases. We can demonstrate this by two curves relating drogue area to integrated divergence: curve A in Figure 6a shows typical observed values, while curve B relates theoretical values computed from eq. (3) due only to the mean flow and large-scale eddies. The ratio of B to A is the approximate fraction of drogue area due to the mean flow and large-scale eddies, while their difference is proportional to the area due to small-scale eddies. Hence about 90-95% of drogue dispersion is caused by flows having length scales larger than drogue groups and the remaining 5-10% is due to small-scale eddies.

Inspection of drogue trajectories (Appendix A) shows that a drogue group tends to disperse in subgroups. This behavior correlates with patchiness in photographs of dye injected into the Puget Sound Model (e.g., Plates I,II). Moreover, patchiness is asymmetrically distributed between flood and ebb tides. During established flood tides three dye patches characteristically disperse between mid-channel and Magnolia Bluff while an eddy forms in West Point's lee. During established ebb tides a characteristic filamentary dispersion sweeps northward around Meadow Point.

Close inspection of our photographs revealed that selected patches formed on both ebb and flood tides and maintained their identity for 12-15 hours. Other dye patterns showed eddy circulations with diameters exceeding one kilometer, yielding additional evidence of large-scale eddies. Finally, we note that drogue and dye plumes do not always match precisely because of dye recirculated from previous tidal stages.

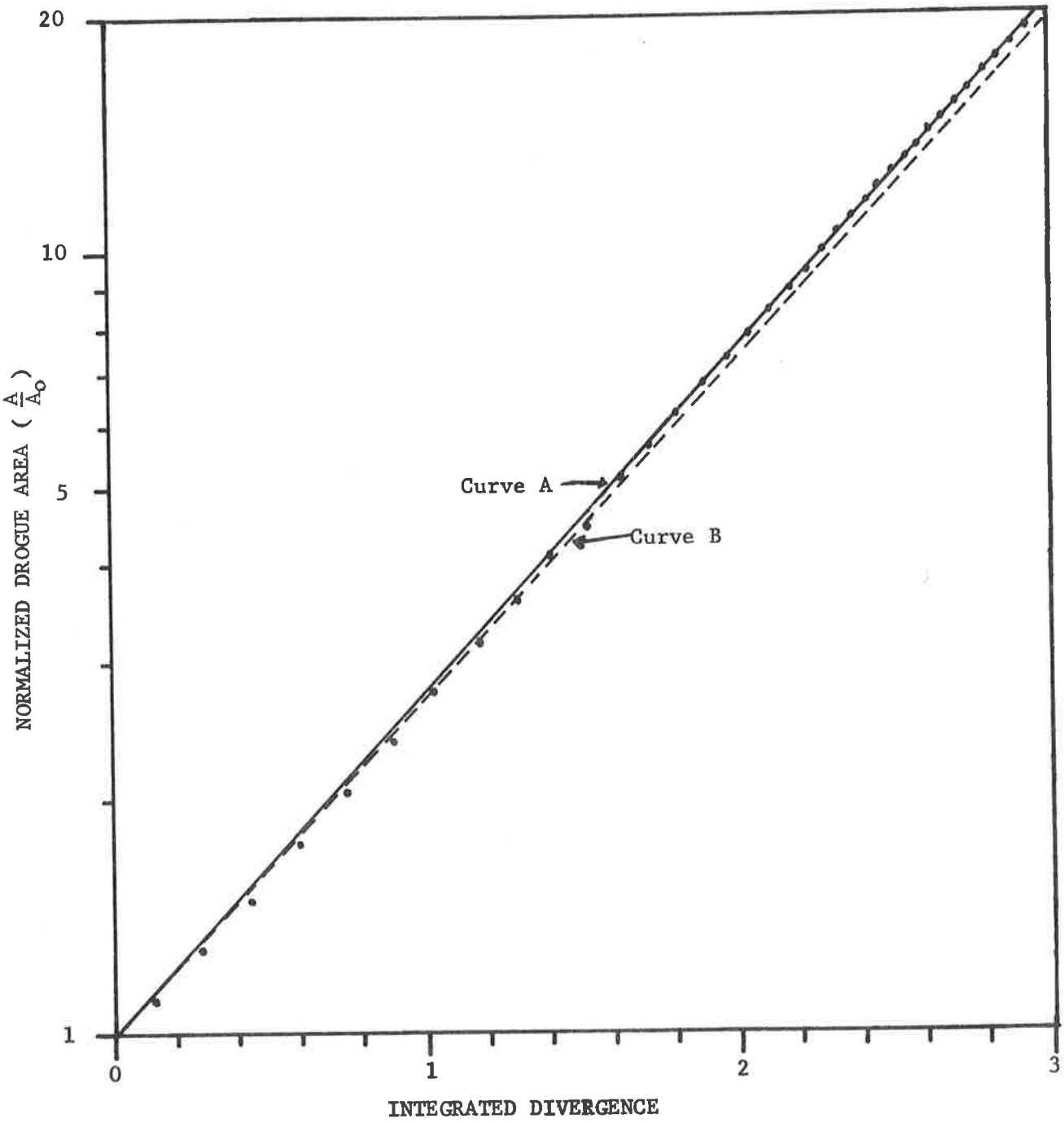

Figure 6a. Normalized drogue area versus integrated divergence for ebb tide of 1 March 1975 (A_o = initial drogue area). Curve A: observed values. Curve B: eq. (3) for large-scale eddies and mean flow. Data from other drogue releases form straight lines having nearly identical slopes and intercepts.

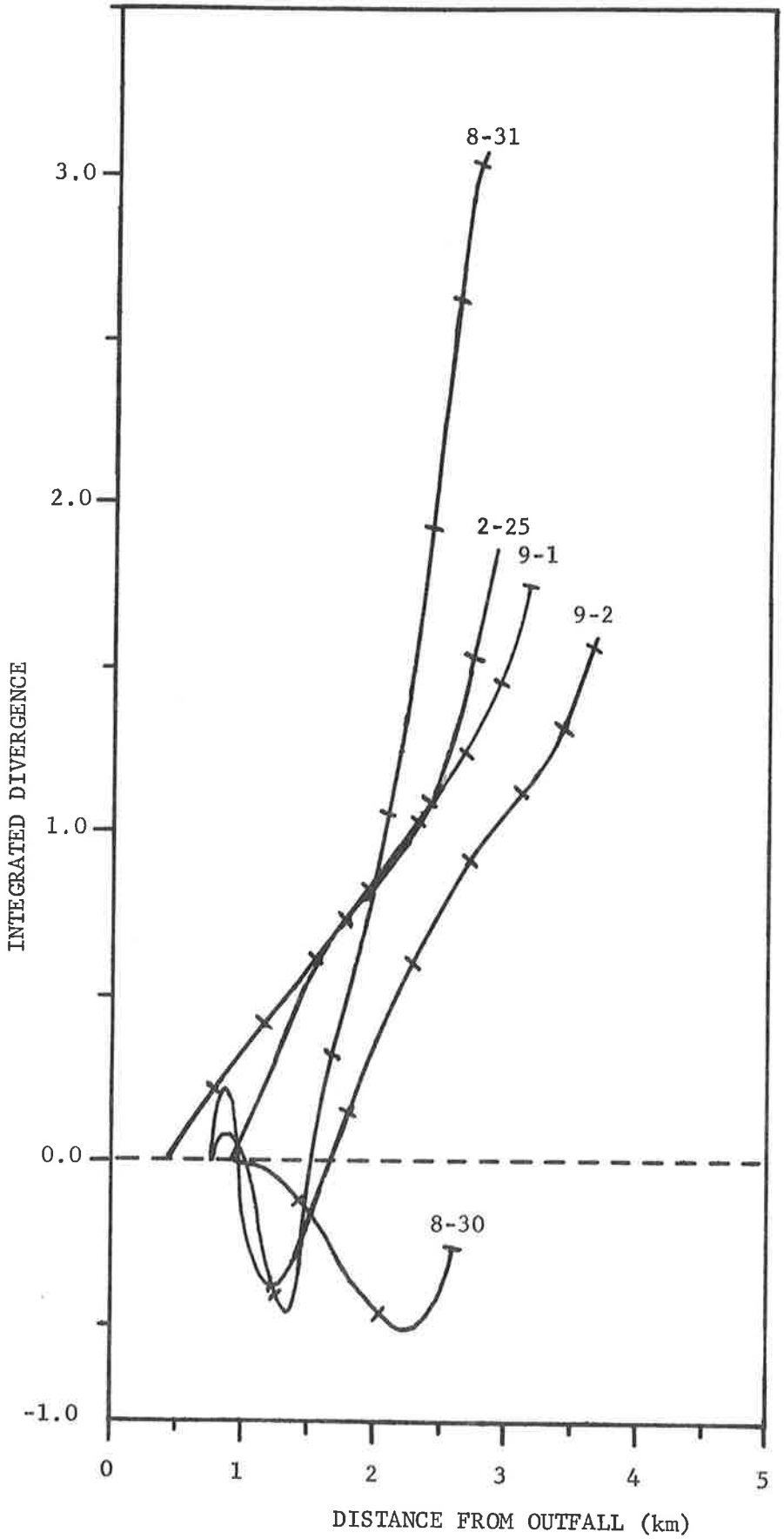

Figure 6b1. Integrated divergence versus distance from West Point outfall for flood tides listed in Tables 1-3. Tics mark half hour intervals.

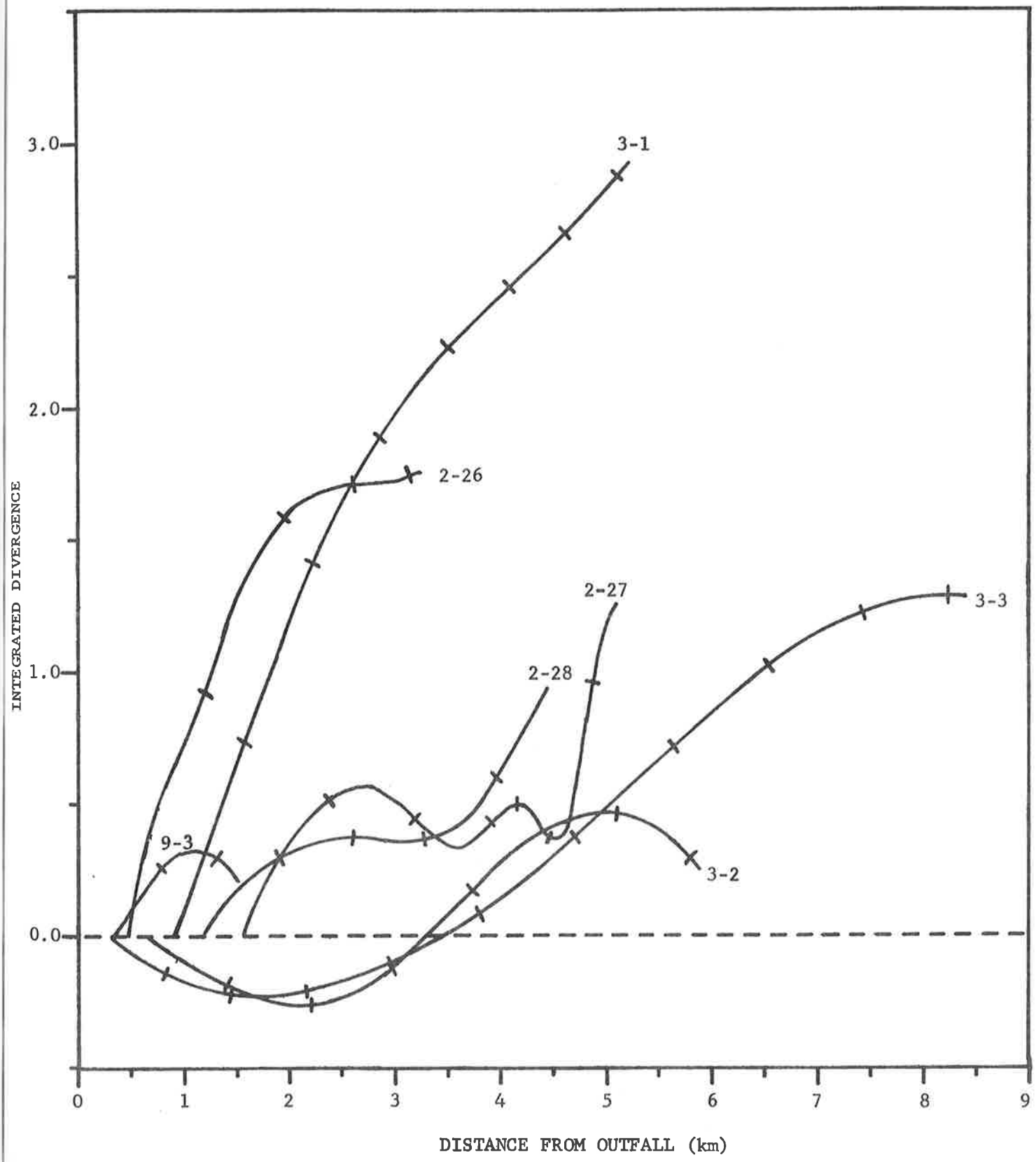

Figure 6b2. Integrated divergence versus distance from West Point outfall for ebb tides listed in Tables 1-3. Tics mark half hour intervals.

B. Dilution of maximum concentrations

Relative dilutions of maximum concentrations* within effluent patches are displayed for individual drogue releases and averaged for five flood and seven ebb tides during which drogue plumes were oriented approximately north-south (Figure 2). These computations suggest that a patch formed during an established flood or ebb tide requires approximately four hours for its maximum concentration to decrease to 10% of its initial value. This interval corresponds to a distance of about five kilometers using average tidal speeds.

Relative dilution decays at a rate proportional to $t^{-1.2}$ after an initial interval of slower decay. Our limited observations during so-called slack tide, in a flood eddy and in areas of high current shear suggest that the decay rate increases to t^{-2} to t^{-4} between established tidal phases depending on the patch's location.

C. Vorticity balance

Conservation of potential vorticity is usually valid for a large-scale motion like the Gulf Stream (Stommel, 1958). For smaller scale motions frictional torque and vertical velocity may become significant. A large fraction of our observations satisfy the balance of potential vorticity and frictional torque in eq. (7) (e.g., Figure 7). However the remaining observations appear to require a more complex vorticity balance which retains terms containing vertical velocity.

*Computed from eq. (13).

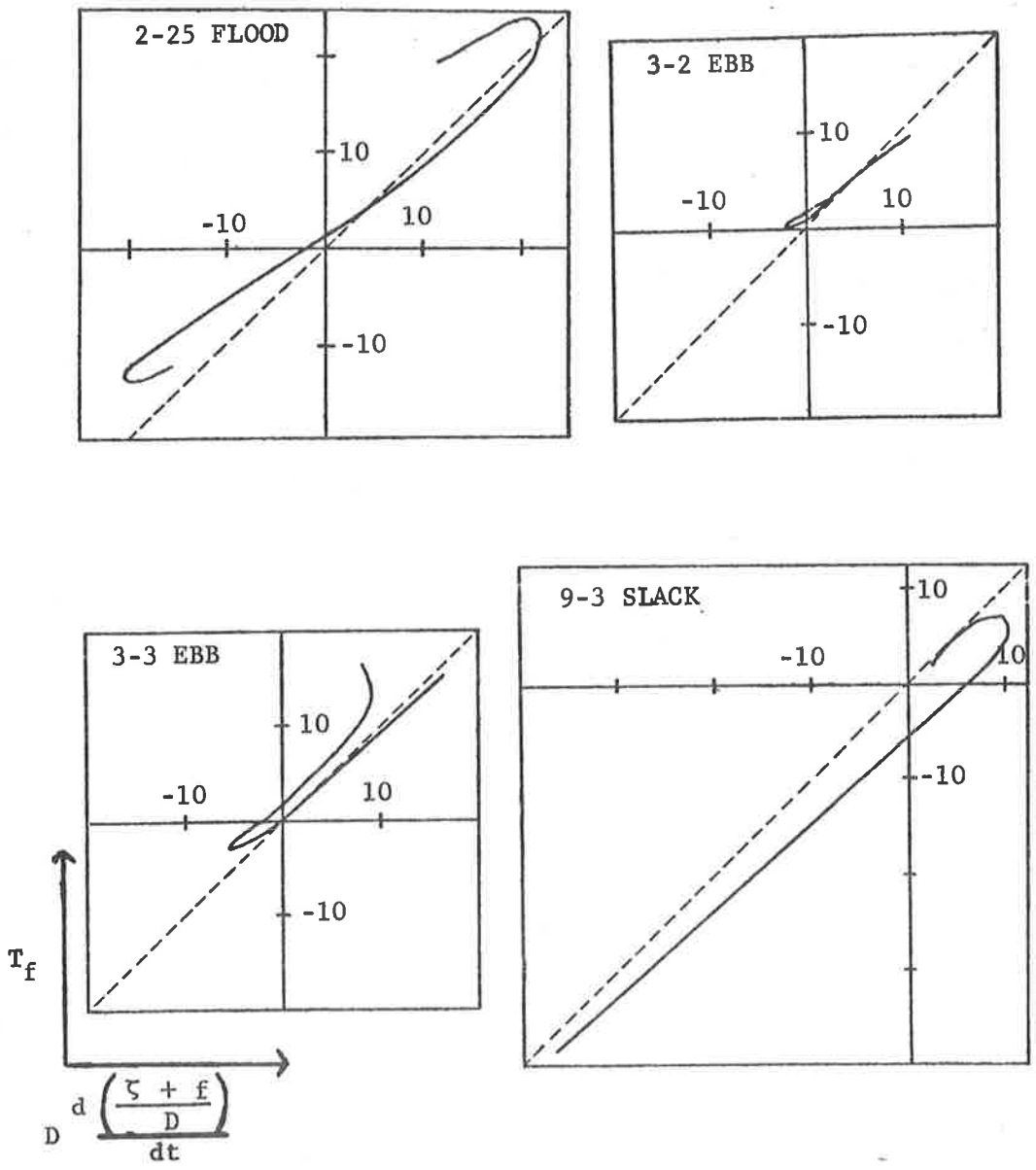

Figure 7. Examples of vorticity balance from eq. 7 in units of 10^{-8} s^{-2}. Dashed line represents equality between frictional torque per unit depth (T_f/D) and rate of change of potential vorticity ($(\zeta + f)/D$). Deviations from the dashed lines result from assumptions used to derive eq. (7) from eq. (5).

V. Conclusion

Our results suggest the following two-step mixing process as a working hypothesis:

1. During established tidal phases the effluent is primarily stirred by the mean flow and large-scale eddies, thereby producing complex patterns of filaments and patches.

2. Between established tidal phases increased fluid acceleration leads to a relative increase of small-scale eddies at the expense of their larger scale parents. In turn these offspring disperse the filaments and patches.

The net result is about a 1:10 dilution of maximum concentration in a patch during established tidal phases and more rapid dilution at a rate in excess of $t^{-1.2}$ during so-called slack tide. However tidal mixing is comparatively inefficient such that some effluent patches may retain their identity through several tidal phases.

On two flood tides drogues travelled around an eddy in West Point lee. Photographs of the Puget Sound Model confirm the presence of this feature. However, drogue plumes do not always match precisely dye plumes because of dye recirculated from previous tidal phases.

Finally, it should be kept in mind that drogues are primarily responsive to horizontal fluid motions. Our results suggest that natural horizontal variability of drogue patterns are sufficient to mask significant differences between observed summer and winter patterns. Moreover, summer and winter observations were obtained at different depths and tidal phases; and photographs of the Puget Sound Model were <u>not</u> available for summer to contrast those reported here for winter. A definitive discussion of summer-winter differences of dispersion patterns must consider additional analyses of

hydrographic conditions and dye observations --- tasks beyond the scope of this study. We have reported our results for both summer and winter in the hopes that they will provide a partial basis for delineating seasonal characteristics.

References

Cramer, H. (1966): Mathematical methods of statistics. Princeton University Press, eleventh edition, 575 pp.

Draper, N.R. and H. Smith (1966): Applied regression analysis. John Wiley and Sons, N.Y., 407 pp.

Ebbesmeyer, C.C. and A. Okubo (1974): A study of current properties and mixing using drogue movements observed near West Point in Puget Sound, Washington. Evans-Hamilton, Inc. Final Report dated November 1974. 95 pp.

Okubo A. (1966): A note on horizontal diffusion from an instantaneous source in a non-uniform flow. Journal of the Oceanographical Society of Japan, 22, 35-40.

Okubo, A. and J.S. Farlow (1967): Analysis of some Great Lakes drogue studies. Proceedings Tenth Conference on Great Lakes Research, pp. 299-308.

Okubo, A. and J.L. Verber (1967): Drogue Studies, Chapter 8 of Lake Currents. Technical Rept. F.W.P.C.A. Great Lakes Region, Illinois, November 1967.

Okubo, A. (1970): Oceanic mixing. Chesapeake Bay Institute Technical Report 62. Reference 70-1, Jan. 1970, 139 pp.

Stommel, H. (1958): The Gulf Stream. Univ. California Press, 202 pp.

Appendix A. Drogue trajectories.

The following figures show trajectories from interpolated drogue positions.

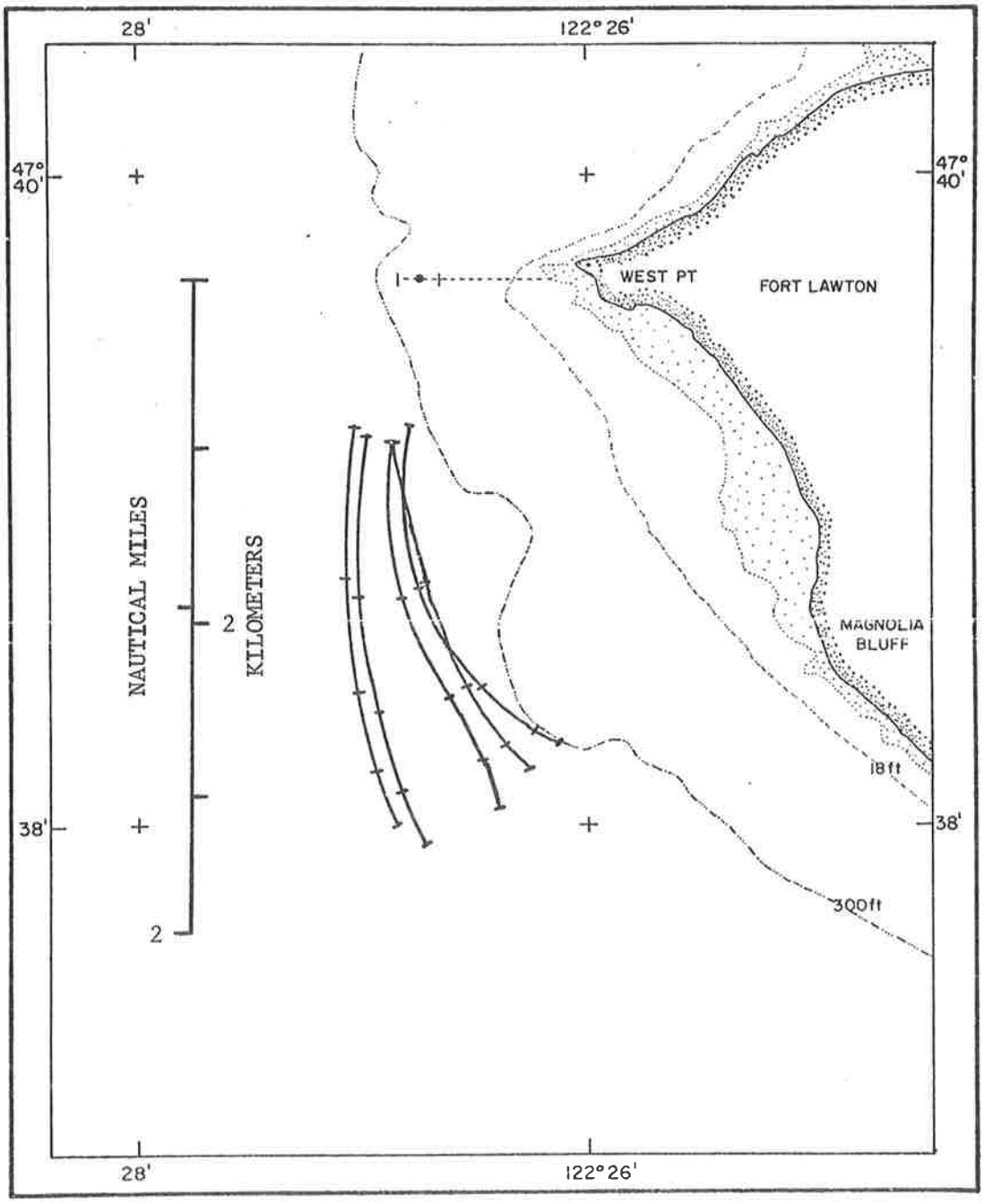

Figure 8a1. Drogue trajectories for flood tide on 25 February 1975. Tics mark half hour intervals.

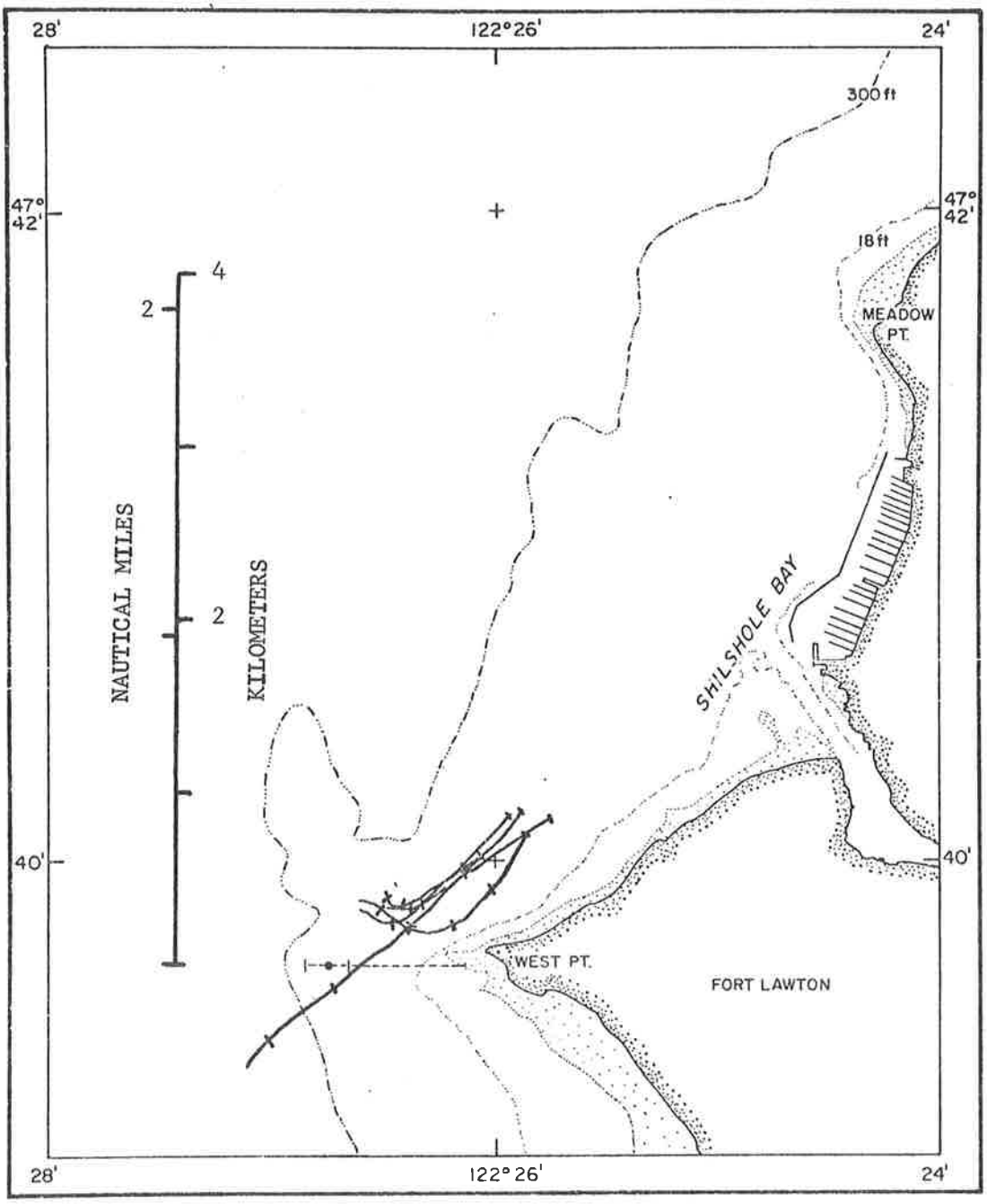

Figure 8a2. Drogue trajectories for Shilshole flood tide on 26 February 1975. Tics mark half hour intervals.

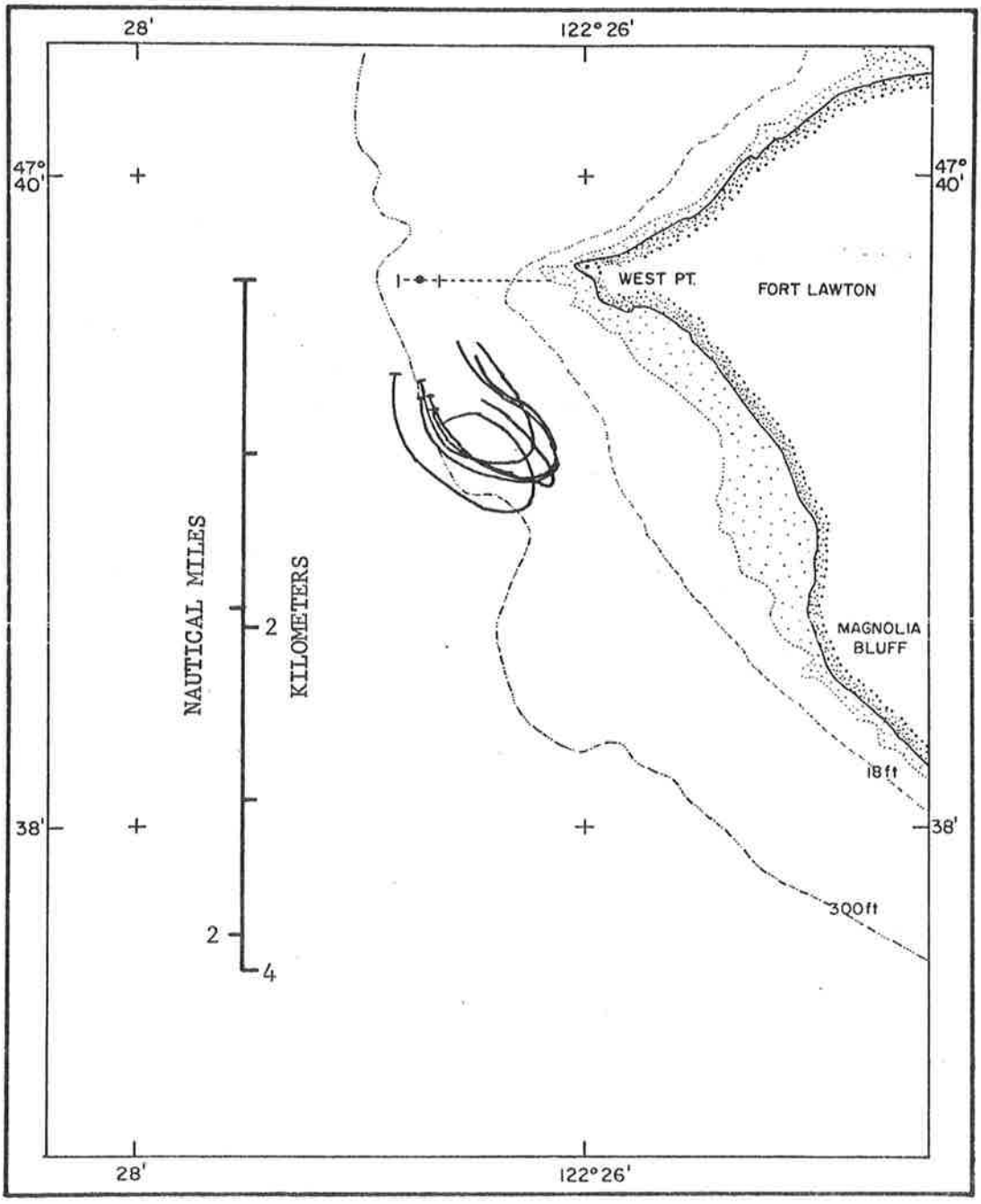

Figure 8a3. Drogue trajectories for flood eddy on 27 February 1975.

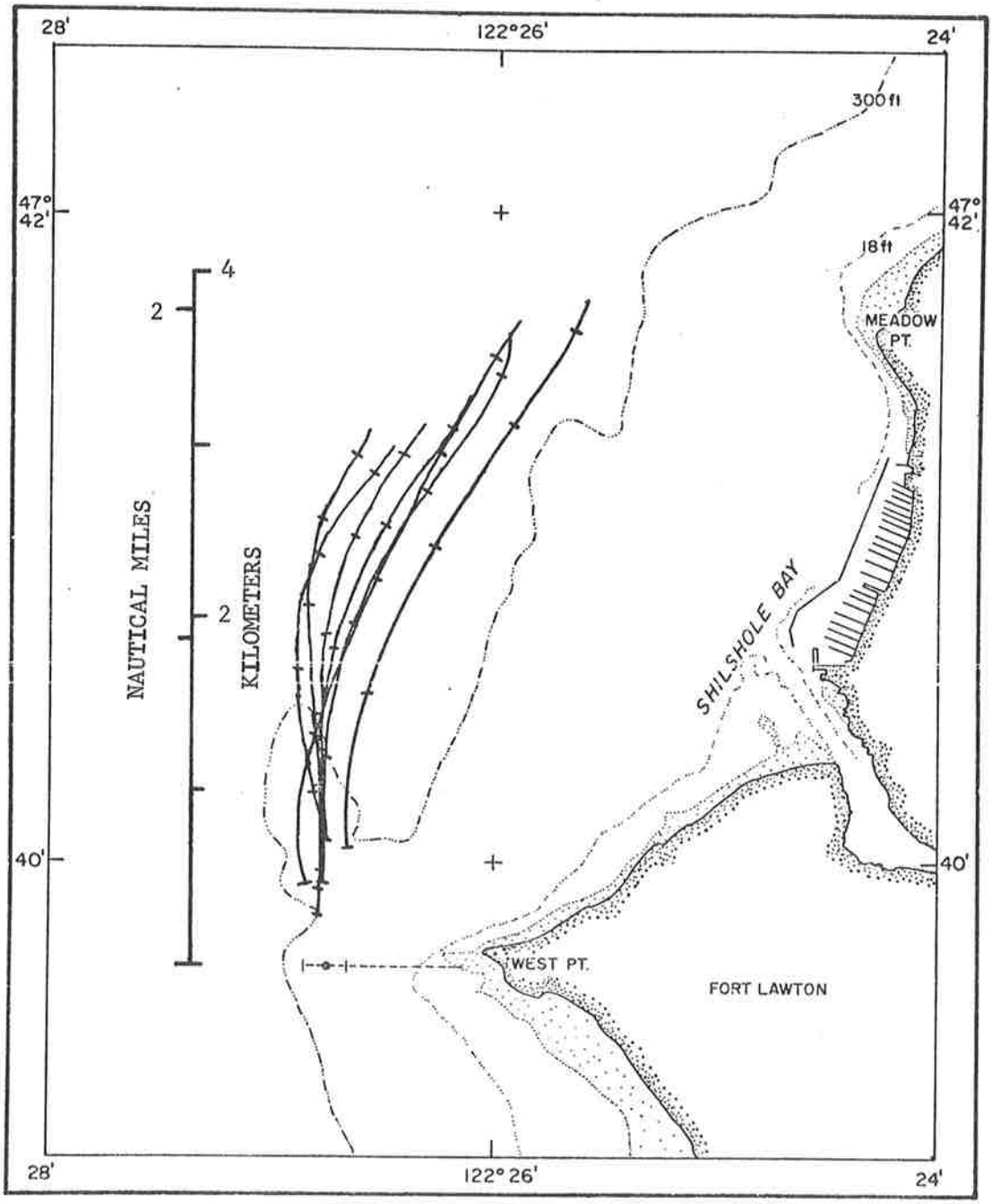

Figure 8b1. Drogue trajectories for ebb tide on 26 February 1975. Tics mark half hour intervals.

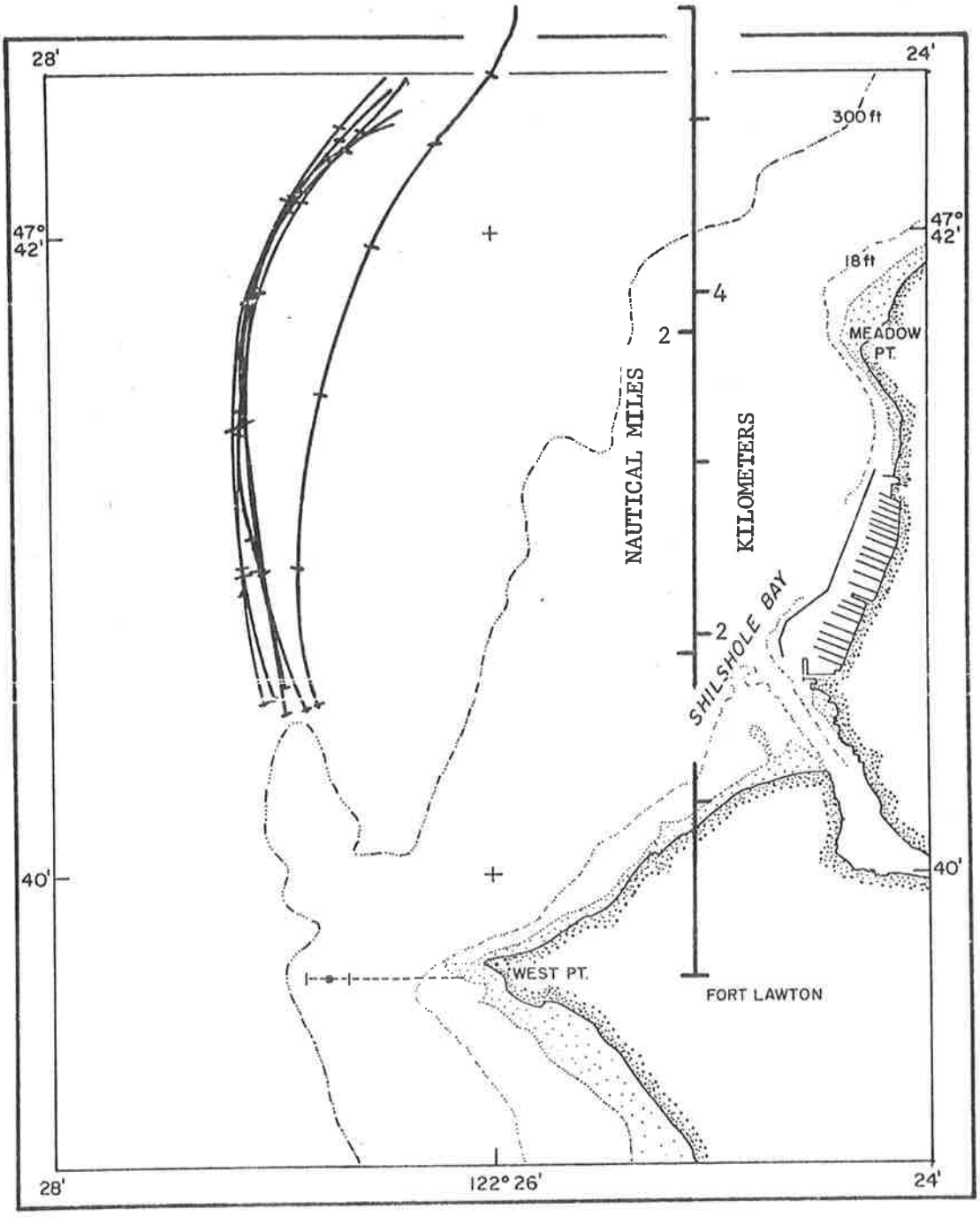

Figure 8b2. Drogue trajectories for ebb tide on 27 February 1975. Tics mark half hour intervals.

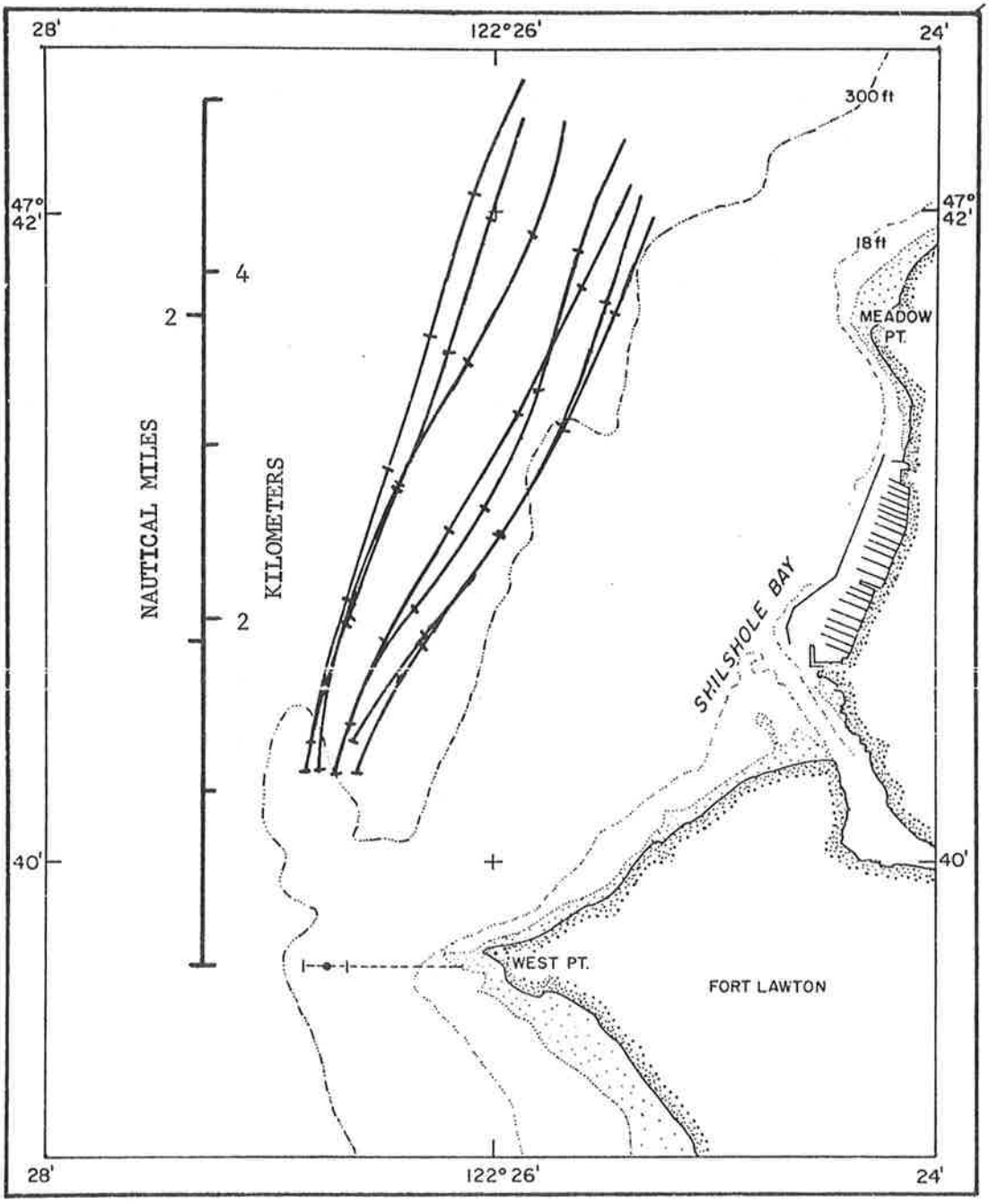

Figure 8b3. Drogue trajectories for ebb tide on 28 February 1975. Tics mark half hour intervals.

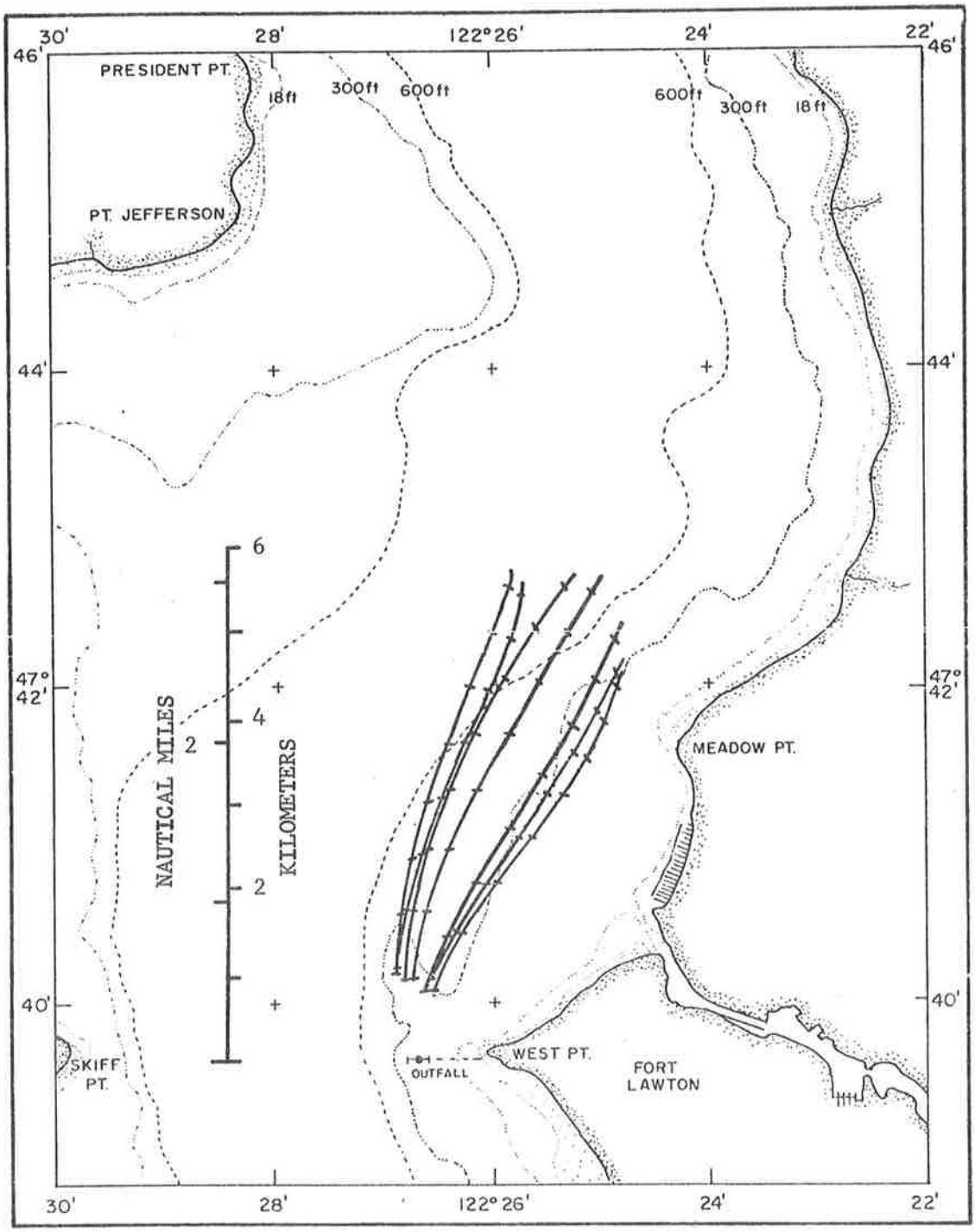

Figure 8b4. Drogue trajectories for ebb tide on 1 March 1975. Tics mark half hour intervals.

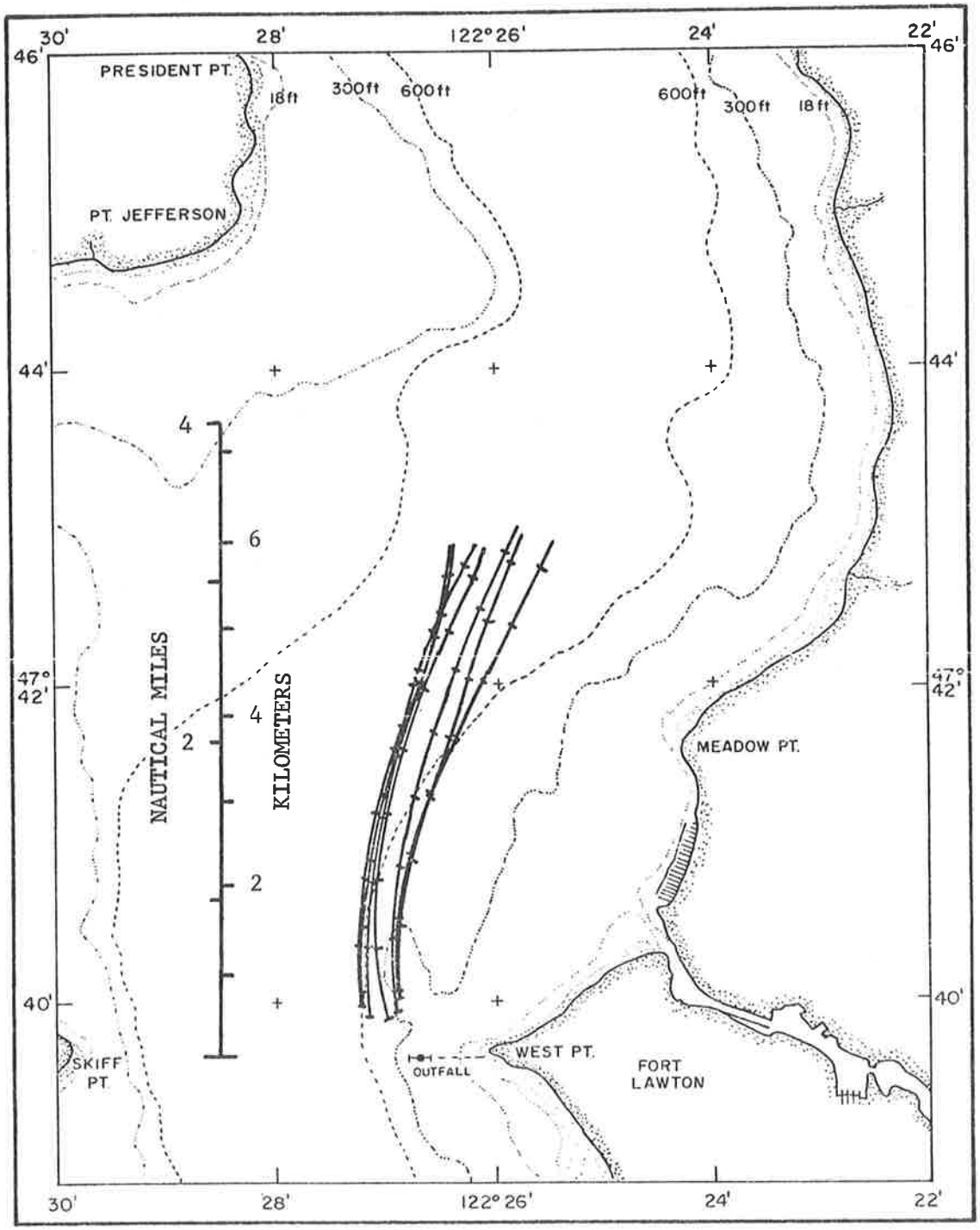

Figure 8b5. Drogue trajectories for ebb tide on 2 March 1975. Tics mark half hour intervals.

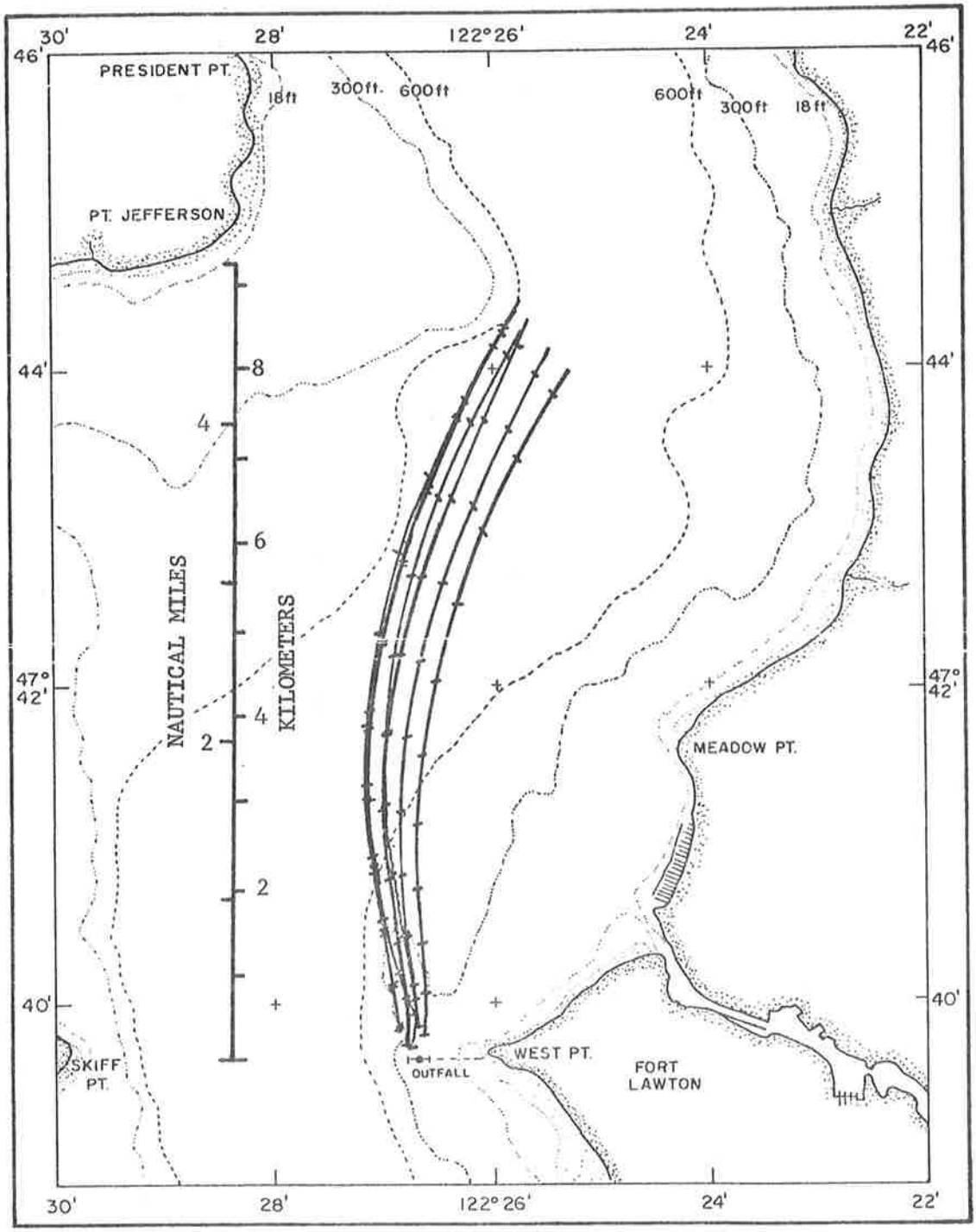

Figure 8b6. Drogue trajectories for ebb tide on 3 March 1975. Tics mark half hour intervals.

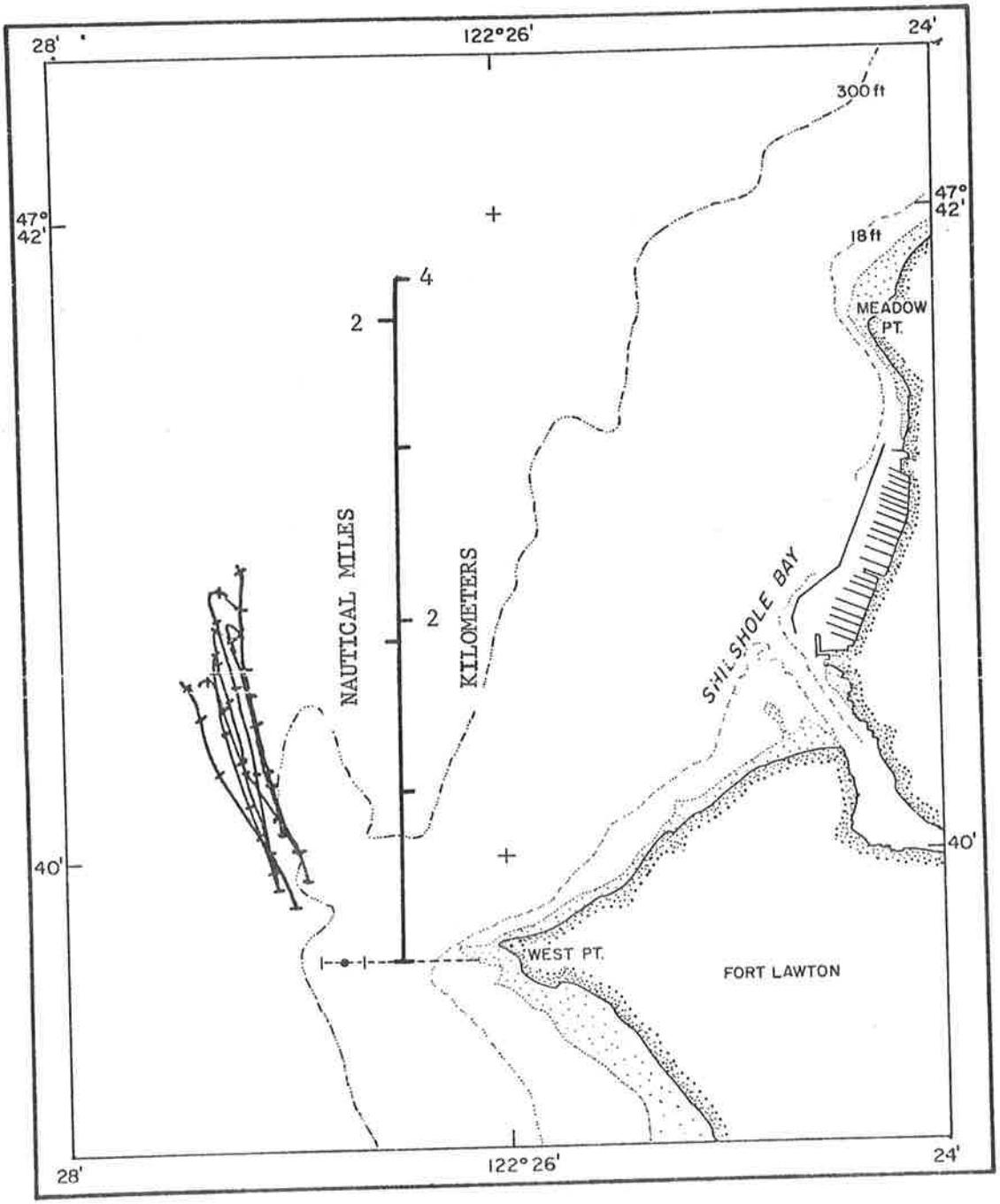

Figure 8c. Drogue trajectories for slack tide on 28 February 1975. Tics mark half hour intervals.

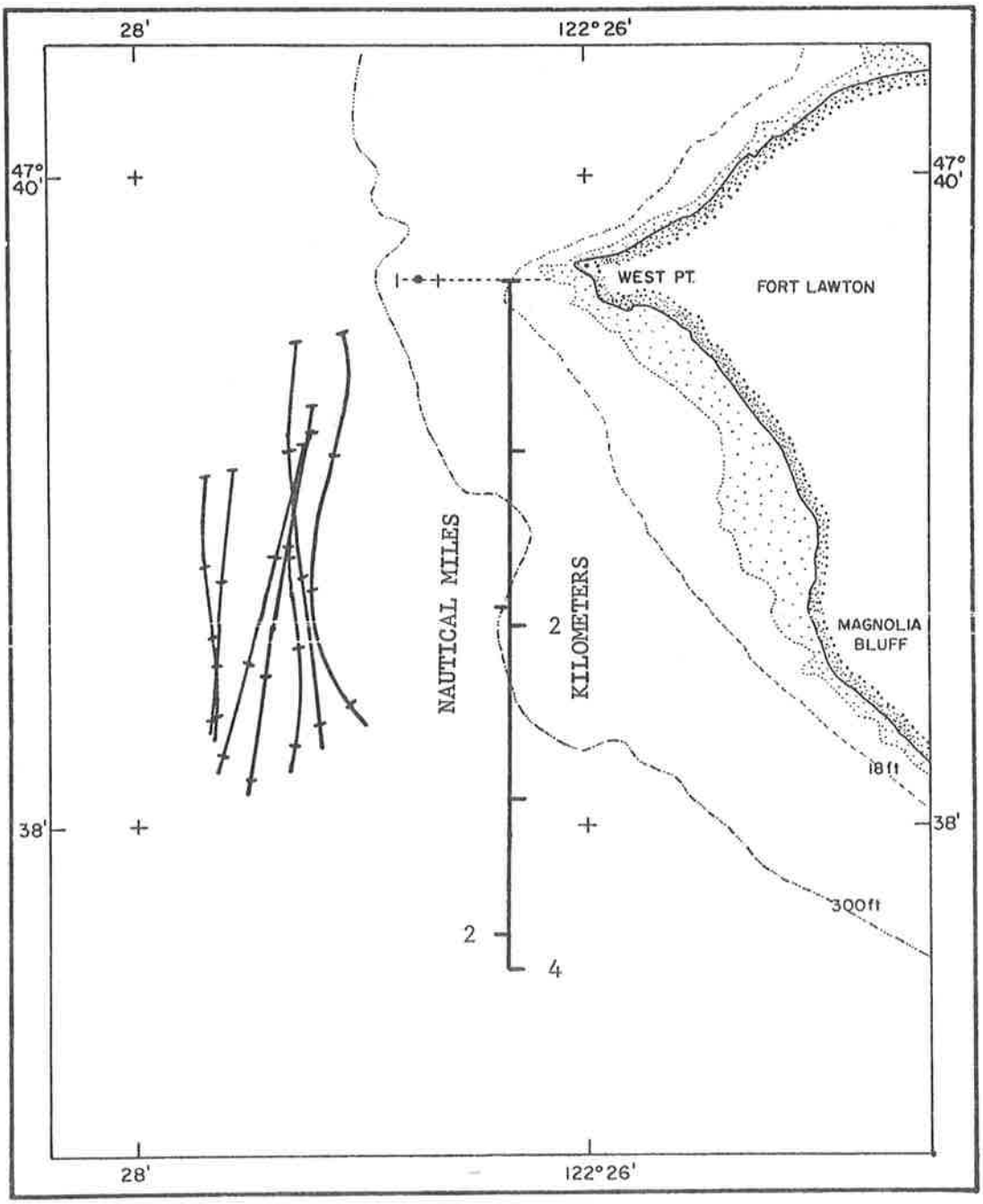

Figure 8d1. Drogue trajectories for flood tide on 30 August 1974. Tics mark half hour intervals.

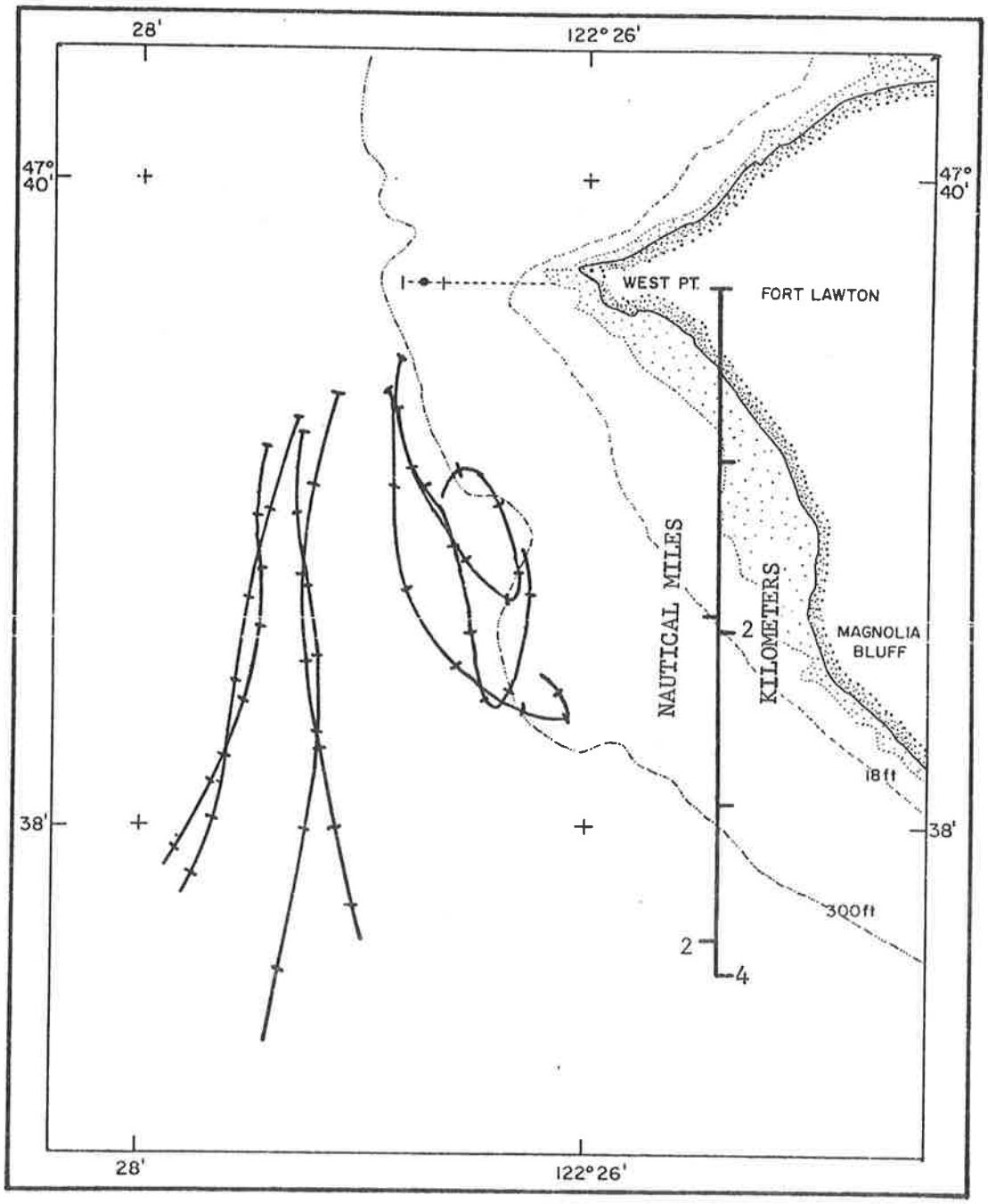

Figure 8d2. Drogue trajectories for flood tide on 31 August 1974. Tics mark half hour intervals.

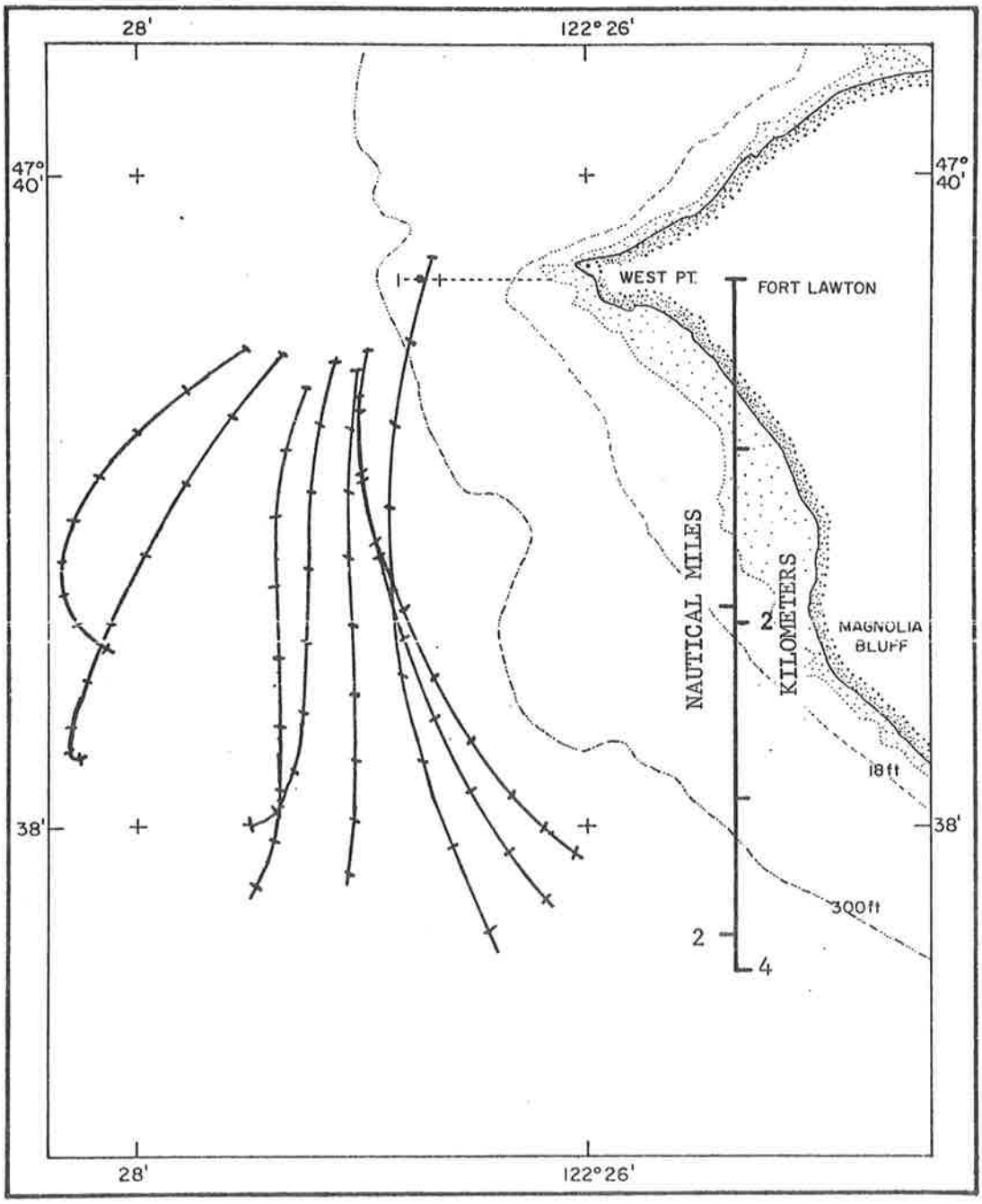

Figure 8d3. Drogue trajectories for flood tide on 1 September 1974. Tics mark half hour intervals.

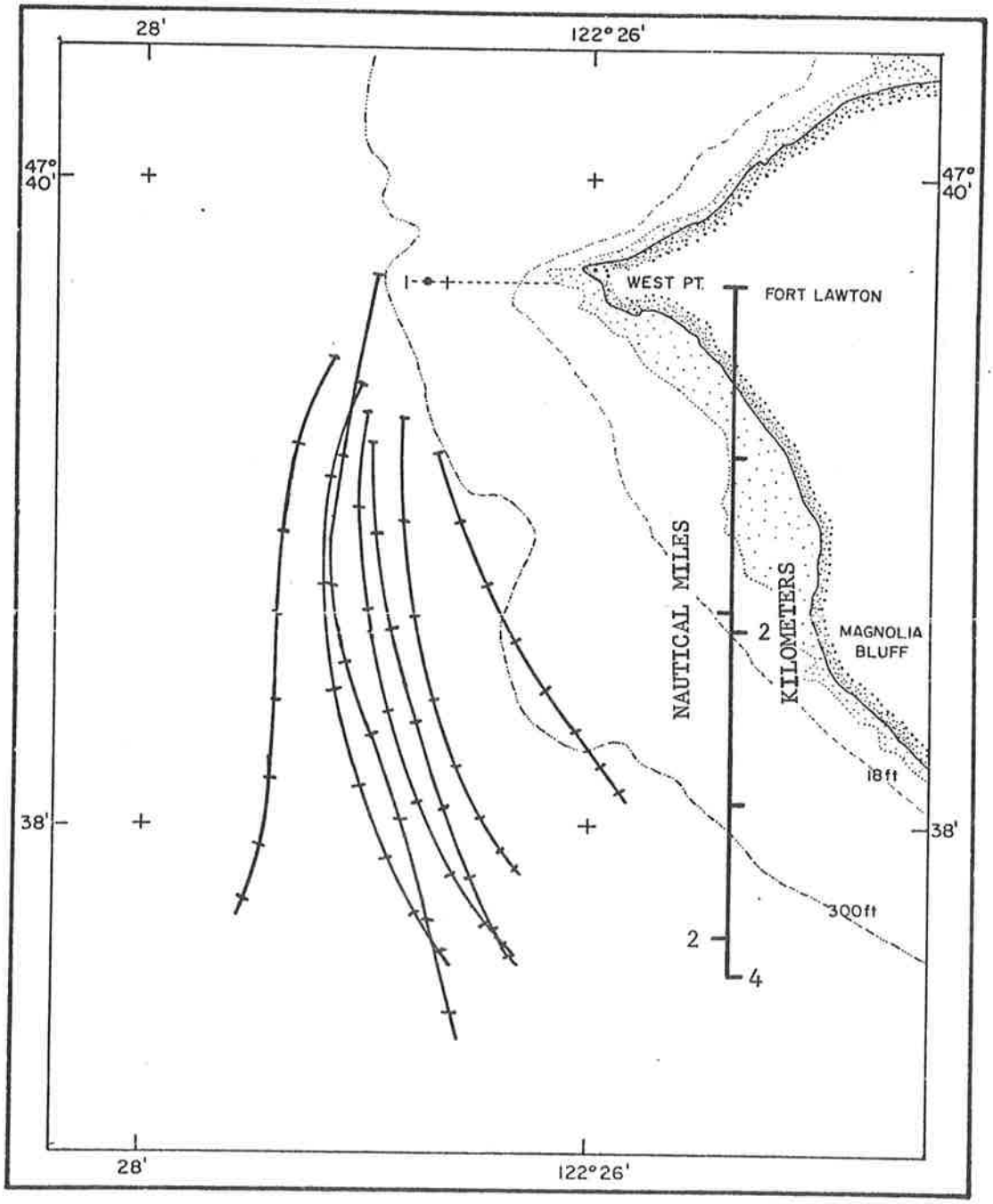

Figure 8d4. Drogue trajectories for flood tide on 2 September 1974. Tics mark half hour intervals.

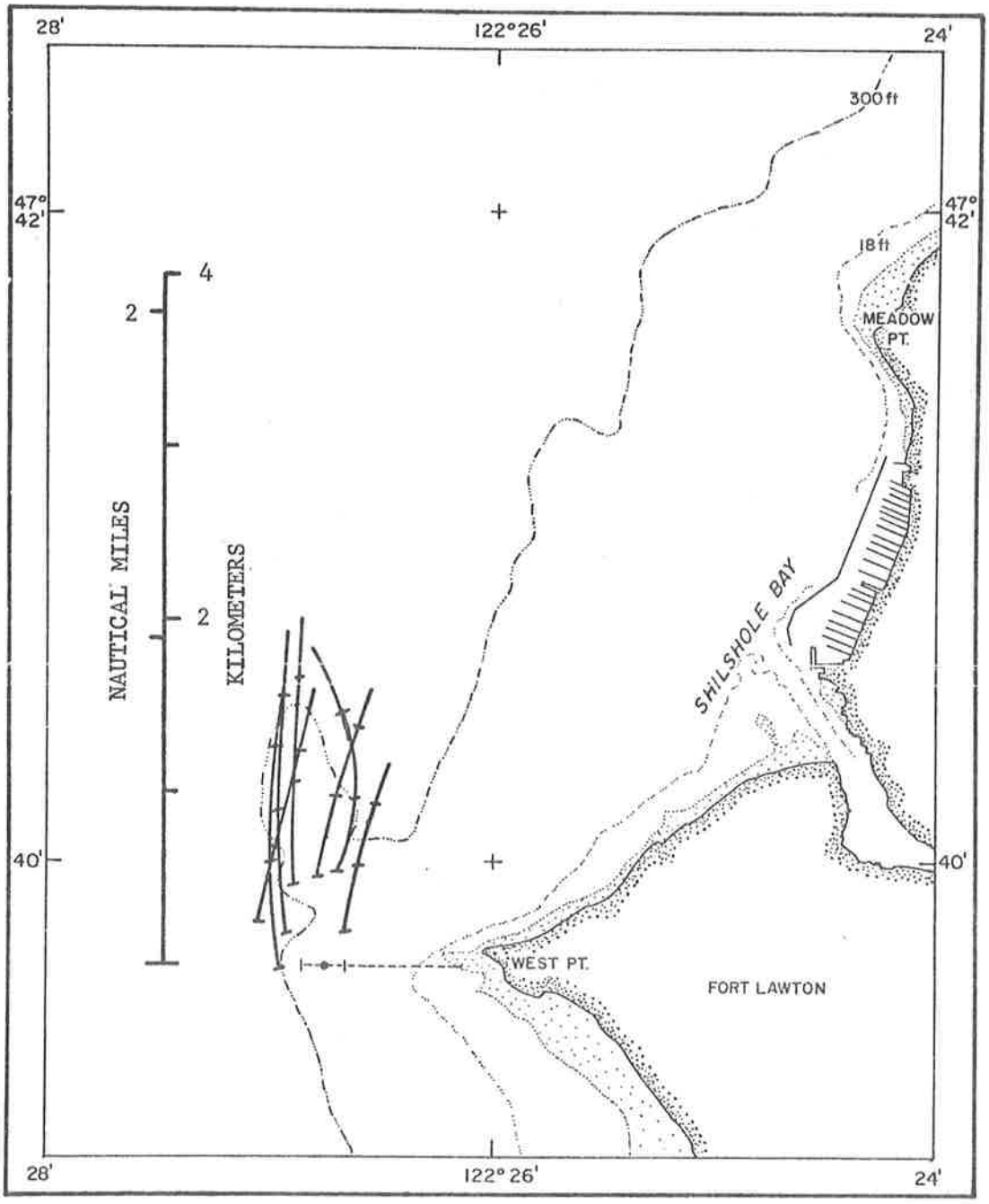

Figure 8e. Drogue trajectories for ebb tide on 3 September 1974. Tics mark half hour intervals.

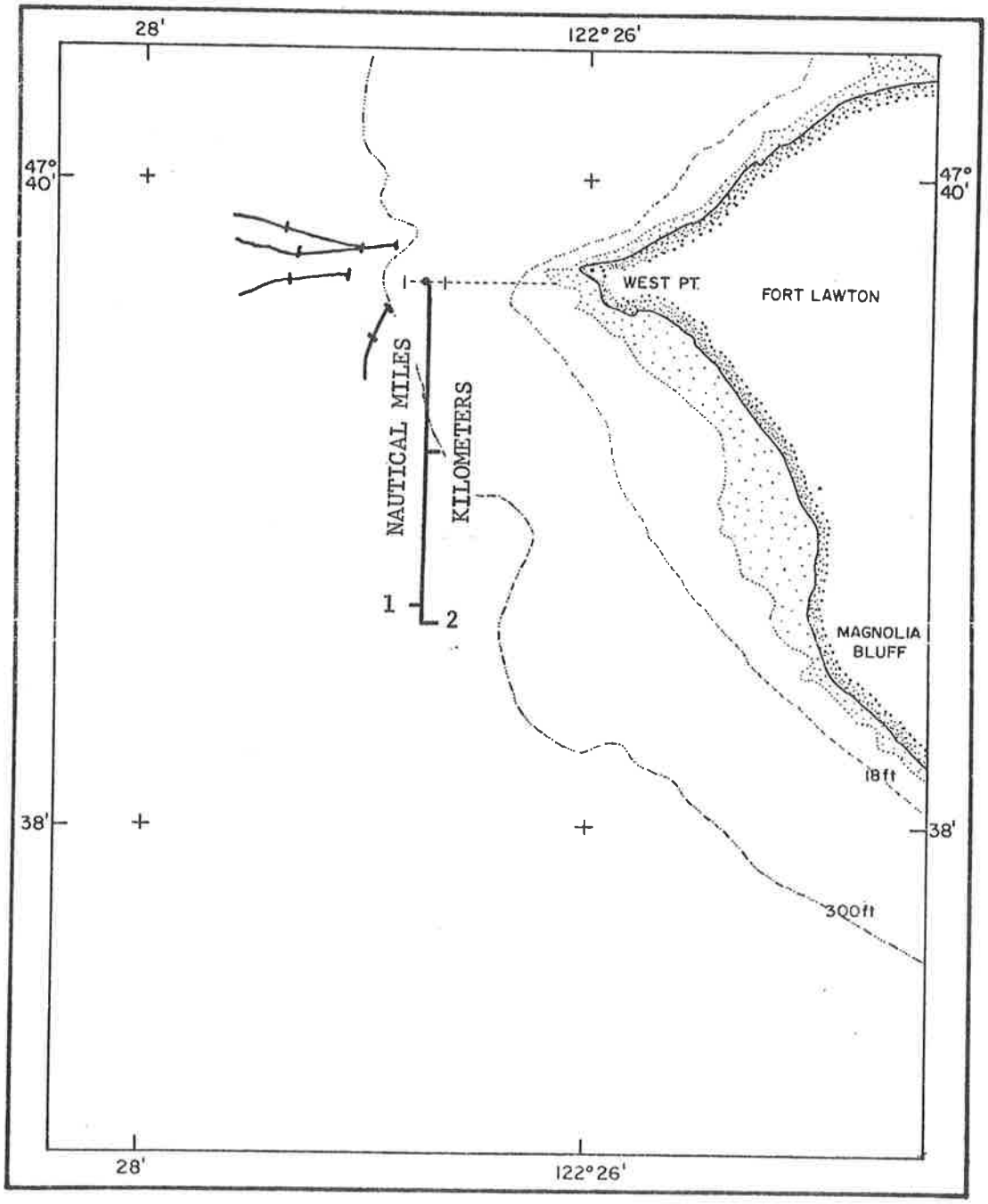

Figure 8f. Drogue trajectories for slack tide on 3 September 1974. Tics mark half hour intervals.

Appendix B

Determination of Vorticity, Divergence, and Deformation Rates from Analysis of Drogue Observations[1]

by

Akira Okubo

Marine Sciences Research Center
State University of New York at Stony Brook
New York 11794

and

Curtis C. Ebbesmeyer

Evans-Hamilton, Inc.
6306 21st Ave. NE
Seattle, Washington 98115

---

[1] Contribution No. 000 from the Marine Sciences Research Center, State University of New York at Stony Brook.

In press, Deep-Sea Res.

ABSTRACT

If several drogues (i.e., four or more) are followed simultaneously not only the mean flow, dispersion, and eddy diffusivities but also the field of mean vorticity, divergence, and deformation rates may be determined as functions of time. Confidence levels of the latter quantities may also be calculated. These new procedures use a matrix approach to linear regression.

Various methods have been developed for experimental studies of oceanic diffusion. However, our present understanding of oceanic diffusion still comes largely from field studies. Among the field methods, the use of drogues is both relatively simple and inexpensive. Yet, their full potential has not been systematically explored in a manner similar to studies of the vorticity and strain rates in arctic sea ice by Hibler, Weeks, Kovacs, and Ackley (1974). This note examines the use of several drogues simultaneously observed in order to separate the mean and turbulent components of fluid flows.

For simplicity, though not of necessity, we will confine our attention to two-dimensional drogue motions. The outline of the data analysis is as follows. Observations of the x,y coordinates are used to calculate the u, v speeds, respectively, of n drogues simultaneously at m times:

$$\begin{aligned} &x_i(k) \quad , \quad y_i(k) \qquad i = 1,2,3,\ldots n \\ &u_i(k) \quad , \quad v_i(k) \qquad k = 1,2,3,\ldots m \end{aligned} \tag{1}$$

Next we expand the u_i, v_i speeds of each drogue at each time in Taylor series about the centroid located at $\bar{x}(k)$, $\bar{y}(k)$:

$$\begin{aligned} u_i(k) &= \bar{u}(k) + \frac{\partial \bar{u}(k)}{\partial x}\,[x_i(k) - \bar{x}(k)] + \frac{\partial \bar{u}(k)}{\partial y}\,[y_i(k) - \bar{y}(k)] + u_i''(k) \\ v_i(k) &= \bar{v}(k) + \frac{\partial \bar{v}(k)}{\partial x}\,[x_i(k) - \bar{x}(k)] + \frac{\partial \bar{v}(k)}{\partial y}\,[y_i(k) - \bar{y}(k)] + v_i''(k) \end{aligned} \tag{2}$$

where

$$\bar{x}(k) = \frac{1}{n}\sum_{i=1}^{n} x_i(k) \quad , \quad \bar{y}(k) = \frac{1}{n}\sum_{i=1}^{n} y_i(k)$$

and where $\frac{\partial \bar{u}}{\partial x}$, $\frac{\partial \bar{u}}{\partial y}$, $\frac{\partial \bar{v}}{\partial x}$, $\frac{\partial \bar{v}}{\partial y}$ are linear velocity gradients at the centroid, and u_i'', v_i'' are the "turbulent" speeds.

In these Taylor series we have assumed that the velocity gradients are *uniform* within the group of drogues and that terms of second and higher order are considered as turbulence. This formulation, as well as those of others (e.g., Okubo, 1966), view the spectrum of oceanic turbulence as separable into two major parts: the large-scale eddies which appear as shears of the mean velocity, and the small-scale eddies responsible for eddy diffusion. In the real ocean, the spectrum of oceanic turbulence contains a wide variety of eddies and is not easily separable in this way. Thus, as the group of drogues spreads, the division between the part of the spectrum assignable to shears and the part assignable to eddy diffusion tends toward smaller wave-numbers and frequencies. Even if the spectrum presents no natural separation, we may assume that the concept of shear-diffusion is still valid locally in time (Ebbesmeyer and Okubo, 1975).

Equation (2) can be expressed more simply as

$$U = RA + E$$
$$V = RB + F \qquad (3)$$

where the following matrix definitions are used:

Position matrices;

$$X(k) = \begin{pmatrix} x_1^*(k) \\ x_2^*(k) \\ \cdot \\ \cdot \\ \cdot \\ x_n^*(k) \end{pmatrix} \qquad Y(k) = \begin{pmatrix} y_1^*(k) \\ y_2^*(k) \\ \cdot \\ \cdot \\ \cdot \\ y_n^*(k) \end{pmatrix} \qquad R(k) = \begin{pmatrix} 1 & x_1^*(k) & y_1^*(k) \\ 1 & x_2^*(k) & y_2^*(k) \\ \cdot & \cdot & \cdot \\ \cdot & \cdot & \cdot \\ \cdot & \cdot & \cdot \\ 1 & x_n^*(k) & y_n^*(k) \end{pmatrix}$$

where the asterisks denote position with respect to the centroid.

Speed matrices;

$$U(k) = \begin{pmatrix} u_1(k) \\ u_2(k) \\ \cdot \\ \cdot \\ \cdot \\ u_n(k) \end{pmatrix} \qquad V(k) = \begin{pmatrix} v_1(k) \\ v_2(k) \\ \cdot \\ \cdot \\ \cdot \\ v_n(k) \end{pmatrix}$$

Current property matrices;

$$A(k) = \begin{pmatrix} \bar{u}(k) \\ \frac{\partial \bar{u}(k)}{\partial x} \\ \frac{\partial \bar{u}(k)}{\partial y} \end{pmatrix} \qquad B(k) = \begin{pmatrix} \bar{v}(k) \\ \frac{\partial \bar{v}(k)}{\partial x} \\ \frac{\partial \bar{v}(k)}{\partial y} \end{pmatrix}$$

Turbulence matrices;

$$E(k) = \begin{pmatrix} u_1''(k) \\ u_2''(k) \\ \cdot \\ \cdot \\ \cdot \\ u_n''(k) \end{pmatrix} \qquad F(k) = \begin{pmatrix} v_1''(k) \\ v_2''(k) \\ \cdot \\ \cdot \\ \cdot \\ v_n''(k) \end{pmatrix} .$$

When the number of drogues exceeds three, the velocity gradients and centroid speeds, i.e., the matrices A and B, may be calculated following the linear regression procedures of Draper and Smith (1966). If $n \leq 3$, then these procedures are not applicable, e.g., if $n = 3$ then turbulent components cannot be determined. Practical considerations of confidence limits as described later dictates that n be approximately six or more.

Application of the linear regression procedures requires that the mean turbulence speeds be zero and that the standard deviation of the turbulence speeds be minimized. For drogue observations we use the "unbiased" sample standard deviation as recommended by Cramer (1966) when calculating the standard deviation from discrete samples drawn from a continuous population:

$$\hat{\sigma}_u(k) = \left[\frac{1}{n-1} \sum_{i=1}^{n} u_i''^2(k)\right]^{1/2}$$
$$\hat{\sigma}_v(k) = \left[\frac{1}{n-1} \sum_{i=1}^{n} v_i''^2(k)\right]^{1/2} . \qquad (4)$$

The result is as follows

$$A = (R'R)^{-1}R'U$$
$$B = (R'R)^{-1}R'V \qquad (5)$$

where R' is the transpose of R and $(R'R)^{-1}$ is the inverse of $(R'R)$. Substituting (5) into (3) the turbulence matrices can be written as

$$E = [1 - R(R'R)^{-1}R']U$$
$$F = [1 - R(R'R)^{-1}R']V \quad . \qquad (6)$$

In reality the turbulence terms consist of two parts: one is the variation due to the real inhomogeniety of velocity gradients within the drogue group, and the other is due to measurement errors in drogue position and velocity. We may estimate measurement errors in several ways. For example, if we make the usual assumption that the real turbulent fluctuations and measurement errors are mutually uncorrelated, and that the measurement errors themselves are uncorrelated with the same zero mean and variance, σ_M^2, we then can obtain the unbiased sample standard deviations for the real

turbulence by subtracting σ_M^2 from $u_i''^2$ and $v_i''^2$ on the right-hand side of eq. (4). Obviously if $u_i''^2$, $v_i''^2 >> \sigma_M^2$, we can regard the total variation due to real inhomogenieties. Measurement errors may also be estimated by substituting positional errors directly into X,Y,R matrices and noting their effect on A,B,E,F matrices.

The standard deviations of the parameters in A and B correspond to the square-root of the diagonal terms of the matrices $(R'R)^{-1}\,\hat{\sigma}_u^2$, $(R'R)^{-1}\,\hat{\sigma}_v^2$, respectively. Then it is convenient to define the following standard deviation matrices

$$\text{S.D. (A)} \equiv \begin{pmatrix} \text{S.D.}(\bar{u}) \\ \text{S.D.}(\frac{\partial \bar{u}}{\partial x}) \\ \text{S.D.}(\frac{\partial \bar{u}}{\partial y}) \end{pmatrix} \qquad \text{S.D. (B)} \equiv \begin{pmatrix} \text{S.D.}(\bar{v}) \\ \text{S.D.}(\frac{\partial \bar{v}}{\partial x}) \\ \text{S.D.}(\frac{\partial \bar{v}}{\partial y}) \end{pmatrix} . \tag{7}$$

Assuming that the turbulence velocities are all from the same normal distribution, the 100(1-a)% confidence limits of A and B may be expressed as

$$\begin{aligned} &A \pm t(n - 2, 1 - \tfrac{1}{2}a)\ \text{S.D. (A)} \\ &B \pm t(n - 2, 1 - \tfrac{1}{2}a)\ \text{S.D. (B)} \end{aligned} \tag{8}$$

where Student's t distribution $t(n-2, 1-\frac{1}{2}a)$ has n-2 degrees of freedom and probability $1-\frac{1}{2}a$.

The stability or instability of the standard deviation of the drogue displacement may be calculated following Okubo (1970). First we define

$$
\begin{aligned}
&\text{Horizontal divergence} && \equiv \gamma(k) = \frac{\partial \bar{u}(k)}{\partial x} + \frac{\partial \bar{v}(k)}{\partial y} \\
&\text{Relative vorticity} && \equiv \eta(k) = \frac{\partial \bar{v}(k)}{\partial x} - \frac{\partial \bar{u}(k)}{\partial y} \\
&\text{Stretching deformation rate} && \equiv \alpha(k) = \frac{\partial \bar{u}(k)}{\partial x} - \frac{\partial \bar{v}(k)}{\partial y} \\
&\text{Shearing deformation rate} && \equiv h(k) = \frac{\partial \bar{v}(k)}{\partial x} + \frac{\partial \bar{u}(k)}{\partial y} \quad .
\end{aligned} \tag{9}
$$

The presence and type of any velocity singularities are then determined according to the graph of $\gamma(k)$ versus $\alpha^2(k) + h^2(k) - \eta^2(k)$ and figures given by Okubo (1970).

The eddy diffusivities K_x, K_y may be obtained by analogy to a combination of mixing length theory and turbulence theory (Obukhov, 1941), i.e., the diffusivity is proportional to the product of a mixing length ℓ and intensity of turbulence velocity $(\varepsilon\ell)^{1/2}$, where ε is the rate of energy dissipation as in the four-thirds power law

$$K(\ell) = c\, \varepsilon^{1/3}\, \ell^{4/3} \quad . \tag{10}$$

Ozmidov (1960) argued that the proportionality constant c should be of order 0.1. In the present work we assume that turbulence intensity equals $\hat{\sigma}_u$, $\hat{\sigma}_v$ and that the mixing length equals the standard deviation of drogue displacement $\hat{\sigma}_x$, $\hat{\sigma}_y$ so that

$$
\begin{aligned}
K_x(k) &= 0.1\, \hat{\sigma}_u(k)\, \hat{\sigma}_x(k) \\
K_y(k) &= 0.1\, \hat{\sigma}_v(k)\, \hat{\sigma}_y(k)
\end{aligned} \tag{11}
$$

where

$$\hat{\sigma}_x(k) = \{ \frac{1}{n-1} \sum_{i=1}^{n} [x_i(k) - \bar{x}(k)]^2 \}^{1/2}$$

$$\hat{\sigma}_y(k) = \{ \frac{1}{n-1} \sum_{i=1}^{n} [y_i(k) - \bar{y}(k)]^2 \}^{1/2} .$$

The foregoing calculations allow determination of the mean field of current shear in addition to eddy diffusivities and the mean current speed versus time. These results may be substituted directly into a comprehensive model for advection and diffusion previously developed by Okubo (1966). In that way detailed comparisons between drogue and dye observations may be obtained.

By treating drogue accelerations in a similar way we may obtain stress components such as in the right-hand side of a simple vorticity balance

$$\frac{d}{dt} (\eta + f) + (\eta + f) \gamma = \frac{\partial F_y}{\partial x} - \frac{\partial F_x}{\partial y} \qquad (12)$$

where f is the vertical component of planetary vorticity and F_x, F_y are x,y components of frictional forces per unit mass. In this balance we have neglected vertical velocities and baroclinic terms. Both the kinematics and dynamics of fluid flows can thus be examined using drogues.

It can be seen that the present analysis may well be applicable to records obtained from an array of several moored current meters.

Acknowledgements: This work was supported by the Office of Naval Research, Contract N-00014-67-A-0103-0014. The cooperation of James J. Anderson and Prof. F.A. Richards at the Department of Oceanography, University of Washington is gratefully acknowledged.

REFERENCES

Cramer, H. (1966) *Mathematical methods of statistics*. Princeton University Press, eleventh edition, 575 pp.

Draper, N.R. and H. Smith (1966) *Applied Regression Analysis*. John Wiley and Sons, N.Y., 407 pp.

Ebbesmeyer, C.C. and A. Okubo (1975) Variance relations between variable shear-diffusion and radially symmetric turbulent diffusion. Deep-Sea Research, (in press).

Hibler, W.D., W.F. Weeks, A. Kovacs, and S.F. Ackley (1974) Differential sea ice drift I: spatial and temporal variations in sea ice deformation. Journal of Glaciology, 13, 437-455.

Okubo. A. (1966) A note on horizontal diffusion from an instantaneous source in a non-uniform flow. Journal of the Oceanographical Society of Japan, 22, 35-40.

Okubo, A. (1970) Horizontal dispersion of floatable particles in the vicinity of velocity singularities such as convergences. Deep-Sea Research, 17, 445-454.

Obukhov, A.M. (1941) Energy distribution in the spectrum of a turbulent flow. Izvestia, Akademiia Nauk, SSSR, Georgraphy and Geophysics series, No. 4-5, 453-466.

Ozmidov, R.V. (1960) On the rate of dissipation of turbulent energy in sea currents and on the dimensionless universal constant in the "4/3-power law." (in Russian) Izvestia Akademiia Nauk SSSR, Geophysics series, No. 8, 1234-1237 (American Geophysical Union Translation, English Edition, Bulletin, Academy of Sciences, SSSR, Geophysics series, No. 8, 821-823).

Appendix C. Determination of Lagrangian Displacement Properties

Observations of the x, y coordinates are used to calculate the Lagrangian Displacement Properties (abbreviated LDP) for n drogues observed at m times:

$$\begin{aligned} &x_i(k) \qquad i = 1,2,3,\ldots n \\ &y_i(k) \qquad k = 1,2,3,\ldots m \end{aligned} \tag{1}$$

We expand the x_i, y_i coordinates of each drogue at each time in Taylor series about the centroid:

$$\begin{aligned} x_i^*(k) &= \frac{\partial x_i^*(k)}{\partial x_i^*(\ 1)}\, x_i^*(\ 1) + \frac{\partial x_i^*(k)}{\partial y_i^*(\ 1)}\, y^*(\ 1) + x_i^{*\prime} \\ y_i^*(k) &= \frac{\partial y_i^*(k)}{\partial x_i^*(\ 1)}\, x_i^*(\ 1) + \frac{\partial y_i^*(k)}{\partial y_i^*(\ 1)}\, y_i^*(\ 1) + y_i^{*\prime} \end{aligned} \tag{2}$$

where asterisks denote position with respect to the centroid

$$x_i^*(k) = x_i(k) - \bar{x}(k)$$

$$y_i^*(k) = y_i(k) - \bar{y}(k)$$

$$\bar{x}(k) = \frac{1}{n} \sum_{i=1} x_i(k), \quad \bar{y}(k) = \frac{1}{n} \sum_{i=1} y_i(k)$$

and where primes denote displacements due to "turbulence".

Equation (2) can be expressed more simply as

$$\begin{aligned} X &= RF + L \\ Y &= RG + M \end{aligned} \tag{3}$$

where the following matrix definitions are used:

Position matrices;

$$X(k) \equiv \begin{pmatrix} x_1^*(k) \\ x_2^*(k) \\ \cdot \\ \cdot \\ x_n^*(k) \end{pmatrix} \qquad Y(k) \equiv \begin{pmatrix} y_1^*(k) \\ y_2^*(k) \\ \cdot \\ \cdot \\ y_n^*(k) \end{pmatrix} \qquad R(k) \equiv \begin{pmatrix} x_1^*(k-1) & y_1^*(k-1) \\ x_2^*(k-1) & y_2^*(k-1) \\ \cdot & \cdot \\ \cdot & \cdot \\ x_n^*(k-1) & y_n^*(k-1) \end{pmatrix}$$

LDP matrices;

$$F(k) \equiv \begin{pmatrix} \frac{\partial x^*(k)}{\partial x^*(k-1)} \\ \\ \frac{\partial x^*(k)}{\partial y^*(k-1)} \end{pmatrix} \qquad G(k) \equiv \begin{pmatrix} \frac{\partial y^*(k)}{\partial x^*(k-1)} \\ \\ \frac{\partial y^*(k)}{\partial y^*(k-1)} \end{pmatrix}$$

Turbulence matrices;

$$L(k) \equiv \begin{pmatrix} x_1^{*\prime}(k) \\ x_2^{*\prime}(k) \\ \cdot \\ \cdot \\ x_n^{*\prime}(k) \end{pmatrix} \qquad M(k) \equiv \begin{pmatrix} y_1^{*\prime}(k) \\ y_2^{*\prime}(k) \\ \cdot \\ \cdot \\ y_n^{*\prime}(k) \end{pmatrix}$$

The matrices F, G may be calculated following the linear regression procedure of Draper and Smith (1966). Application of the linear regression procedures requires that the mean turbulence displacements be zero and that the standard deviation of the turbulence displacements be minimized. For drogue observations we use the "unbiased" sample standard deviation as recommended by Cramer (1966) when calculating the standard deviation from discrete samples drawn from a continuous population:

$$\hat{\sigma}_x(k) = \left[\frac{1}{n-1} \sum_{i=1}^{n} x_i^{*\prime 2}(k) \right]^{\frac{1}{2}}$$

$$\hat{\sigma}_y(k) = \left[\frac{1}{n-1} \sum_{i=1}^{n} y_i^{*\prime 2}(k) \right]^{\frac{1}{2}} \qquad (4)$$

The result is as follows

$$F = (R'R)^{-1} R'X$$

$$G = (R'R)^{-1} R'X \qquad (5)$$

where R' is the transpose of R and $(R'R)^{-1}$ is the inverse of $(R'R)$.